THE UNIVERSITY *of* EDINBURGH

Soil organic matter stability and the temperature sensitivity of soil respiration

Nancy Burns

Thesis submitted in fulfilment of
the requirements for the degree of
Doctor of Philosophy
to the
University of Edinburgh — 2011

Declaration

I declare that this thesis has been composed solely by myself and that it has not been submitted, either in whole or in part, in any previous application for a degree. Except where otherwise acknowledged, the work presented is entirely my own.

Nancy Burns

August 2011

Abstract

Soil respiration is an important source of atmospheric CO_2, with the potential for large positive feedbacks with global warming. The size of these feedbacks will depend on the relative sensitivity to temperature of very large global pools of highly stable soil organic matter (SOM), with residence times of centuries or longer. Conflicting evidence exists as to the relationships between temperature sensitivity of respiration and stability of SOM, as well as the temperature sensitivity of individual stabilisation mechanisms.

This PhD considers the relationship between different stabilisation mechanisms and the temperature sensitivity of SOM decomposition. I used physical fractionation to isolate SOM pools with a variety of turnover rates, from decadal to centennially cycling SOM, in a peaty gley topsoil from Harwood Forest. Mean residence times of SOM as determined by ^{14}C dating was most strongly affected by depth, providing stability on a millienial scale, while OM-mineral associations and physical protection of aggregates provided stability to around 500 years.

Chemical characteristics of organic material in these fractions and whole soils (^{13}C CP-MAS NMR spectroscopy, mass spectrometry, FTIR spectroscopy, thermogravimetric analysis, ICP-OES) indicated the relative contribution of different stabilisation mechanisms to the longevity of each of these fractions. Two long-term incubations of isolated physical fractions and soil horizons at different temperatures provided information about the actual resistance to decomposition in each SOM pool, as well as the temperature sensitivity of respiration from different pools. Naturally ^{13}C-labelled labile substrate additions to the mineral and organic horizons compared the resistance to priming by labile and recalcitrant substrates. Manipulation of soil pore water was investigated as a method for isolating the respiration of SOM from physically occluded positions within the soil architecture.

Contadictory lines of evidence emerged on the relative stability of different SOM

pools from ^{14}C dating, incubation experiments and chemical characterisation of indicators of stability. This led to the interpretation that physical aggregate protection primarily controls SOM stability within topsoils, while mineral and Fe oxide stability provides more lasting stability in the mineral horizon. Less humified and younger SOM was found to have a higher sensitivity to temperature than respiration from well-humified pools, in contrast to predictions from thermodynamics.

Acknowledgements

First of all I would like to thank my supervisor, Dr Joanna Cloy, for her relentless optimism and patience throughout my PhD and especially for continuing to devote an enormous amount of time and energy to it even after leaving the department for a new job. My other supervisors, Prof Keith Smith, Prof Wilfred Otten (University of Abertay, Dundee) and Dr Dave Reay were all sources of valuable guidance at critical points in my PhD. I am very grateful to Dr Maurizio Mencuccini and Dr Iain Hartley (University of Exeter) for examining my thesis.

Very many thanks go to Dr Mark Garnett from the NERC radiocarbon laboratory for his help and advice during the ^{14}C dating experiment, and for his insightful feedback on manuscripts. Thank you very much to Dr David Apperley, Durham University for help with ^{13}C-CPMAS NMR; Silvia Williamson at the University of St Andrews for the thermogravimetric analysis; Colin Chilcott and Ann Mennim for help with the CN analysis and mass spec, and Dr Nicola Cayzer for help with the SEM-EDX. Thank you to Terry Donnelly at SUERC for help calibrating the TDL standards, and tolerating my damage to the vacuum rig. Dr Margaret Graham and Dr Kate Heal were both very generous to offer bench space in their labs. Many thanks go to Prof. John Grace for allowing me to use the TDL (even if sometimes I wished he hadn't).

Special thanks to all the people who helped me to tame uncooperative gas analysers- Rab Howard, Anitra Fraser, Dr Andy Cross (who bore the brunt, teaching me how to use the TDL while writing up his own PhD), Keith, and Mark. Several waterbaths died over the course of this PhD, and Alan Pike gallantly tried to resuscitate several of them.

Thank you to everyone who came on the trips to Harwood forest with me- Sigrid, Andy, Graham, Rab, and Maria Almagro and Nick Nickerson. The first two priming experiments described in chapter 6 were a joint effort between Maria, Nick and

myself when Maria and Nick were both visiting the department.

I doubt I would have made it through my PhD without the supportive environment of the Crew building PhD attic- but if I did it would probably have been faster. Thank you- for the MATLAB and LaTeX help, Silvia, Jonny and Antony; for proofreading, Emily and Jenny; for the solidarity, Howie, Rudra, Tiziana... for distractions, tea-breaks, moral support, and for keeping office ballsports to a minimum, all the attic residents. Thank you, fantastic flatmates (Dave, Jenny and Vanessa) and to various friends I complained to about my PhD (Laura, Romain, Luke, Erin, Hannah, etc...) for keeping me together and for telling me to hang in there when I was fed up.

Thank you to all my funding sources- SAGES and the University of Edinburgh for funding my PhD, SUERC for providing the radiocarbon dates for free, EPSRC for providing the ^{13}C-CPMAS NMR analysis for free, and the UK taxpayer, for funding all of the above, albeit unwillingly. Please continue. Thank you to my Friends at the Quaker Meeting House, who funded the last 9 months of my PhD by employing me part time and not minding if I worked on my PhD on shift. Thank you to the Dunya Ensemble, because you can't do science all the time. Thank you to my family- Mum and Dad, Lucy and John and the Portobello Ashes in particular- for always being there, and for not asking too many questions.

Most of all, thank you Lorna, for giving me a reason to finish, and then making sure I did.

This thesis is dedicated to my grandfather, Michael Ashe (1918-2009), who always said to go and look it up in a book.

Contents

List of Figures

List of Tables

Chapter 1

Introduction

Anthropogenic global warming is undoubtably one of the defining political, economic and scientific issues of the early 21st century. Mean annual temperatures continue to increase, and the first decade of the 21st century was the hottest on record (NASA, 2011), despite exceptionally low solar activity (Lockwood, 2010). IPCC projections estimated a 1.8 °C increase in mean surface temperature by the end of this century (IPCC, 2007) based on the most conservative anthropogenic emissions scenarios. However, fossil fuel emissions from the past decade have already surpassed the projections of the most severe scenarios (Le Quere *et al.*, 2009), which predict a 3 - 4 °C increase by 2100. Even if anthropogenic GHG emissions were to cease completely, warming caused by GHGs already emitted is now irreversible within 1000 years (Solomon *et al.*, 2009). Recent warm summers have seen unprecedented surface melt of the Greenland ice sheet (NASA, 2012), as well as retreating arctic sea ice (Wadhams, 2012), contributing to sea level rise as well as worsening the greenhouse effect due to changes in albedo. Direct impacts of a warmer climate on human activity will include drought (Overpeck and Udall, 2010), food shortages (Lobell *et al.*, 2008), sea level rise (Rahmstorf, 2010), moving boundaries of endemic disease regions (Patz *et al.*, 2005), higher incidence of extreme weather events such as heatwaves and floods (Coumou and Rahmstorf, 2012), and possibly even civil conflict (Hsiang *et al.*,

2011). The direct consequences of climate warming threaten to have very serious consequences for human societies. However, of arguably even greater concern are the impacts of a warmer climate on the natural carbon cycles (terrestrial, aquatic and marine), which hold positive feedback loops with the potential to accelerate warming, and the human costs of warming, beyond control.

Large scale coordinated intergovernmental efforts are urgently needed to mitigate the worst effects of climate change on food and water security and public health, but recent attempts at internationally binding treaties to reduce anthropogenic emissions have been hampered by regional economic interests. Commitment to securing costly, coordinated international legislation on fossil fuel emissions has become a politically polarising position in an era of financial crises. The origin of the observed warming now universally accepted in the scientific establishment is the anthropogenic emission of fossil fuels (BEST, 2011), with a conservative estimated probability of 90 % (IPCC, 2007). However, the estimated 8.7 Pg CO_2-C y^{-1} global emissions from fossil fuels (2008 value, Le Quere *et al.* (2009)) are small in comparison to the 50 - 70 Pg CO_2-C released to the atmosphere annually from soils (Houghton *et al.*, 1996). The moral imperative to reduce fossil fuel emissions remains strong; however, relatively small changes in natural carbon cycling, triggered by anthropogenic changes to the atmosphere and climate or by anthropogenic land use change, and exacerbated by natural feedback loops, have the potential to dwarf the direct effects of anthropogenic emissions.

1.1 Soil in the terrestrial carbon cycle

Globally, soils hold 1576 Pg C (Eswaran *et al.*, 1993), 684–724 Pg to a depth of 30 cm and 1462–1548 Pg to a depth of 1 m (Batjes, 1996). This global soil organic carbon stock makes up around three quarters of the total terrestrial organic carbon stock, and is equivalent to roughly double the amount of carbon in the atmosphere as CO_2.

Global soil organic carbon stocks are large, but also dynamic: organic carbon enters and leaves the soil with turnover times ranging from days to millenia (Trumbore, 2009). The majority of SOC persisting in soils is very old, with a relatively slow turnover. Small changes in the rate of decomposition of old SOC, or in the factors determining the persistence of SOC, could therefore result in a very large source of terrestrial carbon becoming vulnerable to decomposition and released to the atmosphere as CO_2.

Soils accumulate C from plant litter and root exudation, and this dead plant material is gradually transformed by successive degradation and humification processes into humic substances. Some soil organic carbon (SOC) is incorporated into microbial biomass and macrobiota and recycled, and some may be semi-permanently stabilised in physical associations with aggregates and mineral surfaces, before being recovered to the active SOC pool by bioturbation or physical disturbance. SOC leaves the system after it is converted to CO_2 during heterotrophic respiration by microbes and soil animals. Water-soluble SOC compounds may dissolve into the soil water, joining the dissolved organic matter (DOC) pool, where they are more susceptible to microbial respiration. During rainfall, DOC may then be transported downwards into the mineral soil horizons (illuviated), where redox conditions may be less favourable for microbial respiration, leading to stabilisation; or transported horizontally (alluviated) in groundwater flow, entering the aquatic and eventually the marine carbon cycle.

Major carbon cycle models all predict that climate warming will be accompanied by a loss of global SOC stocks, however the extent of the loss is very variable (between 20 and 177 Pg C K^{-1}, (Friedlingstein *et al.*, 2006)) and strongly dependent on the model architecture, in particular the number of pools with different turnover rates that are allowed (Jones *et al.*, 2005). Soil carbon stocks in the UK have been observed to decline consistently over the last 30 years, most likely due to rising temperatures (Bellamy *et al.*, 2005).

1.1.1 Feedback loops

A number of different processes may cause global soil CO_2 emissions to increase under climate warming, resulting in a positive feedback. First of all, the basic rate of heterotrophic respiration of SOM is inherently temperature-sensitive; at a very simple level, respiration is an enzyme reaction governed by standard enzyme kinetics, and at higher ambient temperatures more energy is available to reach the activation energy of the reaction (Arrhenius, 1915). Under equilibrium conditions the positive soil CO_2 flux is balanced by the assimilation of CO_2 in photosynthesis (NPP, 60 Pg C y^{-1}, Cox *et al.* (2000a)), which is also sensitive to temperature and CO_2. However, the positive effect of increased CO_2 on photosynthesis is expected to become saturated at higher levels, while the positive effect of temperature on CO_2 release in soil respiration continues to increase with rising temperatures (Cox *et al.*, 2000a). In addition the light reactions of photosynthesis are expected to be relatively insensitive to temperature, being limited by the non-enzymatic oxidation of chlorophyll. A higher overall temperature sensitivity of heterotrophic respiration reactions than of photosynthesis could result in a positive feedback loop, as CO_2 release increases more than uptake as climate change progresses.

Total soil respiration has been repeatedly shown in field studies to increase with temperature (for example, Bond-Lamberty and Thomson (2010)). However, this only creates a positive feedback loop with climate change if the 'extra' CO_2 released at higher temperatures originates from otherwise stable SOM; since GPP also increases with temperature and CO_2 concentration, it possible that fresh plant inputs to soil also increase with warming, causing soil respiration to increase in a 'carbon neutral' way (Smith and Fang, 2010). Alternately, the same increase in soil respiration with warming could be explained by the recruitment of stable carbon into the available SOC pool, which would represent a net loss of carbon from the system. For this reason it is vitally important to distinguish the temperature responses fresh and older

sources of soil respiration.

Further feedback loops with climate change have been predicted on the basis of the effect of increasing CO_2 concentrations on soil microbial communities, leading to increased respiration (Carney *et al.*, 2007). In addition, microbial respiration in soils and peat also invokes its own positive feedback loop with temperature, as heat is released during respiration, further increasing respiration rates- this is known as the 'compost-bomb' effect (Luke and Cox, 2011).

1.1.2 Land use change

Changes in land use including further deforestation, agricultural conversion and urbanisation are inevitable as by mid-century the world population is expected to reach 9 billion (UN, 2004) and as climate change continues to impact food security (IPCC, 2007). Land use change has a strong control over soil properties (Guo *et al.*, 2007; Paul *et al.*, 2008a; Adachi *et al.*, 2006), and conversion of forests or grasslands to agriculture invariably results in large SOC losses (Brown and Lugo, 1984; Adachi *et al.*, 2006). Increasing SOC stocks using appropriate land management practices (such as minimal tillage and biochar application) is often proposed as a mechanism for mitigating rising atmospheric CO_2 concentrations. However, the extent to which recently incorporated C can be irreversibly sequestered is contested, and interventions designed to increase SOC stocks can result in higher emissions of other GHGs, or land use displacement leading to increased SOC losses elsewhere (for a review see Powlson *et al.* (2011)).

1.2 Soil organic matter stability and temperature response

While the majority of soil respired CO_2 is derived from the rapidly decomposed 'active' pool of soil organic matter (SOM), an esimated 90 % of total SOM in the top 1 m in mineral soils (not including peat) has a turnover rate from decades to millenia

(Davidson and Janssens, 2006). Estimates of the temperature response of soil respiration, unless specifically isolating the response of older material, are necessarily biased towards the response of the active pool. However, there is reason to suggest that some stabilised material may have a different temperature sensitivity than more labile OM. If more stable SOM has a higher temperature sensitivity than the active pool, predictions of the magnitude of soil carbon feedbacks may have been underestimated by biased estimates of soil respiration temperature sensitivity. However, many interacting factors affect both the stability of SOM (Kögel-Knabner *et al.*, 2008; Sollins *et al.*, 2007) and the temperature sensitivity of SOM respiration (von Lützow and Kögel-Knabner, 2009; Ågren and Wetterstedt, 2007), and the relative contribution of different stabilising factors is both site- and soil type-specific (Spielvogel *et al.*, 2008) making it difficult to predict responses. As such the relative temperature response of stable and active SOM remains a controversial topic (Davidson and Janssens, 2006; Kirschbaum, 2006; von Lützow and Kögel-Knabner, 2009).

1.2.1 Quantifying stability

There are essentially three complementary approaches to describing the stability of organic matter, which are all widely used. Firstly, the stability of SOM to decomposition at any one time can be described simply by the rate of decomposition; in this thesis I refer to this type of stability as "current stability". Measurements of current stability address the question *how resistant is this SOM to decomposition?* Alternatively, we might ask *how persistent is this SOM?* It is possible to measure directly how long a substance has persisted in soil by ^{14}C dating (Trumbore, 2000, 2009). I refer to this as "lifetime stability" during this thesis. A third approach to predict the future stability of SOM is to understand the mechanisms contributing to SOM stabilisation, and to estimate the potential for persistence using proxy measurements of physical and chemical characteristics thought to contribute to stabilisation. In comparison, this approach asks the question, *how easy to degrade is this SOM?* I refer to this third approach

as addressing the "theoretical stability" of SOM. Each of these approaches gives useful information about stability which is necessary for predicting the behaviour of the SOM, but which may be contradictory depending on the soil history and interactions between stabilisation mechanisms.

Three main mechanisms are described for the stabilisation of organic matter in soils: intrinsic chemical recalcitrance, physical protection of SOM within aggregates, and mineral sorption (Mikutta *et al.*, 2006; Davidson and Janssens, 2006; von Lützow *et al.*, 2007; Sollins *et al.*, 2007; Marschner *et al.*, 2008). Trumbore (2009) includes a further two mechanisms- climatic stabilization (for example freezing and water saturation, in permafrost and peat) and microbial inhibition.

Intrinsic chemical recalcitrance

OM can be said to be intrinsically recalcitrant if the molecular structure of the compound itself slows decomposition. For example, this can be due to a complex molecular structure with irregular tertiary structure and a lack of enzyme active sites, leading to a high effective activation energy (E_a). Fatty leaf waxes (Feng *et al.*, 2008) and lignins (Benner *et al.*, 1987) are traditional examples, although lignin may be less persistent in soils than previously thought (Marschner *et al.*, 2008; Sollins *et al.*, 2006). Some plant derived molecular structures are known to slow decomposition, but not for longer than around a century. Intrinsically recalcitrant material older than a century is attributed to microbial recycling of plant carbon skeletons (Gleixner *et al.*, 2002). For example, microbial surface-active proteins (hydrophobins, chaplins, glomalins) may be particularly resistant microbial products (Rillig *et al.*, 2007).

A traditionally important paradigm for SOM stabilisation was the production of humic substances- large, polyaromatic macropolymers formed abiotically by condensation reactions between plant and microbial products. However, increasingly evidence suggests the de novo formation of humic polymers is not important for humus formation and stabilisation in soils (Sollins *et al.*, 2007; Schmidt *et al.*, 2011).

Mineral associations

In some soils it has been suggested that the intrinsic quality of SOM has very little impact on decomposition rates, because abundant mineral surfaces cause stronger stabilisation (Marschner *et al.*, 2008). Organic matter forms strong bonds with clay surfaces and mineral oxides via ligand exchange, cation exchange or electrostatic interactions. OM-mineral adsorption is predicted to operate on a near-permanent basis, as the adsorption bonds are effectively irreversible (Marschner *et al.*, 2008; Kögel-Knabner *et al.*, 2008). However, this stability is strongly dependent on crystal structure (Torn *et al.*, 1997), with weakly crystalline minerals providing weaker OM-mineral bonds.

Aggregate protection

OM that is neither intrinsically indigestible nor bound to minerals can persist for a long time in the soil by becoming trapped within aggregates, blocked from access by decomposers. Mineral-OM complexes form loose associations with particulate OM and cluster into self-assembling layered structures of alternating mineral and organic material (Sollins *et al.*, 2009; Lehmann *et al.*, 2007) forming discrete zones of OM with different behaviours (Kleber *et al.*, 2007). OM within these clusters may experience slow decomposition rates because of a combination of physical inaccessibility, reduced oxygen diffusion, and the force of OM-mineral interactions, as well as intrinsic chemical recalcitrance, for example in hydrophobic zones (Kleber *et al.*, 2007).

Soil aggregate status is strongly affected by land-use, with conversion of forested land to agriculture typically causing a reduction in microaggregate-protected C (Six *et al.*, 2002). This means that where aggregate protection provides the dominant source of stability, SOC stocks are more vulnerable to land use than where SOC is primarily stabilised by mineral interactions or intrinsic properties.

1.2.2 Temperature response- Q theory

Defining intrinsic recalcitrance has been problematic, but Bosatta and Ågren (1999) proposed that the 'quality' of SOM should be defined by the number of different enzyme reactions required to mineralise a single carbon atom. A large number of different enzyme reactions implies a low energy return, and results in low decomposition rates. Bosatta and Ågren (1999) used thermodynamics and Michaelis-Menten enzyme kinetics to show that combining the activation energies (E_a) of multiple enzyme steps results in a higher overall activation energy for the whole process, producing a higher temperature sensitivity. SOM of an initially lower quality is by definition more likely to persist in soil, if higher quality (more degradable) material is available as an alternative substrate. However SOM also becomes progressively lower in quality, as the higher quality components are preferentially decomposed and through progressive microbial transformations. Many studies support the relationship between low quality and high temperature sensitivity predicted by Bosatta and Ågren (1999) in what they called "Q-theory" (Hartley and Ineson, 2008; Karhu *et al.*, 2010a; Craine *et al.*, 2010; Biasi *et al.*, 2005). However, the number of enzyme steps are by no means the only control on decomposition.

1.2.3 Temperature response- Mineral adsorption

Thornley and Cannell (2001) proposed that mineral adsorption of OM may contribute to lowering the temperature sensitivity of soil respiration overall by increasing mineral stabilisation with temperature, since the formation of stable OM-mineral bonds by absorption is itself positively temperature sensitive, while their breakdown is thought to be thermally stable. By this reasoning, mineral stabilisation cancels out the temperature sensitivity of soil respiration; in soils where mineral stability is high, mineral-bound material is not sensitive temperature, and the overall temperature response may be attenuated by the formation of new mineral associations.

In addition, the OM material stabilised by minerals can be of a high quality with respect to the Q-theory; labile polysaccharides and peptides are often found in association with minerals (Kleber *et al.*, 2011; Grandy *et al.*, 2007; Kaiser and Guggenberger, 2000). This might suggest that when decomposition does occur, it will have a relatively low temperature sensitivity.

1.3 Aims

This thesis set out to investigate mechanisms of SOM stability in a forest soil. I asked the following questions about the stability of SOM and its effect on the temperature response of respiration:

- What are the dominant mechanisms of stabilisation and destabilisation acting on SOM in forest soils?
- Does aggregate-occluded material have intrinsically different properties from mineral-bound material?
- How is the temperature sensitivity of respiration affected by mineral stability?
- How sensitive to temperature is chemically recalcitrant material?
- Is there a general relationship between temperature sensitivity and the age of SOM?

1.4 Thesis structure

This thesis is structured as a traditional thesis with five self-contained research chapters.

Chapter 3- Chemical characteristics of Harwood forest soils and soil fractions

This chapter investigates the composition of SOM in fractions and horizons, with reference to mechanisms that may cause theoretical stability in these fractions. I investigate trends in degradation with depth, particle size and particle density, and identify several potential mechanisms of stabilisation in the SOM fractions, contributing to the theoretical stability of SOM.

Chapter 4- Soil respiration and temperature response from Harwood forest soils and density fractions

In this chapter, some of the physical fractions and whole soils described in Chapter 3 were incubated at different temperatures as a measure of the current stability of SOM and to establish the temperature sensitivity of different isolated fractions. This chapter addresses the third and fourth research aims, establishing the relative sensitivity to temperature of chemically recalcitrant material and mineral-bound material. Based on the chemical composition of fractions and the Q theory, I hypothesised that respiration in the intra-aggregate organic matter and deeper soil horizons would be more sensitive to temperature.

Chapter 5- Isotopic composition of SOM respired from Harwood forest soils and density fractions

Chapter 5 relates the lifetime stability, measured by ^{14}C age, of fractions and whole soils with the current stability established in chapter 4 and the theoretical stability suggested by chemical characterisation in chapter 3. After long term incubations at

10 and 30 °C, respired CO_2 was collected for ^{14}C dating, to investigate a possible general relationship between temperature and the age of SOM respired.

Chapter 6- Priming effects of labile substrate additions in Harwood forest soil horizons

Lack of available labile substrates is thought to limit respiration of recalcitrant substrates- the experiments described in chapter 6 use naturally ^{13}C labelled sucrose to investigate the priming of SOM respiration by labile substrate additions, assessing whether priming may be a potentially dominant destabilisation mechanism for Harwood SOM.

Chapter 7- Soil porespace and water characteristics in Harwood forest

The experiments described in chapter 7 were designed to address SOM stability due to physical protection in the soil matrix. Intact soil cores were manipulated by selectively draining the saturated soil porespace and incubated in series, in an attempt to separate respiration from macropores and from micropores. This chapter aimed to investigate whether physical protection is a dominant stabilisation mechanism for Harwood SOM.

Chapter 2

Harwood Forest Site Description

2.1 Site Description

2.1.1 Harwood Forest

Harwood forest is a Sitka spruce (*Picea sitchensis* (Bong.) Carr.) forest in Northumberland, UK (55° 12′ 59″ N, 2° 1′ 28″ W). The study site was located in a stand in the centre of the forest that was planted in 1978, under continuous cover forestry after some thinning. The forest itself was established in the 1930s; prior to planting the dominant vegetation was a combination of upland rough pasture and ericaceous moorland. Loblolly pine (*Pinus taeda*) and some deciduous growth is occasionally found at the stand margins. The dominant soil type is a podzolic peaty gley. Harwood stands between 200 and 400 m above sea level, and sees average annual precipitation of 950 mm. The mean annual air temperature is 7.6 °C (Conen *et al.*, 2005). In 2002, soil temperature at 10 cm depth ranged from 3.6 °C to 12.2 °C over the year (Fig. 2.3, Zerva and Mencuccini (2005)).

The soil profile in the stand studied consists of a thick ($\sim$ 2 - 7 cm thick) litter layer, consisting of partially decayed spruce needles, easily separated from a deep and peaty humus horizon (O_i, $\sim$ 5 - 15 cm thick), which is almost black in colour,

spongy and well decomposed with very few plant structures visible to the naked eye. Underneath this is a thick O_e horizon ($\sim$ 10 - 15 cm thick), which is dark brown in colour, denser than the O_i horizon above and contains visible reflective mineral particles. The illuviated mineral A_e horizon underneath this ranges from pale grey or orange to brown in colour. In places the normal order of soil horizons (L, O_i, O_e, A, B) has been inverted (L, O_i, A, O_e, B) due to the ploughing of furrows during afforestation. For this thesis, samples were not taken from any sites with inverted profiles. Descriptions of Harwood forest soil profiles in the literature are inconsistent with respect to the naming of the upper horizons; the horizon descriptions given here are consistent with Swain *et al.* (2010). To avoid confusion, the main horizons studied here (O_i, O_e) will be described hereafter by the sampling depths (5 - 17 cm, 20 - 30 cm).

Figure 2.1: Hemispherical photograph of Harwood forest plots showing contrasting thinned and unthinned forest floor vegetation.

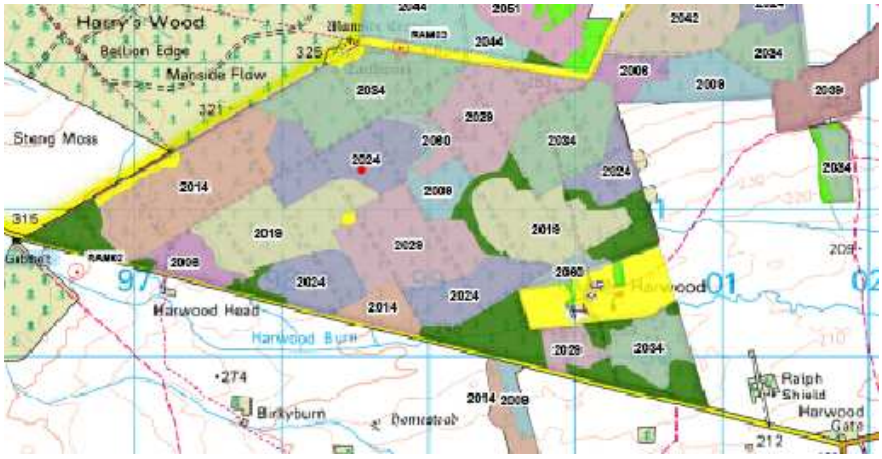

Figure 2.2: Map of Harwood Forest showing planned felling dates. Red dot indicates sampling location.

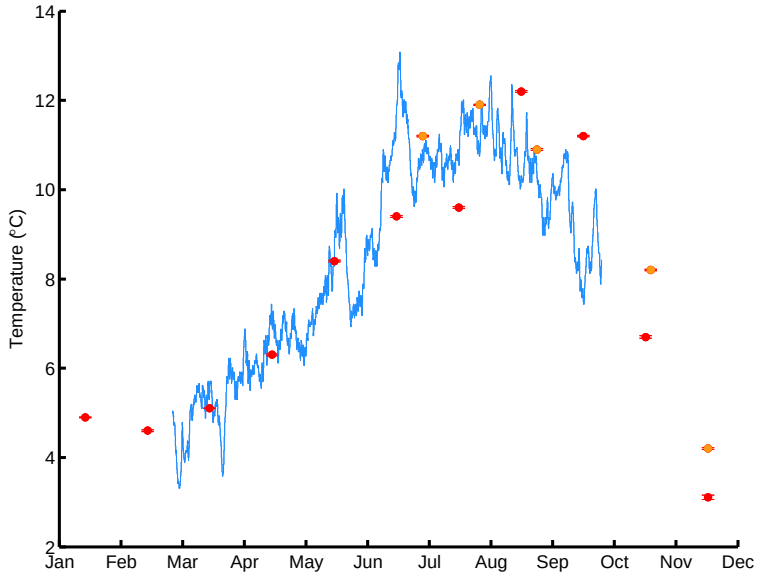

Figure 2.3: Soil temperature at 5 cm depth measured in a 30 year old plot during 2009 (blue line, this study) and at 5 cm depth from a 40 year old stand nearby in Harwood Forest from 2001 (orange points) and 2002 (red points) by Zerva and Mencuccini (2005)

2.1.2 Harwood as a case study for land management impacts on carbon cycling

Harwood forest represents a land management history typical for Northern Britain. Over the twentieth century, around 315,000 ha of peaty gley and peaty ironpan soils, as well as 190,000 ha of deep peatlands, were converted to coniferous forestry, predominantly in the form of Sitka spruce plantations (Cannell *et al.*, 1993). This transition represents the most extensive land-use change experienced in Britain over the last century. Preparation of peaty soils for afforestation involves drainage and physical disturbance, resulting in considerable loss of soil organic carbon protected by anaerobic conditions, to watercourses in DOC and to the atmosphere as CO_2. This may be counterbalanced to an extent by an increased carbon sink in plant biomass and soil organic carbon in the years following afforestation (Zerva and Mencuccini, 2005), depending on management practices during site preparation and harvesting.

Harwood forest is well established as a case study site for the effect of afforestation of peaty gley moorlands on carbon cycling. Mojeremane *et al.* (2012) studied the impacts of site preparation on carbon cycling, comparing three treatments- drainage, mounding and fertilisation. Fertilisation increased soil to atmosphere fluxes of CO_2, CH_4 and N_2O, while drainage caused increased CO_2 emissions and reduced CH_4 emissions, and mounding increased CH_4 but reduced N_2O emissions. The overall impact in CO_2 equivalent was a strong net increase in GHG emissions for fertilisation, a smaller increase for drainage, and a reduction for mounding during the first year only.

While in the early twentieth century, economically unprofitable moorlands gave way to forestry projects, an important economic pressure on upland land use in the early 21st century is wind power. Peatlands tend to be found in upland areas with relatively low population density, in prime position for cheap, efficient and uncontested windfarm developments. However, wind turbine installation also involves

considerable physical disturbance for site preparation and building of access roads. Harwood forest has also been used as a model afforested upland area in a lifecycle assessment of the potential CO_2 'payback time' of windfarm development in upland areas. The payback time of windfarm installation in Harwood forest would be 3 years, rather than 5 months at a site where soil and vegetation disturbance are not an issue (Mitchell and Harrison, 2010).

2.1.3 Harwood forest soil carbon stocks and turnover

Harwood forest soil carbon stocks have been estimated at 21.3 kg C m^{-2}, considerably higher than all other temperate forest sites in the same meta-analysis (Conen *et al.*, 2005). Zerva and Mencuccini (2005) studied sites in and around Harwood forest, using a space-for-time substitution to look at changes in vertical distribution and stocks of soil carbon during successive afforestation, clearfelling and reforestation. During first rotation stand growth, carbon stocks declined in the O_H layer (equivalent to the O_e described here) and accumulated in the O_L (O_i) and A horizons; after clearfelling, carbon stocks declined in both O_L and O_H and continued to accumulate in the A horizon; and during the second rotation of growth, carbon stocks accumulated again in O_L and O_H. These results suggest that after two rotations of forest growth, carbon stocks are restored to that of the unmanaged grassland prior to afforestation.

Ball *et al.* (2011) compared the ^{14}C signatures of SOC and surface CO_2 fluxes in Harwood forest and the surrounding grassland, showing a slightly younger signature for SOC in the forest than the grassland. SOC fixed within the previous year also showed a lower contribution to surface CO_2 fluxes in the forest than in the grassland, consistent with either or both an accumulation of litter in the forest, or increased mineralisation of older SOC. CH_4 and N_2O emissions in Harwood are relatively small, CO_2 emissions make up 93-94 of the total GHG budget in terms of CO_2 equivalent (Ball *et al.*, 2007b).

2.1.4 SOM chemistry

Swain *et al.* (2010) investigated an inverted profile in Harwood forest for C stocks and lignin phenol characteristics. The total lignin yield increased with depth in the organic horizons (O_i -> O_e1 -> O_e2 (buried)), and were still present although in lower quantity in the mineral horizon. High syringyl:guaiacyl and cinnamyl:guaiacyl ratios indicate that the high phenol content of the buried O_e2 horizon is a remnant of pre-afforestation vegetation, rather than fresh input from roots. This suggests that intrinsic chemical recalcitrance of lignin phenols may be important in stabilising OM in Harwood forest on a multi-decadal timescale. However Swain *et al.* (2010) also showed that the acid/aldehyde ratio, a proxy for the oxidative state of guaiacyl phenols, increased with depth, indicating that deeper phenols are also more strongly degraded, suggesting that the enrichment of lignin phenols in the lower horizons has more to do with burial than intrinsic chemical recalcitrance.

2.1.5 Ecosystem flux measurements in Harwood forest

Harwood forest has contributed to understanding of boundary-layer meteorology and ecosystem CO_2 flux estimates by eddy flux measurements, due to the positioning of 3 micrometeorological flux towers in the forest and surrounding grassland (Irvine *et al.*, 1997; Dengel and Grace, 2010). Harwood forest was part of the FORCAST (Forest carbon and nitrogen trajectories) network of European forest research sites in the CARBOEUROFLUX project, contributing to an important interational study on carbon cycling in mineral soils. One such forest site comparison found that the modelled labile fraction in Harwood and other coniferous sites was considerably smaller than that of broadleaf sites (Rey *et al.*, 2008). Leaf area index in Harwood (12 m^2 m^{-1}) was considerably higher than any other forest studied or typical values for Sitka spruce, partly reflecting a variable but moderately high stand density (600 - 3000 trees ha^{-1}) (Rey *et al.*, 2008). These results are contradictory, since high LAI

values are expected to result in a large fine root biomass and hence a large labile SOM fraction.

Chapter 3

Chemical characteristics of Harwood forest soils and soil fractions

3.1 Introduction

The chemical characteristics of SOM fractions with respect to stability has long been an important research area, responding to the demand for measurable characteristics to represent theoretical SOC pools within multi-pool models of soil carbon cycling such as Roth-C or CENTURY (Zimmermann *et al.*, 2007). This research goal can be separated into two aims- firstly, attempts to associate chemical characteristics with OM longevity via particular stabilisation mechanisms, and secondly, attempts to physically separate soil fractions with measurably different indicator characteristics, for the purpose of quantifying SOM under different levels of stability in the field. In the following chapter I will discuss the chemical characteristics associated with different stabilisation mechanisms, the chemical characteristics we can expect of SOM fractions using two common fractionation techniques, and the changing composition

of SOM with depth.

3.1.1 Chemical characteristics of bioavailability

As described in Chapter 1 traditionally SOM stability has been separated into three distinct mechanisms- intrinsic chemical recalcitrance, physical occlusion and association with minerals. Material that is stable as a result of intrinsic chemical recalcitrance by definition has measurable chemical properties that directly confer stability, allowing the possibility of using chemical characteristics as proxy measures for stability. Aggregate occlusion and OM-mineral associations cannot be said to have a direct relation to chemical form, but chemical characterisation still gives indirect insight into the likelihood of aggregate formation or mineral associations, as the strength of OM-mineral or OM-OM association is affected by OM chemical form. The incorporation of SOM into macro-aggregates often involves some degree of microbial processing (Caesar-TonThat *et al.*, 2007) or digestion by macroorganisms such as earthworms (Uvarov and Scheu, 2004), which may result in detectable chemical properties of intra-aggregate SOM and differences between particle size fractions.

Intrinsically recalcitrant SOM

Various chemical characterisation methods are available to determine the intrinsic chemical recalcitrance of organic compounds, based on certain assumptions about what makes a molecular structure recalcitrant to decomposition. Complex irregular polymers such as lignin and polyphenols were traditionally described as intrinsically recalcitrant due to irregular tertiary structure and a lack of consistent active sites for enzymes, and requiring co-metabolism with other substrates with complementary stoichiometry (Jeffries *et al.*, 1981), manifesting in lower mass loss rates than other litter components (Hedges *et al.*, 1985; Haider and Martin, 1975). However, more recent evidence suggests that lignins and other irregular polymers do not necessarily persist in the long term, and that while lignin decomposition is low during the initial

period of rapid mass loss from litter, later on lignin decomposition products are mineralised at least as fast as litter as a whole, becoming an important source of labile DOM (Kalbitz *et al.*, 2006). However, other studies still indicate a low proportion of lignin monomers entering the labile pool after depolymerisation (Feng and Simpson, 2008).

Aliphatic biopolymers such as fatty acids and leaf waxes (cutin from leaves and suberin from roots) can be recalcitrant because of the high energy demand of breakdown (Filley *et al.*, 2008; Prescott, 2008; Feng and Simpson, 2008). Cutin may also be resistant to temperature; Feng *et al.* (2008) used ^{1}H-^{13}C solution-state NMR spectroscopy to show that the cutin content of soil in a heated plot increased after 14 months of +5 °C warming, while both cellulose and, to a lesser extent, lignin-derived methoxy carbon decreased. Since this result was based on a single experimentally heated plot, and the increase in cutin (a leaf wax) was accompanied by an increase in total soil carbon content, more work is required to ascertain whether this result reflects the relative resistence of cutin while other compounds degraded, or a local increase in needle drop. However, older work including litter bag experiments indicated that cutin was not recalcitrant, and degraded at the same rate as bulk soil (Kögel-Knabner *et al.*, 1992).

Organic compounds can be recalcitrant or labile because of nutrient stoichiometry, if element ratios are not in proportion to the needs of decomposers. For example, this is one explanation for the inert behaviour of charcoal, which is high in C but low in H and N. The lignin : N ratio was traditionally considered an indicator of the decomposability of plant litter (Taylor *et al.*, 1989), and similarly the C : N ratio strongly controls rates of carbon mineralisation, which decreases with increasing C:N (Lamparter *et al.*, 2009). Other limiting nutrient concentrations can be expected to affect mineralisation in a similar way.

Well-humified organic material can be more resistant to decomposition, both intrinsically and indirectly via physical stabilisation, because of an increased chance

of forming stable aggregates or mineral associations (Zhang, 1994). Humified OM also takes on intrinsic recalcitrance over the course of successive microbial transformations, as the more intrinsically labile parts of macromolecules are more rapidly mineralised, leaving more recalcitrant materials behind, and shifting the stoichiometry of the remaining material. Microbial processing can also involve polymerisation, potentially increasing the E_a of decomposition reactions.

Aggregate-occluded SOM

While the protection of SOM from decomposition by the physical obstruction of decomposers is essentially stochastic, due to the physical architecture of the soil, certain measurable physical and chemical properties of SOM can increase the chance of incorporation in stable micro-aggregates (Zhang, 1994).

Soil macrofauna such as earthworms and enchaetrids play an important and well-known role in the moderation of soil aggregates by the ingestion, digestion and egestion of SOM. Earthworms in particular are known to selectively ingest mineral matter for the purpose of physical churning of food, contributing to the formation of strong micro-aggregates (Seeber *et al.*, 2006) and putting already humified organic material in contact with mineral surfaces. While earthworm activity is associated with increasing aggregate strength, other macrofauna such as millipedes are known to reduce aggregate stability (Seeber *et al.*, 2006). Mineral chemistry also affects the probability of aggregate formation; soil aggregate stability has been shown to increase with Al and Fe oxide contents (Krull *et al.*, 2003), in particular weakly crystalline ones (D'Angelo *et al.*, 2009).

Mineral-bound SOM

While intrinsic recalcitrance and physical occlusion retard decomposition on short to medium timescales, mineral-OM and metal oxide-OM associations in soils can cause near permanent immobilisation of SOM, and these interactions are considered to be

primarly reponsible for OM stabilisation over timescales of hundreds of years and longer (Marschner *et al.*, 2008; Kögel-Knabner *et al.*, 2008). Leifeld *et al.* (2009) found that along an altitudinal transect where POM longevity was strongly controlled by elevation, the mean residence time of mineral-bound OM was insensitive to elevation but strongly correlated with mineral surface area- indicating that mineral associations trump other environmental variables with respect to stability. OM found in mineral assocations can be intrinsically labile (Kleber *et al.*, 2011); the organic compounds most likely to form successful mineral interactions are those with adhesive properties, such as polysaccharides and hemicelluloses, as well as peptides and humic acids (Grandy *et al.*, 2007; Kaiser and Guggenberger, 2000). Physicochemical properties of the mineral surface also affect the strength of mineral-OM bonds- in particular the surface area, charge density, and degree of hydration. Weakly crystalline minerals typically have a higher surface area and charge density, and so provide more opportunity for SOM stabilisation. Torn *et al.* (1997) suggest that the amount of metal oxides and their crystal form are a controlling factor of SOM stability; in addition, the relative abundance of short range-order minerals significantly reduces C mineralisation (Rasmussen *et al.*, 2008).

Kögel-Knabner *et al.* (2008) identify three functional types of mineral surface sites:

- Surfaces characterised by single coordinated hydroxyl groups (e.g. Fe and Al oxides, allophane, imogolite)
- siloxane surfaces with permanent layer charge (e.g. vermiculite, illite, smectite)
- siloxane surfaces with no layer charge (e.g. talc, pyrophillite, kaolinites)

Kögel-Knabner *et al.* (2008) note that in acidic soils, hydroxylated mineral surfaces are linked to strong protection of SOM, and that Fe oxide stabilisation can be particularly important in soils with podzolic behaviour or gleying. The strength of Fe oxide - SOM interactions is strongly dependent on crystal structure and hydration, as well as redox conditions. Gley soils such as those in Harwood forest are characterised by

patchy and alternating redox conditions; Fe oxides are mobilised as ferrous (Fe^{2+}) ions in reducing patches, and precipitated as ferric (Fe^{3+}) ions in oxidising patches, causing co-precipitation of OM (Kalbitz and Kaiser, 2008).

Harwood forest gley soils (0 – 30 cm depth) were analysed for Al and Fe oxides, and it was found that 5 – 9 % of the total Al and 70 – 100 % of the total Fe present were in the form of Al/Fe oxides (Cloy *et al.*, 2011). The majority of Al oxides were weakly crystalline and the majority of Fe oxides were strongly crystalline, and between 70 and 90 % of the total SOM was associated with either Fe or Al oxides (Cloy *et al.*, 2011).

3.1.2 Fractionation to separate different pools

Particle Size Fractionation

The simplest, most traditional method of separating different functional components of soil is to seive into different particle size classes. Particle size fractionation traditionally separates soil on the basis of soil texture classes- coarse and fine sand, silt and clay. Separation can be done by dry, moist (Stemmer *et al.*, 1998) or wet (Paul *et al.*, 2008b) seiving and is often combined with either density (Six *et al.*, 2002; John *et al.*, 2005) or chemical fractionation (Plante *et al.*, 2010), to further separate some of the fractions. Drying soils before moist or wet seiving strongly affects the yield and distribution of SOC between fractions (Paul *et al.*, 2008b), depending on the mineralogy, as some clays show irreversible flocculation on drying, causing stable microaggregates to form stable macroaggregates.

Some studies have used particle size fractionation to isolate fractions for incubation, to measure rates of soil respiration from different fractions directly (Plante *et al.*, 2010; Leifeld and Fuhrer, 2005; Gartzia-Bengoetxea *et al.*, 2009), while other studies use the chemical properties, isotopic composition (Paul *et al.*, 2008a) and the mass balance (Six *et al.*, 2002) of particle size fractions to make inference about SOM

cycling.

Separated particle size fractions show some consistent trends in chemical properties indicating differences in SOC cycling regardless of soil type- C:N ratios are typically lower in smaller size fractions, reflecting higher microbial transformation in silt and clay fractions (Stemmer *et al.*, 1998; John *et al.*, 2005), although this trend is not universal and is dependent on mineralogy (Paul *et al.*, 2008a). Stemmer *et al.* (1998) measured enzyme activity in particle size fractions of four soils, and found that invertase activity (the enzyme involved in sucrose breakdown) was highest in the silt and clay fractions, whereas xylanase, which is important for hemicellulose degradation, was highest in the coarse and fine sand fractions.

Density Fractionation

While particle size fractionation separates macro-aggregates from micro-aggregates, there may be some cross-over in mineral-stabilised SOM. Material falling into the coarse sand fraction in a particle size separation may be either large particulate SOM or macroaggregates with a high mineral content. Density fractionation typically aims to separate light, un-aggregated and mineral-free material from heavy mineral-bound material and light, occluded material within aggregates. Common high density solutions used to separate density fractions include sodium iodide (NaI) (Sohi *et al.*, 2001), sodium polytungstate (SPT) (Magid *et al.*, 1996; Crow *et al.*, 2007), Ludox (a colloidal silica suspension Magid *et al.* (1996)) or NaCl (Bol *et al.*, 2003). Separation often involves a disaggregation step or a particle size separation. Magid *et al.* (1996) compared different density fractionation procedures and found that large light particles of fresh SOM were retained in the heavy fraction unless a particle size fractionation was performed first. However, this can also be avoided by disrupting the aggregates of the initial heavy fraction before re-fractionating (Sohi *et al.*, 2001).

Depending on the density of the separation medium, light particulate material is usually found to comprise of fresh, recently decomposed plant material, and

recently-added litter is predominantly retained in this fraction Magid *et al.* (1996). Light material released after disaggregation (intra-aggregate material) is often shown to be more humified and older than light material, with a lower C:N ratio (John *et al.*, 2005) and a higher O-alkyl-C : Alkyl-C ratio. Heavy fractions comprise OM in association with soil minerals, and usually but not always (Crow *et al.*, 2007) older than bulk or light fraction C (Bol *et al.*, 2003), with lower C:N content than light or occluded light material (John *et al.*, 2005; Sollins *et al.*, 2006) and lower SOC. Mineral-bound material may be high in chemically labile components such as polysaccharides and peptides (Grandy *et al.*, 2007).

The proportion of SOC found in the intra-aggregate fraction of the scheme described in Sohi *et al.* (2001) has been proposed as a possible indicator measure for changing SOC stocks- soils that had recently undergone land management changes had a higher proportion of SOC in the intra-aggregate fraction (Sohi *et al.*, 2010). However, this indicator does not predict the direction of change to SOC stocks, as the intra-aggregate portion seems to increase regardless of whether total C stocks rise or fall.

Chemical fractionation

Acid (HF, HCl, and NaOCl) resistant fractions are often used to indicate intrinsically recalcitrant OM, on the basis that compounds with a complex molecular structure and high E_a are the most resistant to chemical oxidation. However this is complicated by the action of mineral associations in providing resistance to chemical oxidation to thermally labile compounds. Sleutel *et al.* (2009) found that intrinsically 'labile' materials such as carbohydrates, peptides and short-chain lipids are protected from NaOCl treatment in mineral associations and aggregate structures, just as they would be protected from biological attack.

Aims

I characterised bulk soils from different depths, SOM density fractions (see Figure 3.2) and particle size fractions (see Figure 3.1) from Harwood Forest (see section 2.1.1) using a number of chemical and physical techniques, all with the aim of assessing chemical and physical factors contributing to the overall longevity of SOM. I intended to investigate how relevant the fractions separated by particle size and density fractionation are to the fast, slow and passive SOC turnover pools used in models of SOC cycling, and which mechanisms of stability apply to each fraction. I hypothesise that intra-aggregate material will be well humified, and SOM in 20 - 30 cm whole soil will be strongly stabilised by mineral associations.

3.2 Methods

Sampling strategy

Full soil profile samples Samples for soil profile C and N contents and FTIR (Section 3.3.1) were collected from five semi-random locations in Harwood forest, using a 2 cm diameter corer, in April 2008. Each sample was separated in situ into five horizons: litter, O_i, O_e, A and B horizons.

O_i horizon particle size fractionation samples Soil samples for fractionation by particle size according to Stemmer *et al.* (1998) (Section 3.2.1) were collected from Harwood forest in June 2008, using a spade to collect a 10 cm x 10 cm x 10 cm block from two sites. These soils were fractionated and analysed for key chemical characteristics, as a preliminary test to assess the suitability of this fractionation scheme for isolating stable and labile organic carbon forms. This method separates soil into coarse (> 2000 μm) and fine (> 200 μm) sand fractions, silt (> 63 μm) and clay (< 63 μm) fractions, by wet seiving after low-energy sonication to disaggregate macroaggregates. I present data from particle size fractions disaggregated by sonication at 25, 100 and 300 J g^{-1}.

O_i horizon density fractionation samples Samples for density fractionation and for chemical analysis of fractions (used subsequently for incubation and isotopic analysis of separate fractions and whole soils, Chapters 4 – 5) were taken from four equally spaced points in a square around the base of the eddy flux tower. Each pit was 15 m from a corner of the tower. Samples were taken by digging a small pit, removing the litter layer (0 - 5 cm) and coarse roots, and collecting material ~ 1 kg from the O_i horizon (~5 - 17 cm) with a trowell. Each whole soil sample was seived at 5 mm, and two pairs of samples were combined by gentle rotation in a cylindrical tub for 2 minutes, forming two composite samples as recommended by Robertson *et al.* (1999).

Each of the two composites, hereafter named A and B, originated from two of the four sampling points.

Whole soils from the O_e horizon (20 - 30 cm) were collected from near the same four sites and composited by the same rationale in January and December 2009, and these samples were used for comparison with the density fractions in subsequent experiments (see also Chapters 4 and 5).

3.2.1 Particle Size Fractionation

Section 3.3.2 describes results using a SOM particle size fractionation procedure adapted from Stemmer *et al.* (1998). Field moist whole soil from 5 - 17 cm depth was dispersed in distilled water and ultrasonicated at 50 J g^{-1} before wet seiving at 2000 μm, 125 μm, and 53 μm, yielding a coarse sand fraction (150 - 2000 μm) and a fine sand fraction (53 - 150 μm). Throughflow smaller than 53 μm was centrifuged at 150 x g for 2 minutes. The supernatant was retained and the pellet was resuspended in distilled water; this centrifugation step was repeated three times to separate a silt fraction (pellet) free of clay particles (supernatant). The supernatants from this step were then centrifuged at 3900 x g for 30 minutes to separate the clay fraction (pellet) from soluble sugars (supernatant). After this step the pellet was resuspended and the process repeated once.

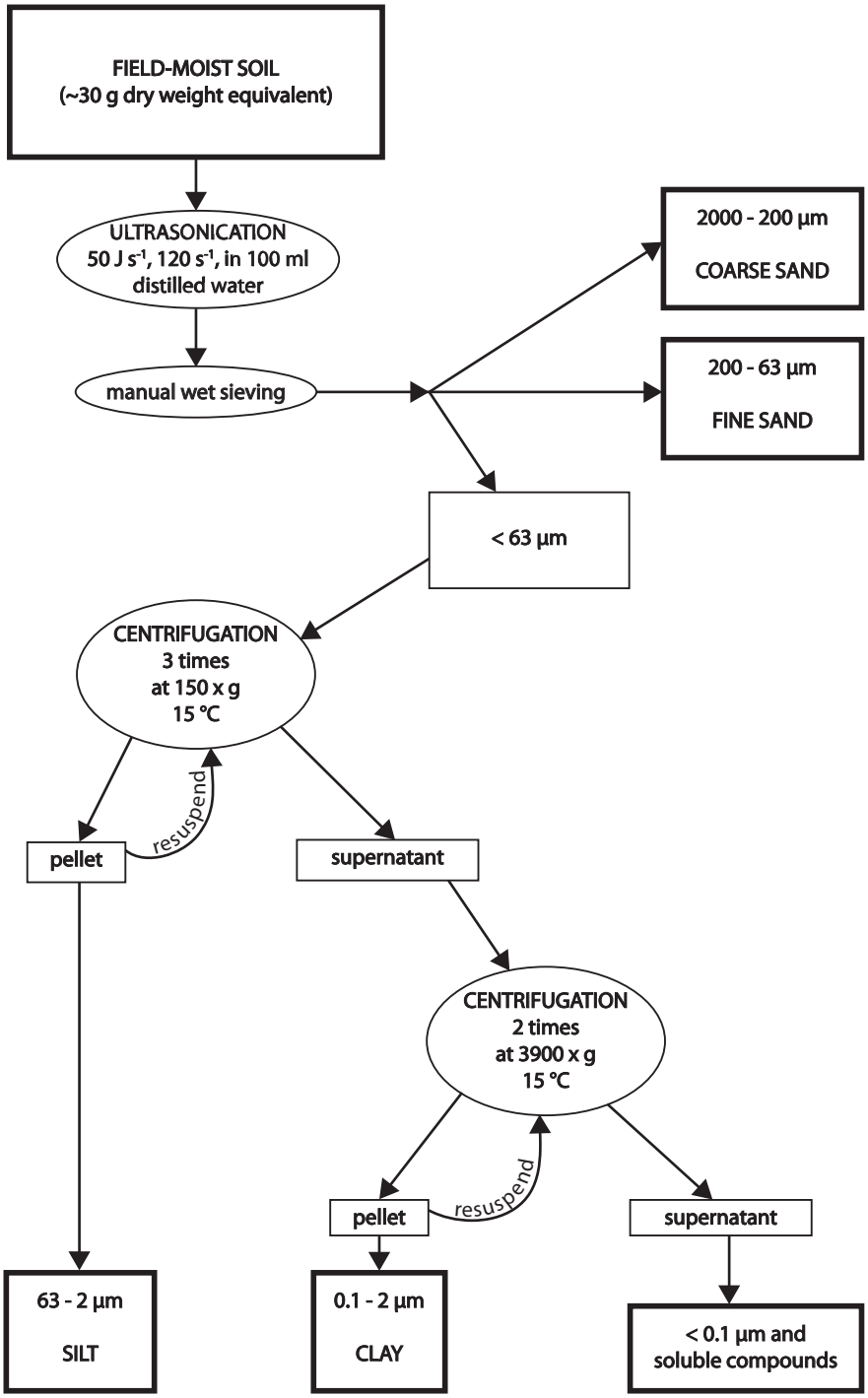

Figure 3.1: Diagram of particle size fractionation method taken from Stemmer *et al.* (1998)

3.2.2 Density fractionation

Field moist whole soil from 5 - 17 cm was floated in a 12M NaI_{aq} solution, with a density of 1.8 g cm^{-3} at room temperature. Samples were mixed by inversion for 30 seconds then centrifuged at 8000 x g for 30 minutes. SOM suspended in the supernatant or floating on top was designated 'light' material, and was filtered at 0.45 μm on Whatman GF/A glass microfibre filter paper, using a micropore filtration system, and rinsed thoroughly with deionised water. The pellet was then resuspended in NaI solution by shaking, and the resulting solution was ultrasonicated using an ultrasonic probe (Misonix, NY USA) at 25 J ml^{-1} over ice. The centrifugation step was then repeated again. Material in the supernatant was designated 'Intra-aggregate' material, and the remaining pellet 'Mineral-bound'. Both the decanted supernatant and the pellet (resuspended in deionised water) were then filtered at 0.45 μm and rinsed thoroughly before all three fractions were dried at 40 °C. NaI solution was recycled between runs by stirring with activated charcoal for one hour and filtering. These fractions are operationally defined, and the pool sizes are strongly affected by the choice of solution density and sonication energy, which were chosen to represent the most functionally relevant separation of aggregates and of bond strength within aggregates (Sohi *et al.*, 2001).

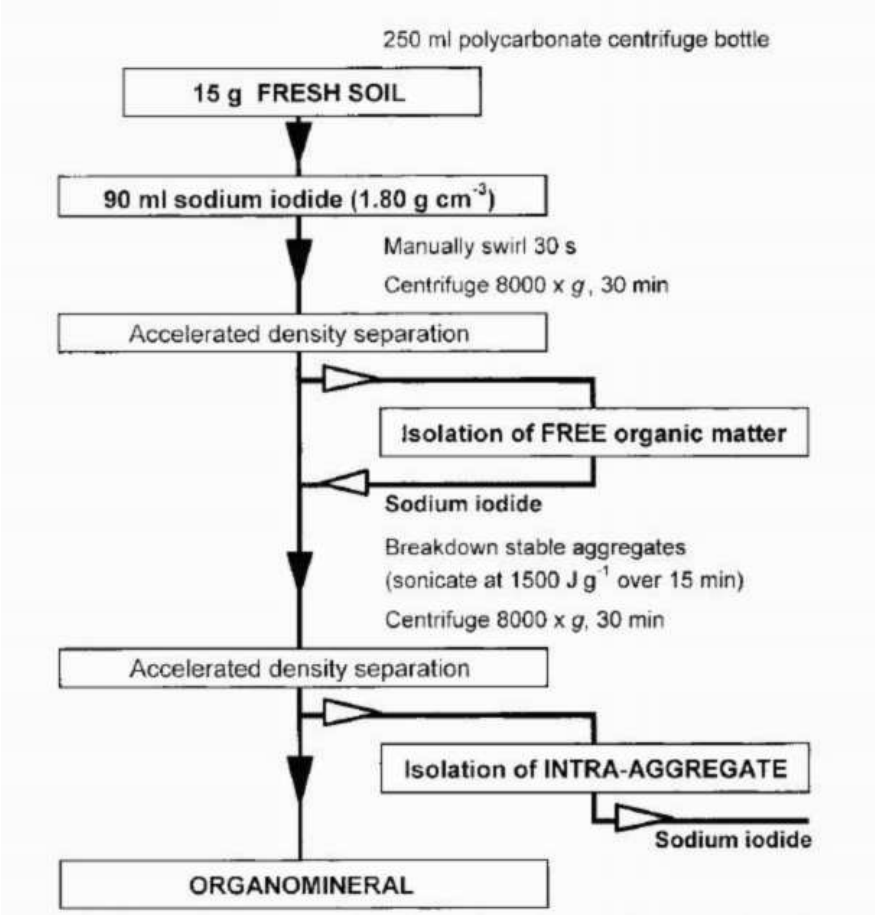

Figure 3.2: Diagram of density fractionation method taken from Sohi *et al.* (2001)

3.2.3 Moisture, ash and OM contents, and pH

The moisture content of field-moist whole soil samples was determined by drying overnight in a 105 °C drying oven. Subsamples ($\sim$ 1 g) were accurately weighed out into pre-dried, pre-weighed Pyrex beakers at room temperature, dried for at least 12 hours, and allowed to cool to room temperature in a dessicator before reweighing. Moisture content (weight %) was determined using the formula:

$$\text{Moisture content (\%)} = \frac{(\text{mass of field-moist soil} - \text{mass of dry soil})\ x\ 100}{\text{mass of field-moist soil}} \quad (3.1)$$

Ash and OM content of dry soil was determined by the loss on ignition method. Subsamples of dry soil were accurately weighed out into pre-dried, pre-weighed Pyrex beakers at room temperature, and heated to 450 °C for four hours in a muffle furnace. Samples were allowed to cool to room temperature in a dessicator before reweighing. OM content (% dry mass) is given by the formula:

$$\text{Organic matter content (\%)} = \frac{(\text{mass of dry soil} - \text{mass of residual ash})\ x\ 100}{\text{mass of dry soil}} \quad (3.2)$$

Ash content (% dry mass) was defined as the mass remaining after ashing, equivalent to 100 - organic matter content (%):

$$\text{Ash content (\%)} = \frac{\text{mass of residual ash}\ x\ 100}{\text{mass of dry soil}} \quad (3.3)$$

pH was measured by mixing 10 g soil into a slurry with 10 ml de-ionized water and leaving to stand for one minute before testing with a pH meter.

3.2.4 Carbon and nitrogen contents

SOM samples were analysed for C and N contents using a Carlo-Erba NA 2500 elemental analyser (Carlo-Erba, Milan, Italy). In addition, carbon and nitrogen isotopic composition ($\delta^{13}C$ and $\delta^{15}N$) was analysed for some SOM samples by mass spectroscopy (VG PRISM III mass spectrometer, Manchester UK). Samples were dried as for determination of moisture content (see above), ground finely either by hand in a ceramic mortar and pestle or an automated ball mill (Retsch mixer mill 400, Retsch, Haan, Germany), weighed into ultraclean tin capsules in subsamples of 8 - 20 mg, and analysed. Total soil C was assumed to be equal to total organic carbon as Harwood forest parent material is not calcareous (Zerva *et al.*, 2005). In some cases only one replicate from each sample was analysed. C and N analysis of SOM density fractions and whole soils used in the incubations described in Chapter 4 were analysed

on the Carlo-Erba elemental analyser in triplicate for quality control. The mean standard error of C content for these samples was 0.93 %, and the mean standard error of N contents was 0.04 %. These values can be used as a proxy for the analytical precision of other measurements taken by the same machine.

3.2.5 FTIR

Infra-red spectroscopy provides information about the chemical composition of organic compounds, using the absorption properties of CH_2 groups with different vibrational structure (stretching, scissoring, rocking, wagging and twisting) to characterise the contribution of different organic functional groups to the total OM. A Michelson interferometer enables scanning of a wide range of wavelengths, and the discrete raw data are converted to spectra by a Fourier transform algorithm. Quantitative applications of spectra are limited, but is nevertheless a useful tool for qualitative comparison of the relative abundance of OM functional groups.

Dry ground soil samples were mixed 1:100 by mass with KBr crystals, and ground into a fine powder. 100 mg of the mixture was pressed into a pellet using a flat die pellet mill. Three pellets were analysed from each sample. The pellets were analysed on a Jasco FT/IT-460 Plus (Easton MD, USA) and the spectra were processed using Spectra Manager II.

For density fraction and whole soil (20 - 30 cm) samples, samples were analysed before and after ashing to remove OM content, to remove interference from the mineral matrix. After analysis of unashed samples the pellets were recovered, placed in an ashing furnace at 450 °C overnight, ground, pressed and reanalysed, to obtain the FTIR spectra for the inorganic component of the same samples. Several other studies have used the FTIR spectra of ashed soil samples to separate the OM spectra (Kaiser *et al.*, 2011; Chefetz *et al.*, 1998; Cox *et al.*, 2000b). Kaiser *et al.* (2007) compare the effects of 500, 700 and 900 °C heating on the mineral structure, and based on their results a 450 °C treatment is not likely to have caused significant distortion of the

mineral structure.

3.2.6 ^{13}C CP-MAS NMR

NMR spectroscopy provides information about molecular structure via the absorption of electromagnetic radiation. ^{13}C NMR exploits the nuclear spin of ^{13}C atoms, which give a different chemical shift signal depending on the electron density surrounding each ^{13}C atom. Because ^{13}C atoms comprise only around 1.1 % of the total C, the chance of ^{13}C atoms occuring so close together as to interfere with the chemical shift causing signal splitting is very small. This property of ^{13}C NMR means that relatively clean spectra can be produced even from complex solid state samples, providing information about molecular structure with minimal destruction. Cross-polarisation transfers excitation energy from nearby protons to the measured ^{13}C, using Hartmann-Hahn matching. By exciting ^{13}C atoms indirectly via the more abundant protons rather than directly, a stronger signal can be produced. Spinning of the sample at the 'magic angle' of 54.74 ° to the field direction during analysis increases the resolution of the resulting spectra, narrowing the otherwise broad peaks.

Solid-state NMR was performed on Harwood forest density fraction and whole soil samples at the University of Durham, EPSRC NMR facility. The spectrometer frequency was 100.562 MHz, contact time 1 ms, relaxation time 1 s, and spin-rate 6800 Hz. The total number of scans taken for each spectra was between 3248 and 25000. The number of scans per sample was optimised to give the best resolution available for each sample, but was capped at 25000 (for 20 - 30 cm whole soil and mineral-bound fractions) for time and cost reasons.

3.2.7 TGA

Thermo-gravimetric analysis was performed at the University of St Andrews, School of Chemistry, on a Netzsch STA 449C (Selb, Germany). Samples were packed into Al_2O_3 crucibles and heated from 35 to 650 °C, increasing at a rate of 10 °C min^{-1}, in

an argon atmosphere. The decreasing mass of the sample was measured every 0.025 min.

3.2.8 ICP-OES

Density fractions, whole soils from 5 - 17 cm and 20 - 30 cm and DOM extracted on a separate occasion (see section 4.3.1) were analysed for trace metal contents using a Perkin Elmer Optima 5300 DV ICP-OES (Perkin Elmer, Beaconsfield UK), equipped with a gem-cone cross-flow nebuliser, following a HF-HNO_3 microwave digestion adapted from a modified US EPA Method 3052 Protocol (Yafa and Farmer, 2006). Samples were dried and ash content estimated (see section 3.2.3); subsamples $\sim$ 0.25 g) were microwave-digested in 48 % HF (Aristar grade). The digest solutions were reduced to $\sim$1 ml on a hotplate and made up to 25 ml with 2 % v/v HNO_3 (Aristar grade, 69 %) before analysis. Analytical precision for metal concentrations on the ICP-OES is typically $\leq$ 5 % (Cloy *et al.*, 2008).

3.2.9 Statistical analyses

All statistical analyses were performed using MATLAB version R2009a, statistical toolbox. One-way and two-way ANOVAs were used to test for differences in chemical properties between fractions and depths (Chapter 3).

3.3 Results

3.3.1 Soil horizons

C and N content

OM content and C and N contents declined down the soil profile as expected (Fig. 3.3), and in a stepwise fashion reflecting the differences in horizons (L, O_i, O_e, A, and B); OM content and C and N drop rapidly after the transition to the B horizon, which is distinctly paler in colour. Below the top two horizons, the C:N ratio increased close to linearly with depth.

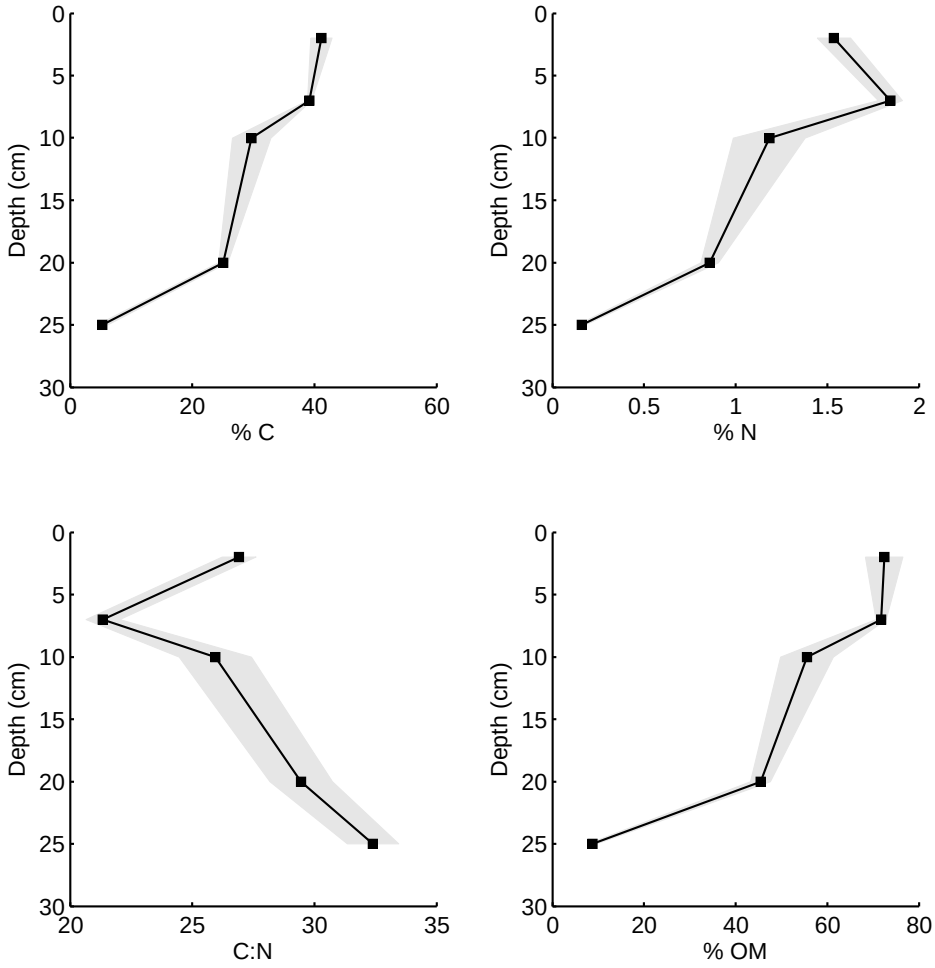

Figure 3.3: Elemental composition and ratios and OM content of whole soil from five horizons. Squares represent the mean (n = 5) and grey shaded areas represent $\pm$ 1 SE

FTIR

FTIR spectroscopy revealed small differences in chemical composition between horizons. Because it is not possible to quantify these differences, the results from one representative replicate of each profile are shown here, for simplicity.

The region below $\sim$ 1100 cm $^{-1}$ reflects soil minerals; these are understandably highest in the mineral horizons (A1, A2e and B, see also Fig. 3.3) although in the leached A2e layer this peak region is not very pronounced. The double peak region around 2900 cm $^{-1}$ is an indication of aliphatic -CH, -CH_2 and -CH_3 groups. There is only a very weak signal in this region in the litter layer, with stronger peaks in the A1 and B horizons and moderate peaks in the O horizon and leached A2e horizon. Peaks in the region around 1600 cm $^{-1}$ and 1700 cm $^{-1}$ are indicative of ketone groups and carboxyl groups, respectively. The ratio of ketone : carboxyl moieties seems to increase with depth from the organic horizon downwards, but is also high in the litter.

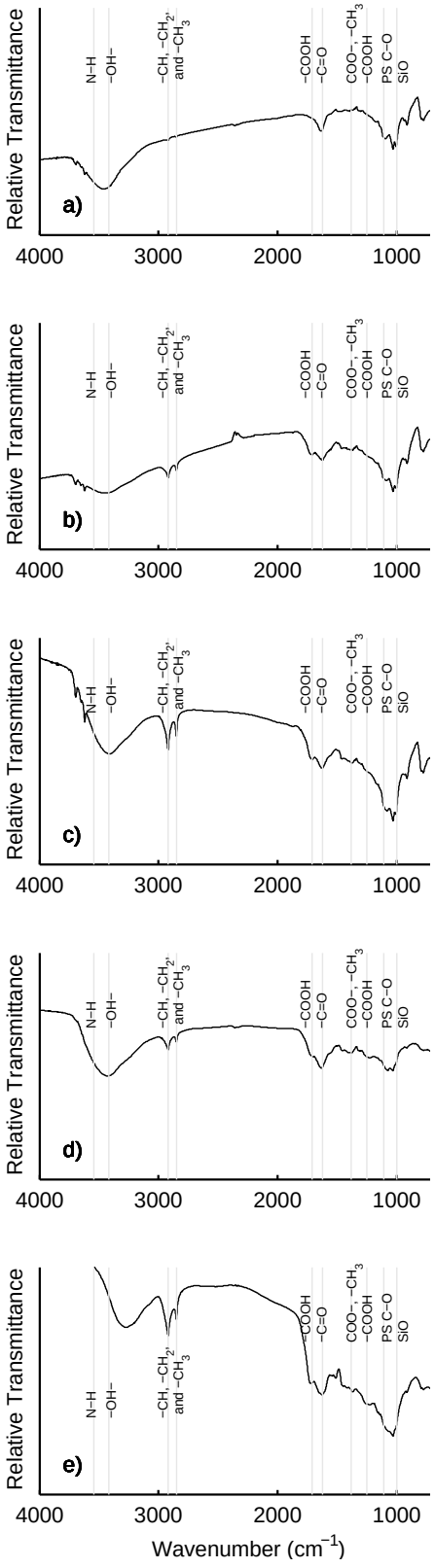

Figure 3.4: Fourier Transform Infrared spectroscopy of whole soil from different horizons: a) Litter (2 cm) b) Organic horizon (7 cm) c) A1 mineral horizon (10 cm) d) A2e leached mineral horizon (20 cm) e) B mineral horizon (25 cm).

pH

Whole soil material taken from the O horizon (5 - 17 cm) in four locations for fractionation and subsequent incubations had a mean pH of 4.4 $\pm$ 0.1 (n = 4, 95% C.I. 4.1 - 4.9). The four samples were combined and composited such that the mean pH of composite A was 4.5 (4.3, 4.7) and composite B was 4.3 (4.2, 4.5). These values are within the typical range of a peaty soil, although less acidic than previous measurements in Harwood forest (Ball *et al.* (2007b) found a pH of 3.6 in a 30 year old stand.) As Leifeld *et al.* (2008) discuss, the effect of pH in acid forest soils can counteract the intrinsic lability of the 'light' fraction, which should be taken into account. pH values for isolated fractions were not measured in this case as the pH was expected to be distorted by the fractionation process.

3.3.2 SOM particle size fractions

C, N and OM contents

For coarse, fine, and silt fractions, both C and N contents (and by extension OM content) decreased with decreasing particle size, while the clay size fraction was high in both C and N in relation to the other fractions. This finding matches Stemmer *et al.* (1998)'s original observation that C and N were both highest in the clay fraction. In common with Stemmer *et al.* (1998), I found that C:N ratios also decrease with decreasing particle size, with the exception of the coarse sand fraction which had a lower C:N ratio than the fine sand. This general relationship may be a reflection of high C:N ratios in undecomposed structural carbohydrates in the sand fractions combined with more microbial transformations in the silt and clay contributing to their breakdown into smaller particles. Leifeld and Fuhrer (2005) meanwhile found no consistent differences in C:N between < 63 μm and > 63 μm size fractions (clay and other) in an arable field and a grassland.

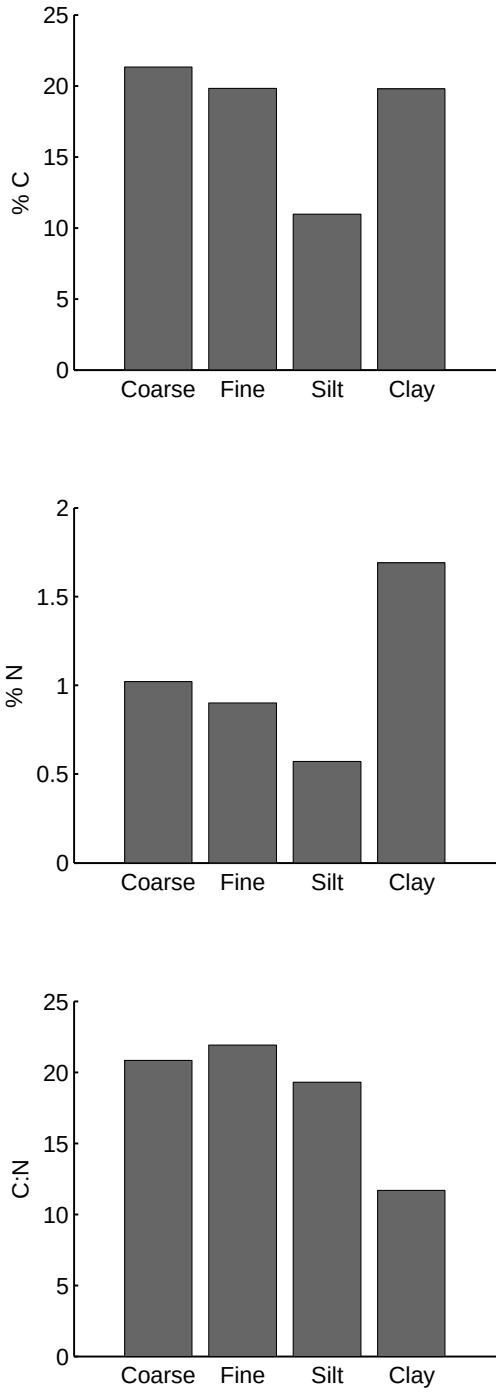

Figure 3.5: Carbon and nitrogen content and C:N ratio of SOM particle size fractions, disaggregated by ultrasonication at 25 J g $^{-1}$

FTIR

I compared particle size fractions disaggregated at low (25 J g $^{-1}$) and high (300 J g $^{-1}$) sonication energies. The choice of sonication energy affects the fraction yield. A higher sonication energy can be expected to cause a decrease in the coarse sand fraction and an increase in silt and clay as more moderately stable microaggregates are dispersed. However, whether material from these microaggregates should be considered as whole microaggregates in the larger size fraction, or dispersed intra-aggregate material in the smaller size fraction, is an arbitrary decision.

The clearest effect of the higher sonication energy is a softening of peaks in the mineral matrix absorption region (< 1100 cm $^{-1}$) in all fractions (Fig. 3.6, e-h). This may indicate that mineral structures were disrupted by the high sonication energy, in which case it is likely that organic structures were similarly distorted by this process, for example losing mineral associations, and tertiary and quaternary structure of macromolecules.

The clay fraction separated at 25 J g $^{-1}$ (Fig. 3.6 c) showed a strong distinctive peak at around 1350 cm $^{-1}$ which was not present in any other fraction, indicating COO- and -CH_3 groups.

The polysaccharide C-O band occuring at 1150 cm $^{-1}$ should be interpreted with caution as the strength of absorption can be affected by the adjacent Si-O peak which marks the beginning of a region dominated by the mineral matrix. However, comparison of these regions in the 25 J g $^{-1}$ fractions (Fig. 3.6 a-d) indicates that polysaccharides are higher in silt than clay, and higher in coarse sand than in fine sand. The higher concentration of polysaccharides in the silt fraction may reflect the high affinity of sugars for mineral surfaces (Guggenberger *et al.*, 1994), since the silt fraction has the lowest OM content (Fig. 3.5) and the high polysaccharides in the coarse fraction may reflect a higher proportion of intact plant material in comparison with the fine fraction.

Our results seem to show slightly higher aliphatic peaks ($\sim$ 2900 cm $^{-1}$) in the silt fraction, which also had the highest mineral content. COOH groups indicated by the band at around 1750 cm $^{-1}$ seem to be higher in the clay fraction than the other fractions, although the adjacent ketone groups are of a comparable size in all fractions.

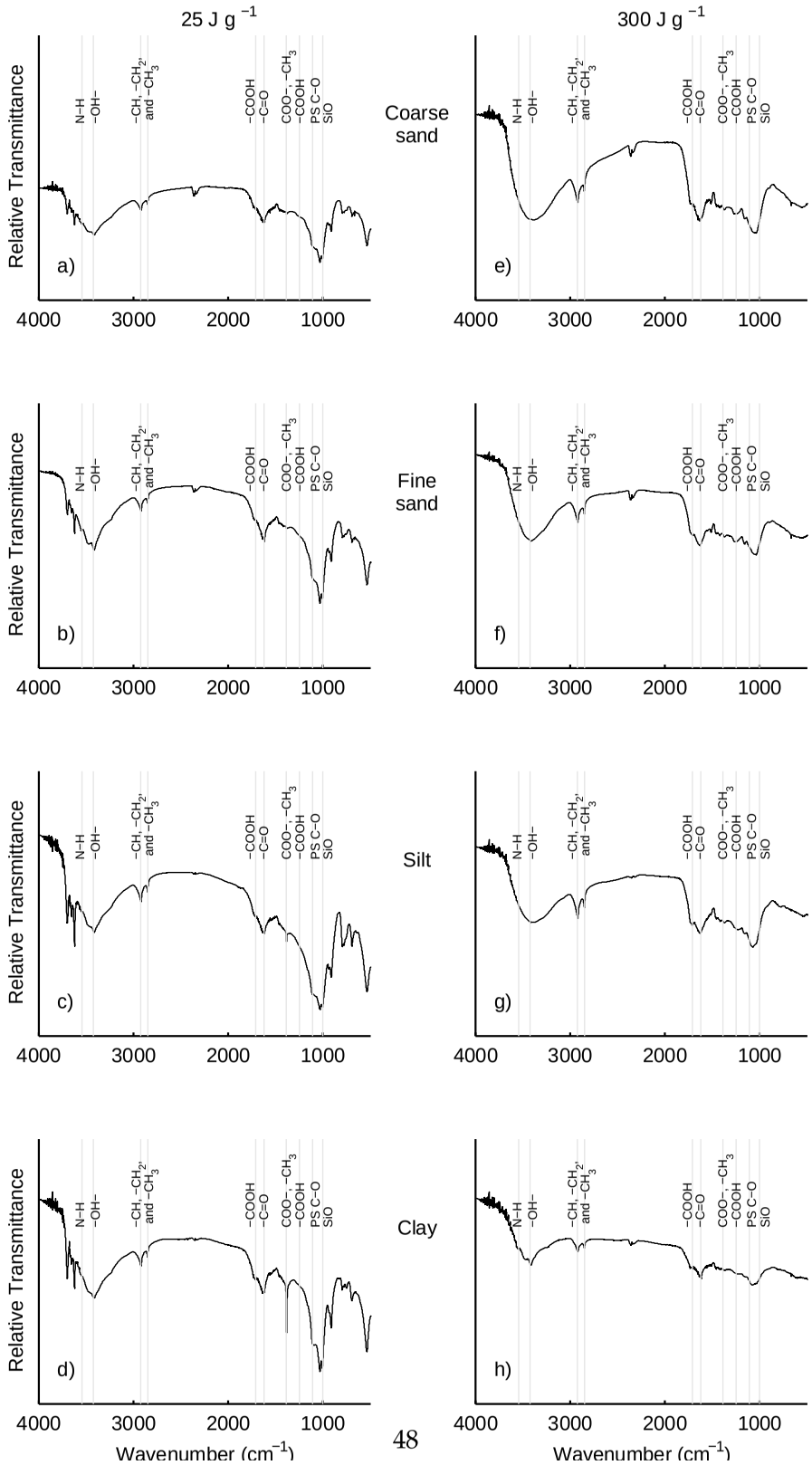
25 J g −1
300 J g −1
Relative Transmittance
Coarse sand
Fine sand
Silt
Clay
a)
b)
c)
d)
e)
f)
g)
h)
N–H
–OH–
–CH, –CH2, and –CH3
–COOH
–C=O
COO–, –CH3
–COOH
P S C–O
SiO
4000
3000
2000
1000
Wavenumber (cm−1)

Figure 3.6: Fourier Transform Infra-red spectroscopy of SOM particle size fractions, disaggregated by ultrasonication at either 25 J g^{-1} (a-d) or 300 J g^{-1} (e-h)

3.3.3 SOM density fractions and whole soils

This section presents the chemical characteristics of density fractions (See section 3.2.2 and Sohi *et al.* (2001)), from 5 - 17 cm Harwood forest soil. These fractions were subsequently incubated (see Chapter 4) and analysed for isotopic composition (see Chapter 5) alongside their parent whole soils and whole soils from the same sites at 20 - 30 cm. For comparison, the chemical characteristics of these whole soils will also be presented here alongside those of the SOM fractions.

C, N and OM contents

Carbon contents were higher in the light and intra-aggregate fraction SOM than in mineral bound material. At 5 - 17 cm, C:N ratios were consistently higher in the intra-aggregate and mineral-bound fractions than light fraction or whole soil (Table 3.7). In addition, C:N ratios were considerably higher in the 20 - 30 cm whole soil than 5 - 17 cm whole soil (Fig. 3.7), consistent with earlier results from the full profile (Fig. 3.3)

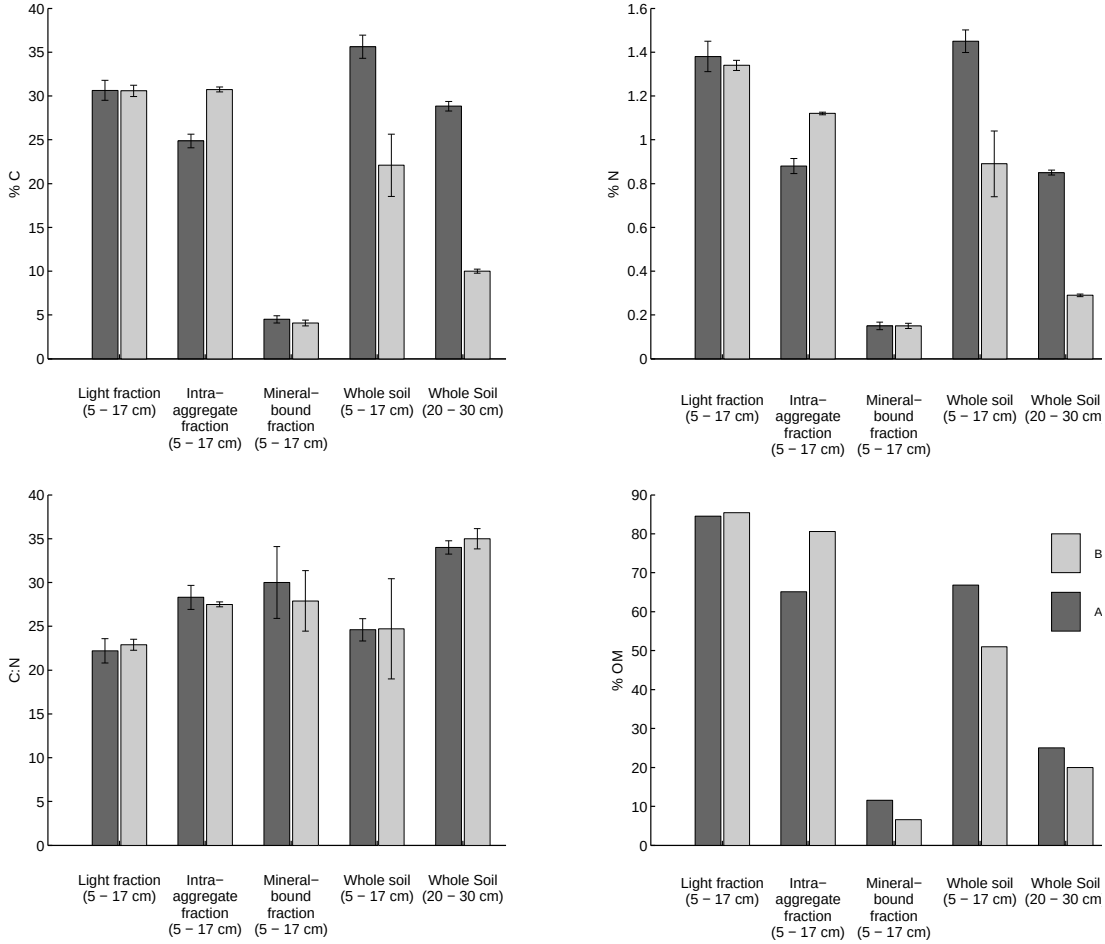

Figure 3.7: Carbon and nitrogen content and C:N ratio of SOM density fractions. Error bars (C, N and C:N) refer to 1 S.E. (n = 3)

Fraction mass balance

Using mass balance calculations I estimate that for both A and B composites, approximately 82 % of total soil carbon was found in the light fraction, 12 % in the intra-aggregate fraction and 6 % in the mineral-bound fraction. Only small amounts of DOC were lost during fractionation.

FTIR

The FTIR spectra of the fractions and whole mineral soil (Fig. 3.8) showed four important absorption band regions. Absorption bands for alcohol, phenol and water O-H groups (3300 - 3400 cm^{-1}) were particularly strong in the 5 - 17 cm fractions. Absorption bands for aliphatic CH, CH_2 and CH_3 groups (2850 - 2960 cm^{-1}) and for amide C=O, aromatic C=C, and N-H groups ($\sim$ 1590 cm^{-1}) were smaller in the 20 - 30 cm whole soil, relative to the fractions.

Strong absorption bands for polysaccharide C-O groups (1030 - 1170 cm^{-1}) and/or Si-O bonds of soil minerals (1000 - 1100 cm^{-1}) were apparent in all samples. Comparing the spectra from unashed and ashed samples (Fig. 3.8) it appears that a portion of the absorption in this region in the light and intra-aggregate fractions is attributable to polysaccharides. In the 5 - 17 cm mineral-bound fraction and 20 - 30 cm samples, polysaccharide groups are likely to be masked by the mineral matrix Si-O groups. Bands in the region of 3695 cm^{-1} are likely to represent kaolinite surface hydroxyl groups. This is the only region for which relative absorption was always higher in the spectra of ashed samples, because after ashing the inorganic material is a higher proportion of the overall mass. The ratio of aliphatic : aromatic peaks (2900 and 1630 cm^{-1} respectively) is lowest in the mineral-bound fraction, despite a high mineral content. This suggests that although kaolinite - aliphatic C interactions are an important source of mineral-OM stability in many soils, they are not in this case.

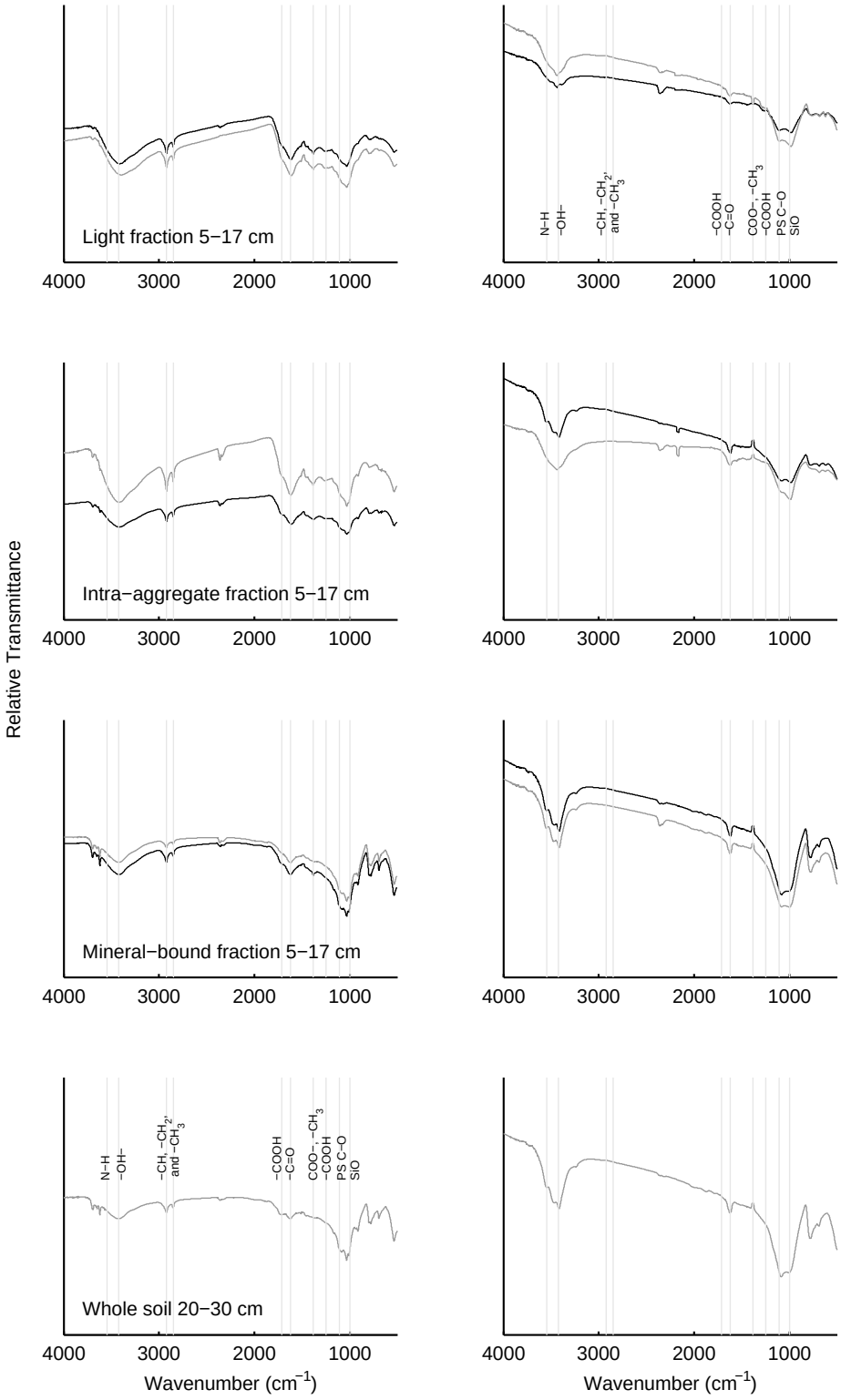
Relative Transmittance
Light fraction 5−17 cm
Intra−aggregate fraction 5−17 cm
Mineral−bound fraction 5−17 cm
Whole soil 20−30 cm
N−H
−OH−
−CH, −CH2− and −CH3
−COOH
−C=O
COO−, −CH3
−COOH
PS C−O
SiO
4000
3000
2000
1000
Wavenumber (cm−1)

Figure 3.8: Fourier Transform Infra-red spectroscopy of whole soil and SOM density fractions (left) and mineral residue from the same samples after ashing (right). Black lines show composite A, grey lines composite B.

^{13}C CP-MAS NMR Spectroscopy

Alkyl and O/N-alkyl groups were dominant in all fractions and whole soils (Figs. 3.9 and 3.10). Alkyl-C compounds formed a greater proportion of total C in 20 - 30 cm soils than all 5 - 17 cm samples (ANOVA, $p < 0.05$). Within the 5 - 17 cm samples, the alkyl-C component was lowest in the light fraction. The dominant alkyl peak at 30 ppm includes two distinct sub-peaks, which to my knowledge have not been described elsewhere. In both composites, the peak to the right is more prominent in the 20 - 30 cm whole soil, while the peak on the left is larger in the 5 - 17 cm whole soil, although lower in all 5 - 17 cm fractions. More work is clearly required to identify the source of these peaks, but I tentatively suggest that they could simplistically be explained as suberin- and cutin-derived components, since the 20 - 30 cm horizon is likely to be higher in suberin from root sloughing and the 5 - 17 cm soil is likely to be higher in undecomposed cutin. Alternatively, the left-hand peak may be a water-soluble sugar that was lost from the fractions during flotation.

The alkyl-C:O-alkyl-C ratio was higher in the 20 - 30 cm soils than in any of the 5 - 17 cm samples (Fig. 3.11), and amongst the fractions of 5 - 17 cm soil the ratio was around double in the intra-aggregate fraction, and lowest in the light fraction, consistent with other findings from a different soil type (Sohi *et al.*, 2001). A high alkyl-C : O-alkyl C ratio is an indicator of humified or microbially transformed SOM; this ratio is shown to increase over time in freshly added leaf litter (Webster *et al.*, 2000). Within each category the ratio was higher for composite A than for composite B, but the relationship between categories was consistent for both composites. Later results provide a convincing explanation for the difference between replicates (see section 5.2.4).

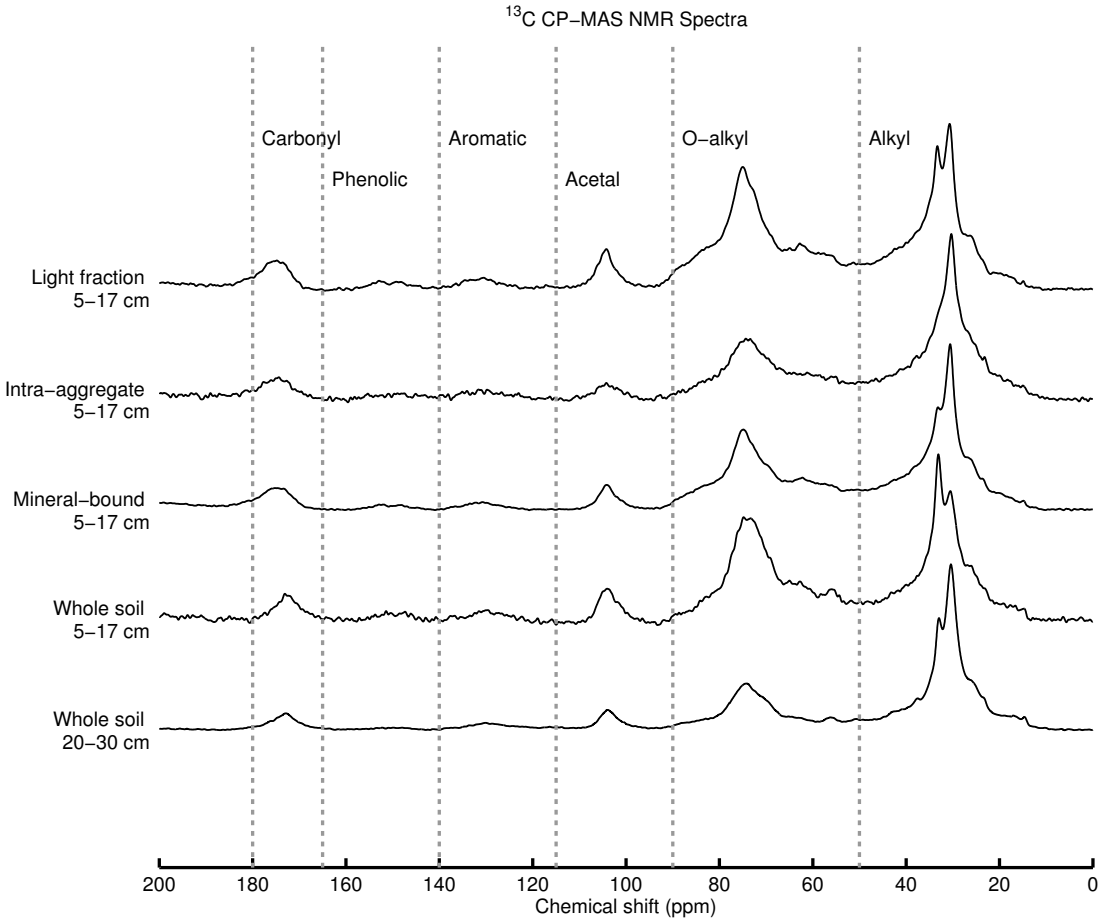

Figure 3.9: ^{13}C CP-MAS NMR spectroscopy for composite A density fraction and whole soil samples.

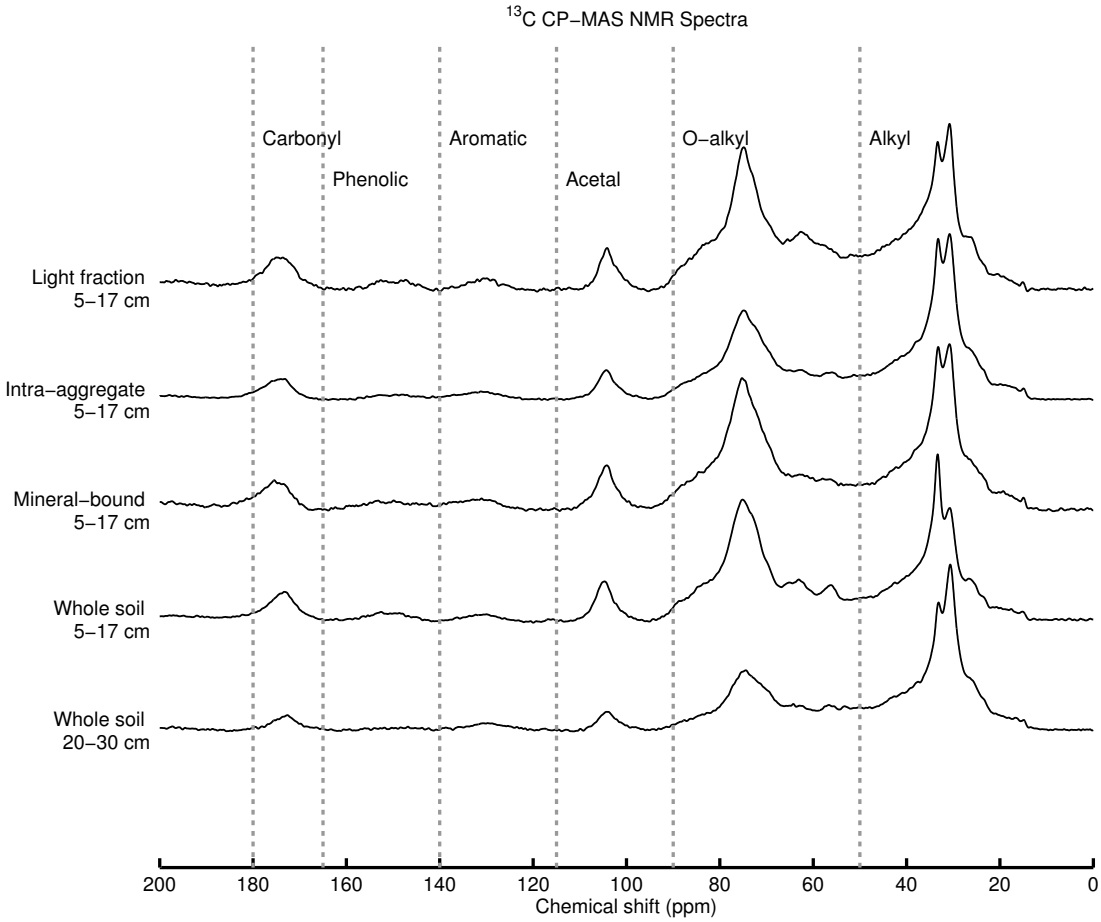

Figure 3.10: ^{13}C CP-MAS NMR spectroscopy for composite B density fraction and whole soil samples.

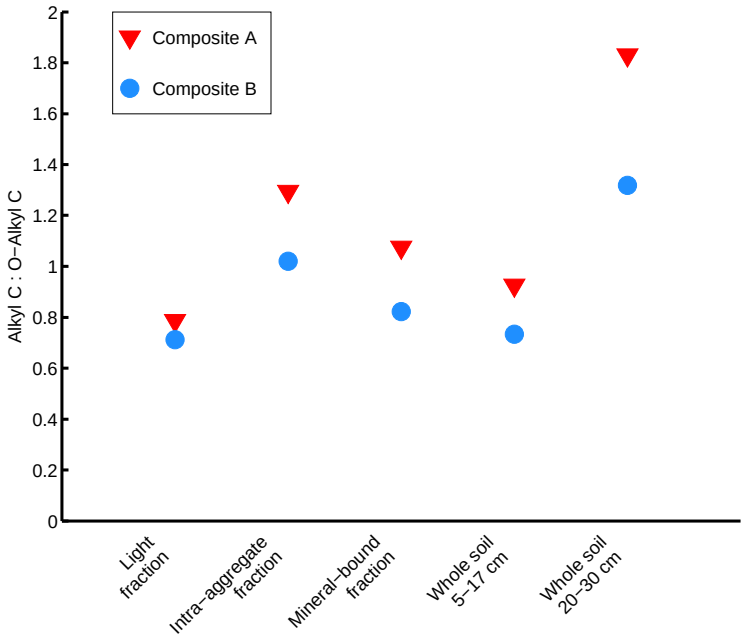

Figure 3.11: Ratio of Alkyl-C to O-Alkyl-C components of fractions and whole soils, determined by ^{13}C CP-MAS NMR spectroscopy, calculated from the integrated area under each peak as a percentage of total peak area.

Thermogravimetric Analysis

Three main peaks are visible in the derivative thermogravimetry (Fig. 3.12), at approximately 100, 300 and 500 °C. Mass lost from below 150 °C can be assumed to originate from bound water. Organic material oxidised at lower temperatures (such as in the peak at 250 - 350 °C) is described as labile, while mass loss at higher temperatures represents recalcitrant material, resistant to oxidation at 300 °C. T_{50} was lower in the mineral-bound fraction than light or intra-aggregate fractions (Table 3.1).

TGA showed no significant differences between the light and intra-aggregate fractions (Fig. 3.12), despite the differences shown in the NMR and FTIR spectra. Comparison of peak areas showed higher mass loss in the second (300 °C) peak range for mineral-bound OM, compared to light and intra-aggregate material (ANOVA, $p < 0.01$). Mass loss of mineral-bound fraction material was lower in the recalcitrant peak ranges (ANOVA, $p < 0.01$), with no significant differences in the third (500 °C)

peak range.

The large labile peak and lower T_{50} of the mineral-bound material (Table 3.1) indicate the presence of polysaccharides (Rovira *et al.*, 2008), and are typical results for a heavy fraction separated at high density (Tonon *et al.*, 2010).

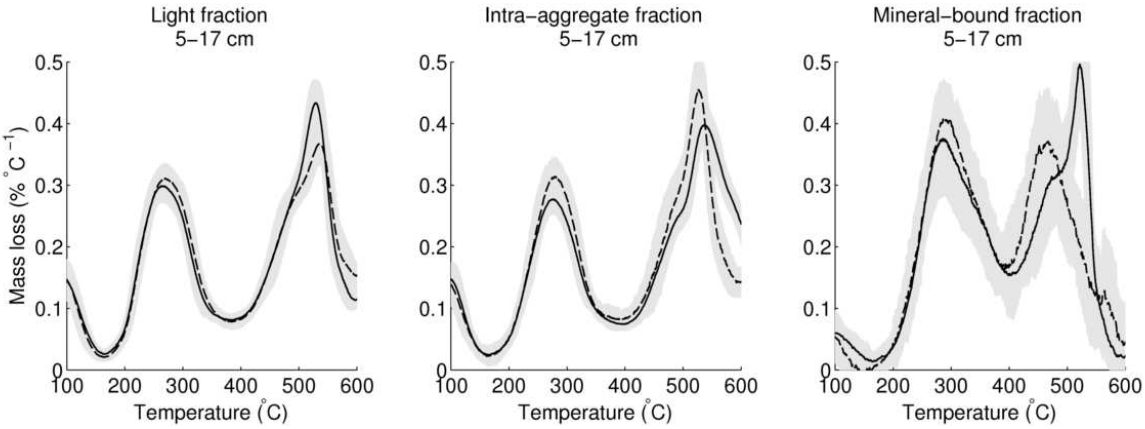

Figure 3.12: Derivative thermogravimetric analysis of SOM fractions: percentage of remaining mass lost per 1 °C (derivative of the total mass loss). Solid line is composite A, dashed line is composite B. Lines are smoothed by a moving window average of width 20 °C. Shaded area represents 1σ of this window.

Table 3.1: Thermogravimetric characteristics of 5 - 17 cm SOM fractions. T_{50} is the temperature by which 50 % of the mass of organic matter in the sample was combusted. A_R is the area of the 'recalcitrant' peak as a fraction of the total OM mass loss.

Fraction	Composite	T_{50} (°C)	A_R (%)
Light	A	408	45.9
	B	424	44.3
Intra-aggregate	A	459	45.5
	B	421	45.8
Mineral-bound	A	379	48.3
	B	370	46.6

ICP-OES

ICP-OES analysis of trace metals showed that all fractions and whole soils had high concentrations of Fe, Al, P and Ti. However, only Ti content seemed to be correlated to ash content, while trace metals that act as plant micronutrients (Mg, Ca, Cu, P, Fe and S) were higher in the light fractions than the mineral-bound fractions. Likewise, some plant-associated metals were much lower at 20 - 30 cm than 5 - 17 cm (Mg, Ca, P). Fe concentrations showed a very strong positive correlation with C content of fractions and whole soils ($r = 0.95$, $p < 0.0001$, Fig. 3.13). Within each composite, the amount of Fe present per g C consistently followed the order mineral-bound » whole soil 5 - 17 cm > intra-aggregate > light fraction, with composite A values consistently higher than composite B.

Al concentrations were higher in the intra-aggregate fraction than the light or mineral-bound, and Cu concentrations were higher in both whole soils than in any fractions, although not retained in the DOM, perhaps indicating an interaction with I^- anions during the fractionation procedure. Of all the elements studied, only P was significantly retained in the DOM fraction.

Table 3.2: Trace elemental composition of whole soils, SOM fractions, and DOM as measured by ICP-OES. standard deviations were calculated as the standard deviation from the mean value for three consecutive determinations of the concentration of a sample solution. Total elemental concentrations for solid samples were corrected for 105 °C moisture contents

		Al mg kg $^{-1}$	Ca mg kg $^{-1}$	Cr mg kg $^{-1}$	Cu mg kg $^{-1}$	Fe mg kg $^{-1}$	Mg mg kg $^{-1}$	Ni mg kg $^{-1}$	P mg kg $^{-1}$	S mg kg $^{-1}$	Ti mg kg $^{-1}$	V mg kg $^{-1}$
5 - 17 cm												
Whole soil	A	10573 ± 120	28 ± 0.2	16 ± 0.3	23 ± 0.2	4832 ± 62	197 ± 2	1.68 ± 0.07	784 ± 7	182 ± 1	1950 ± 445	22 ± 0
	B	8473 ± 10	62 ± 1	10 ± 0	14 ± 0	2820 ± 8	146 ± 1	7.1 ± 0.0	382 ± 6	80 ± 1	1438 ± 243	15 ± 0
Light fraction	A	5835 ± 63	143 ± 1	9.1 ± 0.1	7.1 ± 0.1	3478 ± 22	227 ± 0	4.0 ± 0.1	1460 ± 18	1524 ± 11	548 ± 298	10 ± 0
	B	7040 ± 64	316 ± 2	7.7 ± 0.5	6.4 ± 0.3	2930 ± 36	218 ± 4	1.0 ± 0.1	1422 ± 3	1506 ± 1	388 ± 138	9.7 ± 01
Intra-aggregate	A	7754 ± 33	96 ± 0	12 ± 0	4.0 ± 0.1	2978 ± 22	305 ± 3	2.3 ± 0.1	3307 ± 23	1080 ± 12	1480 ± 160	16 ± 0.1
	B	10452 ± 64	222 ± 5	15 ± 0	5.3 ± 0.1	3303 ± 36	414 ± 5	3.5 ± 0.1	5662 ± 13	1489 ± 7	949 ± 317	17 ± 0.1
Mineral-bound	A	6470 ± 142	26 ± 1	8.4 ± 0.3	0.84 ± 0.14	1305 ± 28	121 ± 0	0.42 ± 0.04	142 ± 0	171 ± 2	1892 ± 360	17 ± 0
	B	5391 ± 58	< 3 (LOD)	5.9 ± 0.2	< 0.3 (LOD)	732 ± 9	98 ± 2	< 0.07 (LOD)	80 ± 3	131 ± 2	1790 ± 259	14 ± 0
DOM	A	1.1 ± 0.0	4.5 ± 0.0	< 0.01 (LOD)	0.22 ± 0.03	< 0.04 (LOD)	1.8 ± 0.0	< 0.001 (LOD)	284 ± 11	2.9 ± 0.0	0.043 ± 0.009	< 0.001 (LOD)
	B	1.0 ± 0.0	3.4 ± 0.1	0.011 ± 0.002	0.24 ± 0.00	< 0.04 (LOD)	0.54 ± 0.01	0.011 ± 0.000	100 ± 4	2.2 ± 0.0	< 0.002 (LOD)	< 0.001 (LOD)
20 - 30 cm												
Whole soil	A	4020 ± 23	< 3 (LOD)	27 ± 0	9.0 ± 0.5	3666 ± 21	25 ± 1	3.5 ± 0.0	323 ± 4	283 ± 5	2095 ± 2	40 ± 0
	B	3554 ± 40	< 3 (LOD)	15 ± 1	11 ± 0	1619 ± 20	< 1 (LOD)	7.1 ± 0.1	193 ± 3	93 ± 4	1714 ± 16	28 ± 0

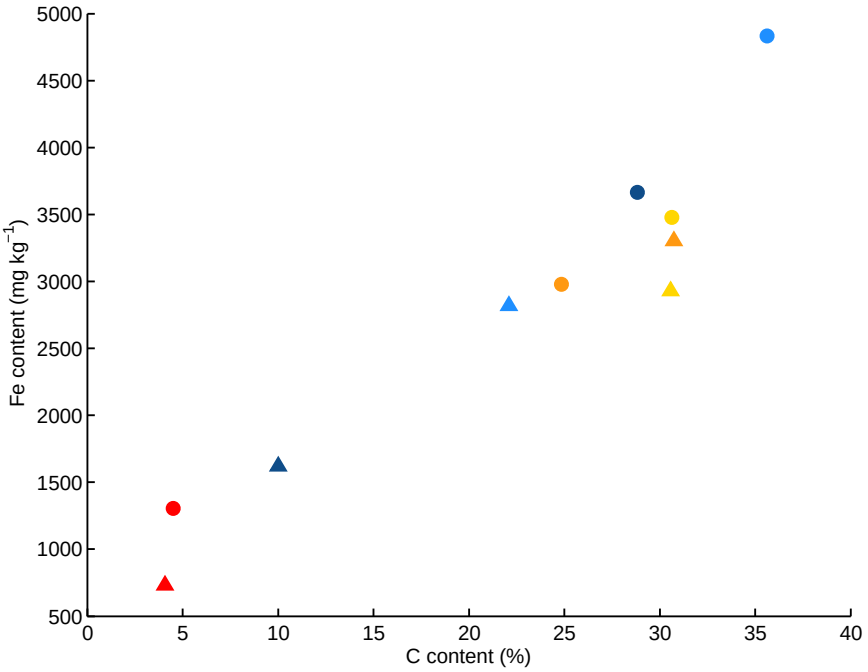

Figure 3.13: Fe association with SOC in Harwood forest fractions and whole soils. Pale blue - whole soil 5 - 17 cm; dark blue - whole soil 20 - 30 cm; yellow - light fraction 5 - 17 cm ; orange - intra-aggregate 5 - 17 cm; red - mineral-bound fraction 5 - 17 cm. Circles are composite A, triangles are composite B.

3.4 Discussion

Chemical characterisation SOM from Harwood soil horizons, particle size fractions and density fractions revealed strong differences in chemical composition down the profile, some differences between density fractions and small differences between particle size fractions, indicating that burial and to some extent mineral associations and microaggregate formation play a role in the stabilisation of SOM in Harwood forest.

Soil carbon and OM content are all generally high, for the soil type, in the upper horizons of Harwood forest soil (See Fig. 3.3). Conen *et al.* (2005) found carbon stocks of 21.3 kg m^{-2} at this site, to 45 cm depth, while the global mean for Humic Gleysols

in the top 50 cm is 19.4 kg m^{-2} (Batjes, 1996). These samples were taken without consideration of bulk density, so it is not possible to calculate an unbiased estimate of carbon stocks integrating depth. I estimated soil carbon stocks from 0 – 20 cm to be 30.7 kg m^{-2}, using the bulk density of later samples (see Chapter 7).

3.4.1 Elemental ratios

Carbon to nitrogen ratios in organic matter reflect the availability of plant material to microbial degradation, insofar as organic matter with a low nitrogen content and a high carbon content is likely to experience nutrient-limited decomposition. However, in the presence of an external N supply (for example, due to mycelial N transport (Fellbaum *et al.*, 2012)), microbial degradation can also result in a decrease in C:N ratios (Conen *et al.*, 2008), as energy-rich high carbon compounds are preferentially mineralized. The C:N ratios of Harwood forest soil are high (Figs. 3.3 and 3.5), reflecting the acidic (see section 3.3.1), peaty nature of Harwood soils; the usual range of C:N for UK topsoils is 10 - 12 (Stevenson, 1994). The global mean C:N ratio from 0 – 30 cm has been estimated at 12.7 for gleysols and 25.8 for histosols (peat) (Batjes, 1996). Although Harwood forest soil has been described as a peaty gley soil, some Fe precipitation is visible in the soil profile, suggesting podzolisation. The high C:N ratios here are also more characteristic of a podsol, for which the global mean C:N is 23.8 (Batjes, 1996).

Although C:N typically decreases with depth due to increased microbial processing (Haberhauer *et al.*, 1998), C:N ratios in Harwood increased with depth (Fig. 3.3). C:N has previously been shown increasing with depth at the same site (20.6 from 5 - 15 cm, 29.9 from 20 - 30 cm, Cross and Grace (2010)) and in the surrounding unplanted grassland (19.2 at 5 cm to 30.8 at 30 cm, Ball *et al.* (2007a)), although the trend is not consistent between similar-aged stands within Harwood forest (Ball *et al.*, 2007a). Karhu *et al.* (2010b) showed C:N ratios that decreased with depth as expected in Boreal spruce and pine plantations, while C:N of particulate OM (POM) (> 63 μm

and < 1.85 g cm^{-3}, equivalent to the light fraction described here) from the same horizons increased with depth. The light fraction here accounted for 82 % of total soil carbon in the 5 - 17 cm soil fractionated here (see section 3.3.3), which may account for the C:N ratio of bulk soils increasing with depth like the POM fraction in Karhu *et al.* (2010b). The light fraction or POM is primarily composed of relatively intact plant structures; a possible explanation for the increasing C:N with depth is that cross-linking proteins are initially more rapidly decomposable than the relatively recalcitrant structural carbohydrates, leading to a gradual depletion of N with time manifesting as an increase in C:N down the soil profile. Mycorrhizae may also play a role in the upwards redistribution of mineralized N (Fellbaum *et al.*, 2012). The dip in the C:N ratio in the 5 - 17 cm horizon can be attributed to a build up of humic acids and a high degree of microbial transformation here.

C:N ratios were lower in the light fraction than in both intra-aggregate and mineral-bound fractions, in contrast to expectations and clear established trends from other studies using density fractionation (Conen *et al.*, 2008; Dorodnikov *et al.*, 2011). Conen *et al.* (2008) predict lower C:N ratios in mineral-bound SOM due to progressive C loss during microbial transformations: a possible explanation for the lower C:N ratio in light material in Harwood is that uncomplexed OM has in fact undergone a higher degree of microbial transformations than aggregate-associated material without forming aggregates.

3.4.2 Functional group chemistry

Results from ^{13}C-CPMAS NMR show that the dominant carbon forms in Harwood SOM are alkyl- and O-alkyl carbon, while FTIR results show also that carboxyl, ketone and methyl groups are prevalent in all depths and fractions. While neither analysis can be interpreted strictly quantitatively, the relative size of peaks gives some information about the distribution the major groups of organic compounds in fractions and horizons which can be related to the age, degradability and stability

of SOM. While the very low incidence of lignin-derived signals (such as might be found in the NMR spectra at 150, 130 or 112 ppm) is surprising, the very high alkyl-C content in these forest soils can be partly explained by a high content of cutins and suberins deriving from needle and root waxes respectively (Kögel-Knabner *et al.*, 1992).

Haberhauer *et al.* (1998) studied the composition of three forest soils including one peaty podzol under an Irish Sitka spruce forest. Their results show an increase in the ketone : carboxyl peak ratio with depth, consistent with our FTIR results, and suggesting a general enrichment of aromatic groups in progressively older horizons. They also show decreases in FTIR peaks in the range from 1510 to 1230 cm $^{-1}$ with depth, which were not apparent in our results. However, Baldock *et al.* (2004) suggest that over the timescale of soil formation, it is alkyl rather than aromatic C which accumulates with age. NMR results in this study also tentatively suggest that alkyl-C may have accumulated with age in the lower horizon, while no firm conclusions can be drawn from the NMR data regarding the small aromatic peaks.

A strong increase in Si-O peaks at 1100 cm $^{-1}$ and < 1000 cm $^{-1}$ reflect an increasing overall mineral content with depth (see also Fig. 3.3), and is consistent with (Haberhauer *et al.*, 1998). Haberhauer *et al.* (1998) did not observe any differences between the horizons in the 2900 cm $^{-1}$ peak region, but the sharp increase in the polysaccharide peak at 1050 cm $^{-1}$ in these samples was also found in all three soils in their study. The decrease in polysaccharides seen here in the leached mineral layer is consistent with what might be expected of mobile, water-soluble sugars.

Lehmann *et al.* (2007) used synchrotron-based FTIR to show that aliphatic groups were spatially correlated with well hydrated kaolinite surfaces, although polysaccharide groups were not, and overall carbon distribution in aggregates was essentially random. Our results seem to show slightly higher aliphatic peaks ($\sim$ 2900 cm $^{-1}$) in the silt fraction, which also had the highest mineral content. However, this relationship is not reflected in the density fractions, where the O-H peak is high even in the

light and intra-aggregate fractions.

The alkyl-C:O-alkyl-C ratio was higher in the 20 - 30 cm soils than in any of the 5 - 17 cm samples (Fig. 3.11), and amongst the fractions of 5 - 17 cm soil the ratio was around double in the intra-aggregate fraction, and lowest in the light fraction, consistent with other findings from a different soil type (Sohi *et al.*, 2001). A high alkyl-C : O-alkyl C ratio is an indicator of humified or microbially transformed SOM; this ratio is shown to increase over time in freshly added leaf litter (Webster *et al.*, 2000).

3.4.3 Metal ion chemistry

Turchenek and Oades (1979) compared the metal concentrations of density and particle size fractions and found that as in this study, Mg, Ca, Cu, P and Fe were concentrated in the lighter fractions while Ti, Fe, Si and P were concentrated in the heavy fractions. Ducaroir and Lamy (1995) analysed light (< 1.0 g cm $^{-3}$) and heavy fractions of a fine sand fraction of a cultivated soil and showed much higher levels of S, Cu, Ni Pb and Zn in the lighter fraction, which was also the case for both light fractions in this study, despite the much higher density cut-off.

Fe oxide stabilisation is known to be a very important source of mineral-OM associations in podzolic soils such as this (Kögel-Knabner *et al.*, 2008; Sollins *et al.*, 2009). The very strong positive correlation between Fe and C contents here (Fig. 3.13) seems to indicate an important role for Fe-humus complexes and Fe-oxide interactions in the stabilisation of Harwood SOM. Alternatively, it may reflect an important role for organic matter in the precipitation of Fe oxides from aqueous solution.

Light fraction samples had a slightly lower Fe content per g C than the other fractions, confirming that the light fraction is less mineral-associated than the other fractions and whole soils, although the Fe concentration was still high. (Sohi *et al.*, 2001) found that C:Fe ratios consistently at least doubled from the light fraction to the intra-aggregate fraction, across three soil types. Here, C:Fe ratios were an order

of magnitude higher than the C:Fe ratios reported by Sohi *et al.* (2001), increasing by only ~ 15 % from light to intra-aggregate fraction. The relatively small effect of fractions on the relationship between C and Fe, combined with the high overall C:Fe (~1:400 molar ratio) implies that OM-Fe associations play a small but strong role in OM protection, and moreover that OM is more important for Fe oxide stabilisation in soils than vice versa.

3.5 Conclusions

I characterised Harwood forest soils from different horizons, and particle size and density fractions of the 5 - 17 cm O_i horizon. Soil horizons show an expected decrease in C, N and OM with depth, and also an increasing C:N ratio with depth which was not expected. FTIR spectroscopy indicates a general increase in aromaticity with depth as well as mineral horizons (but not the leached mineral horizon) rich in aliphatic groups. Within the particle size fractions, C and N contents were high in the clay fraction but otherwise decreased with decreasing particle size, and C:N ratio decreased with particle size; FTIR spectroscopy indicated that polysaccharide content was higher in the silt and coarse sand fractions than clay and fine sand, and also that the highest aliphatic content was found in the silt fraction. Amongst density fractions, C, N and OM contents were similar in the light and intra-aggregate fractions and very low in the mineral-bound fraction, but C:N ratio increased from <light < intra-aggregate < mineral-bound. ^{13}C CP-MAS NMR of density fractions and two horizons indicated that all samples are rich in alkyl-C, and that the alkyl-C : O-alkyl-C ratio, an indicator of humification, is highest in the intra-aggregate fraction and the 20 - 30 cm whole soil. TGA analysis indicated that the 20 - 30 horizon may be rich in polysaccharides, and ICP-OES analysis of trace metals indicated that Fe oxide stabilisation is very important in this soil.

Chapter 4

Soil respiration and temperature response from Harwood forest soils and density fractions

4.1 Introduction

Determining the temperature sensitivity of respiration from different SOC pools has been a research priority for many groups (see Davidson and Janssens (2006), von Lützow and Kögel-Knabner (2009) and Conant *et al.* (2011) for reviews). Since physical fractionation has shown some promise for the separation of pools with different turnover times (Zimmermann *et al.*, 2007; Sohi *et al.*, 2001), incubating isolated physical fractions representing SOM pools was an obvious next step (Leifeld and Fuhrer, 2005; Plante *et al.*, 2010; Crow *et al.*, 2006; Swanston *et al.*, 2002). Incubation of isolated fractions presents several methodological problems however. Many people have questioned the extent to which isolated fractions can be said to behave in the same way after isolation, whether because of physical changes during fractionation, inhibitory effects of separation media (Crow *et al.*, 2006; Magid *et al.*, 1996) or the

absence of other SOC pools with which co-metabolism might occur.

Some previous efforts to incubate isolated fractions have focused on particle size fractionation methods (Leifeld and Fuhrer, 2005; Plante *et al.*, 2010; Sey *et al.*, 2008) while others have used density (Crow *et al.*, 2006; Swanston *et al.*, 2002) or chemical fractionation (Plante *et al.*, 2010). Particle size fractionation of Harwood forest soils in this study yielded fractions that were insufficiently different in intrinsic chemical properties to justify separate incubation (see section 3.3.2). Since the difference in decomposability between particle size fractions is likely to depend mostly on the physical structure of aggregates and the location of SOM with respect to surfaces, cracks and pore spaces, incubation of isolated particle size fractions is likely to be sensitive to packing artefacts. Limits to decomposition experienced *in situ* are therefore unlikely to be reflected by incubation of separates. Ideally, fractions incubated in isolation should represent pools with turnover rates dependent on intrinsic properties. I used density fractions separated as described by Sohi *et al.* (2001) because my results indicated that density fractionation showed more potential to separate SOM semi-permanently sorbed to mineral surfaces and highy degraded SOM within aggregates from 'fresh' SOM.

Another common approach to using physical fractionation to investigate the respiration of different SOC pools while avoiding the potential problems involved in incubating isolated fractions is to fractionate soils after incubation of whole soils at different temperatures (Karhu *et al.*, 2010a; Creamer *et al.*, 2011). Mass balance and isotope mass balance can be used to infer the proportion of SOC lost from each fraction during the whole soil incubation. After the incubation of isolated fractions and whole soils in this study, I re-fractionated the incubated whole soils and fractions after incubation at two temperatures, to measure the relative loss of different fractions within the whole soils, and conversion from one fraction to another in the fraction incubations.

A further commonly used method of separating labile and stable respiration responses in incubation studies is to use the decline in respiration rates over time as the initial stock of labile substrate becomes depleted (Karhu *et al.*, 2010b; Hartley and Ineson, 2008; Townsend *et al.*, 1997). Slowly degrading SOM cut off from organic carbon inputs is not realistic, because decomposition of recalcitrant SOM is affected by the presence of labile SOM. However the labile depletion approach is arguably one of the least artificial and least invasive methods available to study the decomposition of labile and recalcitrant materials. Comparing respiration in soils at different temperatures over the course of a long term incubation, Townsend *et al.* (1997) showed that 'intermediate' SOC was just as sensitive to temperature as 'active' SOC. Hartley and Ineson (2008) later used the same approach to show that the SOC remaining after a long pre-incubation was in fact more sensitive to temperature than the 'active' SOC respired at first– providing evidence to support the prediction based on the Q theory that recalcitrant or humified SOM should be more temperature sensitive due to a larger molecular weight.

4.2 Aims

In this chapter I present data from two long term incubations of whole soils (5 - 17 cm and 20 - 30 cm) and soil density fractions (5 - 17 cm), designed to estimate the temperature sensitivity of respiration in different SOC turnover pools. I hypothesise that the relative rates of respiration in density fractions will follow the order *Light fraction >> intra-aggregate fraction > mineral-bound fraction*, based on the stabilising effect of mineral surface and metal interations in the mineral-bound fraction, and on the high proportion of well-humified material in the intra-aggregate fraction. (See Fig. 3.11). I expect relative respiration rates amongst the whole soils to be lower in the 20 - 30 cm than 5 - 17 cm soil. According to Q theory, and based on the high degree

of humification, I expect respiration to be most temperature sensitive in the intra-aggregate fraction, and more temperature sensitive at 20 - 30 cm soil than at 5 - 17 cm. Based on the predicted insensitivity of mineral-OM interactions to temperature, I expect temperature sensitivity to be lowest in the mineral-bound fraction.

4.3 Methods

Soil density fractions were separated by the Sohi *et al.* (2001) method described in Chapter 2, from two composite 5 - 17 cm soil samples collected in October 2008 and stored at 4 °C until fractionation. During the main experiment for establishing respiration rates at four different temperatures over five months, rates of CO_2 evolution were determined by gas chromatography (GC). This incubation will hereafter be referred to as the "GC incubation". Subsamples were also incubated at two different temperatures in sealed vessels for up to nine months, for the purposes of collecting the accumulated CO_2 for isotopic analysis. This incubation will be referred to as the "cumulative incubation".

4.3.1 Sample preparation

Samples were collected from Harwood forest in October 2008 in two composite replicates as described in Chapter 2. Isolated fractions (light, intra-aggregate and mineral-bound) and whole soils from 5 - 17 cm, in two composite replicates as described in Chapter 2, were dried immediately after fractionation for at least 24 hours at 105 °C, and stored in airtight containers. These samples were sterilised by γ-irradiation at the Isotron facility, Sheffield, UK, to reduce differences in microbial biomass between fractions due to the fractionation procedure. The samples were subjected to 26 kGy, sufficient to kill all living soil organisms while minimising organic matter transformation. Irradiated samples were left for two weeks before reinoculation, to prevent residual free radicals released during the irradiation from affecting the inoculum.

Fresh whole soil samples for preparation of inoculum solution were collected from the same sites and depths as the previous collections, during September 2009. The soil samples were seived at 2 mm and combined into composites in the same manner as the previous samples. Each 100 g soil subsample was mixed with 1 l distilled water and four 10 mm ø glass beads, and shaken in an end-over-end shaker (Laboshake Rotoshake RS12, Gerhardt, Germany) for two hours at 10 Hz (rotation arc radius 50 cm) to separate macroaggregates. The supernatant was retained after centrifugation at 100 x g and filtered through a seive to remove particles > 63 μm. Sterilised samples were rewetted to 60 % WHC using this inoculum solution. All samples (including whole soils) were mixed 2:1 (by mass) with ashed, carbonate-free white quartz sand prior to rewetting, and 2 ml of a carbonate-free nutrient solution diluted to 5 ml l^{-1} (Formulex, Growth Technology, Taunton, UK; see Appendix B) was added to the inoculum solution. Subsamples of the inoculum solutions were analysed by mass spectroscopy for total organic carbon and $\delta^{13}C$, and were found to contain 1000 - 1200 mg/L TOC.

Alongside the sterilised and reinoculated samples, whole soil subsamples from 5 -17 cm and 20 - 30 cm were prepared without sterilisation for incubation in the GC incubation (both 5 - 17 cm and 20 - 30 cm whole soils) and in the cumulative incubation (20 - 30 cm whole soils only). The 5 - 17 cm whole soils in this case were the 'fresh' samples collected for the preparation of inoculum in September 2009. One of the 20 - 30 cm whole soils was collected in January 2009 and the other in September 2009. All the 'unsterilised' samples were air-dried and then re-wet to 60 % WHC before incubation. Water holding capacity (WHC) was determined by weighing soil into a Buchner funnel lined with filter paper, saturating with deionised water, allowing to drain overnight in a humid environment, and then drying at 105 °C. The WHC is the gravimetric water content of the subsample after draining overnight.

4.3.2 GC incubation

Incubation conditions

Samples incubated for GC measurement were contained in either 50 ml Erlenmeyer flasks, 15 ml glass test tubes, or 1.8 l adapted Kilner jars, all sealed with pierced parafilm, except during the measurement period when these were replaced with Subaseal® rubber septum stoppers. One sample of each type (Light fraction, intra-aggregate fraction, mineral-bound fraction, sterilised whole soil from 5 - 17 cm, unsterilised whole soil from 5 - 17 cm, and unsterilised whole soil 20 - 30 cm) from each composite (A and B) was incubated at each temperature, 10, 15, 25 and 30 °C. Measurements began two weeks after inoculation. One headspace sample was taken at the time of sealing, using a cone-tipped SGE gas-tight syringe (SGE, Melbourne Australia). During sampling, the containers were vented by a second needle in the septum, to maintain laboratory air pressure inside the containers. The sample was flushed 6 times before taking a sample of 3 ml, which was compressed to 2 ml and released before injection into the GC to normalise injection pressure to laboratory air pressure. The containers were left sealed for between one and six hours depending on the rate of accumulation, and then a second headspace sample was analysed. During the second headspace sampling the venting needle was not used. The GC incubation ran for five months in total: measurements began after two weeks, and ran twice a week at the start of the incubation, decreasing to twice a month by the end of the incubation.

CO_2 determination by GC

Headspace gases were analysed for CO_2 content by gas chromatography (GC) on a Perkin Elmer Autosystem XL GC system (Perkin Elmer Life Sciences, Wellesley MA, USA) fitted with a thermal conductivity detector on a 1.5 m column of Porapak Q. The oven temperature was 50 °C, and the carrier gas was helium. GC peaks were

analysed using PeakSimple software. 400, 1000, 1500, and 2000 ppm CO_2 standards (BOC) were analysed to calibrate at the start and end of each run; 400 and 2000 ppm standards were analysed every ten samples during the run. Headspace CO_2 concentrations were measured at the beginning and end of each measurement period, which lasted between two and six hours. Respiration rates (F) were calculated in μg CO_2-C g soil-C^{-1} d^{-1} from the change in headspace CO_2 concentration (C_v, in ppm_v), the headspace volume of the flask (V, in L), the duration of the measurement period (t), the dry mass of the soil (W, in g), the carbon content of the soil (S, in %), and the temperature of the incubation (T, in K) using the following equation:

$$F = \frac{C_v \times M \times P}{R \times T} \times \frac{V}{W \times S/100 \times t} \tag{4.1}$$

where M is the molecular weight of C (12 μg μmol^{-1}), P is the barometric pressure (1 atm) and R is the universal gas constant (0.0821) (Robertson *et al.*, 1999).

4.3.3 Cumulative incubation

Samples incubated for collection and radiocarbon dating of CO_2 were left to accumulate in sealed Kilner jars. Two sampling ports were drilled into the jar lids attached to Nalgene tubing and the joints were sealed with Plastidip®. Air inside the sealed jars was scrubbed of atmospheric CO_2 by drawing through soda lime. The jars were left sealed until 5 - 10 ml CO_2 had accumulated (between 35 and 278 days), providing sufficient respired CO_2 for isotopic analysis without limiting microbial activity. Headspace CO_2 was measured before sampling using a continuous-loop infrared gas analyser, scrubbed of CO_2 using sodalime and connected to the nalgene sampling tubes (EGM-4, PP Systems, Hertfordshire UK). Headspace CO_2 was collected for isotopic analysis using a zeolite molecular sieve sampling system (Hardie *et al.*, 2005). Headspace gases were drawn through a molecular sieve cartridge, trapping CO_2.

CO_2 was then recovered cryogenically while the cartridge was heated to 500 °C to release the CO_2. For quality assurance, a known CO_2 gas standard was released inside a scrubbed incubation jar and the CO_2 collected using the same method. A further gas standard was released inside a scrubbed jar containing NaI residues, to test for a physical fractionation of C isotopes due to sorption and resorption. This jar was incubated for two weeks before collection and reanalysis of headspace CO_2.

4.3.4 Temperature sensitivity of soil respiration

The temperature sensitivity of respiration during the GC incubation was calculated from two standard models of temperature response. The first is a simple exponential curve described by the equation

$$R(T) = R_0 e^{a_0 T} \tag{4.2}$$

where $R_0 > 0$ and is the rate of respiration at 0 °C, and $a_0 > 0$ and is the temperature sensitivity coefficient. The exponential relationship assumes that the temperature sensitivity is constant with respect to temperature. For this reason it is only appropriate for intercomparison within a small temperature range and at low temperatures, where temperature does not yet restrict enzyme activity. The Arrhenius equation was also applied to the same data for comparison:

$$R(T) = R_0 e^{a_1 / RT} \tag{4.3}$$

where $R_0 > 0$ and is the maximum rate of respiration and where $a_1 < 0$, and is equal to $-E_a$, the activation energy of the oxidation reaction (kJ K^{-1} mol^{-1}), R is the ideal gas constant, and temperature is in K. Q_{10} is calculated from this relationship as the factor of increase over a 10 °C increase in temperature.

$$Q_{10} = (R_2 / R_1)^{(10/(T_2 - T_1))} \tag{4.4}$$

In the exponential model, Q_{10} is constant across temperatures, while in the Arrhenius model it is not. For the purposes of comparison Q_{10}s given here for the Arrhenius equation are calculated between 10 and 30 °C. Q_{10} values from the cumulative incubation were calculated from the initial rate of CO_2 accumulation measured at day 35, and were calculated from measured respiration rates using equation 4.4

4.4 Results and discussion

4.4.1 Soil respiration from different SOM fractions

Respiration rates during the GC incubation showed a near-exponential relationship with temperature for all SOM fractions and whole soils at both depths (Fig. 4.1). Respiration rates per g C were considerably lower in all isolated fractions than in the bulk soil from 5 - 17 cm (Friedman test and χ^2, all $p < 0.01$). This could be the result of small amounts of Na/I residues remaining from fractionation, which were found in association with organic matter (see Appendix A). Composite A and B mineral-bound fractions at 30 °C had very different rates of respiration- composite A rates were consistently between 3 and 10 times higher than composite B. Since there were only two samples it was not possible to identify either one as an outlier, and so all subsequent temperature response calculations for the mineral-bound fraction were made using only 10, 15 and 25 °C values. Excluding the composite A 30 °C sample with very high respiration rates, there were no significant differences at any temperature in respiration rates per g C between fractions at 5 - 17 cm (Friedman test and χ^2, $p > 0.05$). Including both 30 °C mineral-bound samples, respiration rates at 30 °C were higher in the mineral-bound fraction than in either the intra-aggregate or light fractions (Friedman test and χ^2, $p < 0.05$). This result is the opposite of what was expected, since mineral protection is considered to be a long-term stabilisation mechanism. However, higher respiration rates are consistent with chemical characterisation of the fractions, which showed a high proportion of chemically labile

material in the mineral-bound fraction (Thermogravimetric Analysis and FTIR, Sections 3.3.3 and 3.3.3). Chemically labile material stabilised by mineral interactions in soils was relatively bioavailable after fractionation. This suggests that any protection of SOM in close mineral interactions is the result of microaggregates, which were broken down during fractionation, rather than the OM-mineral bonds themselves. However, it should be noted that the tenuous difference in respiration rates between isolated fractions was small in comparison to the difference between soil horizons, and between sterilised and unsterilised soil.

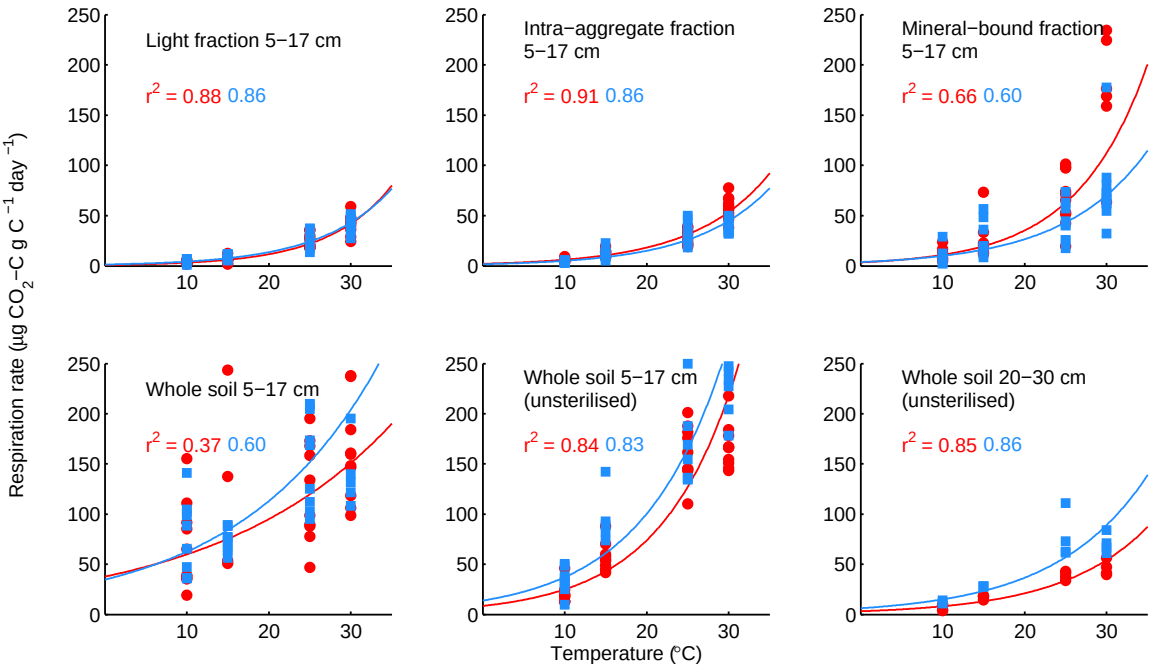

Figure 4.1: Soil respiration from three soil fractions and from whole soil at two depths, spanning five months (two months for 20 - 30 cm whole soil). Lines and r^2 values respresent the best fit of equation 4.2 to all values at all temperatures within a single composite (40 datapoints, but n = 4). Red lines show composite A, blue lines show composite B.

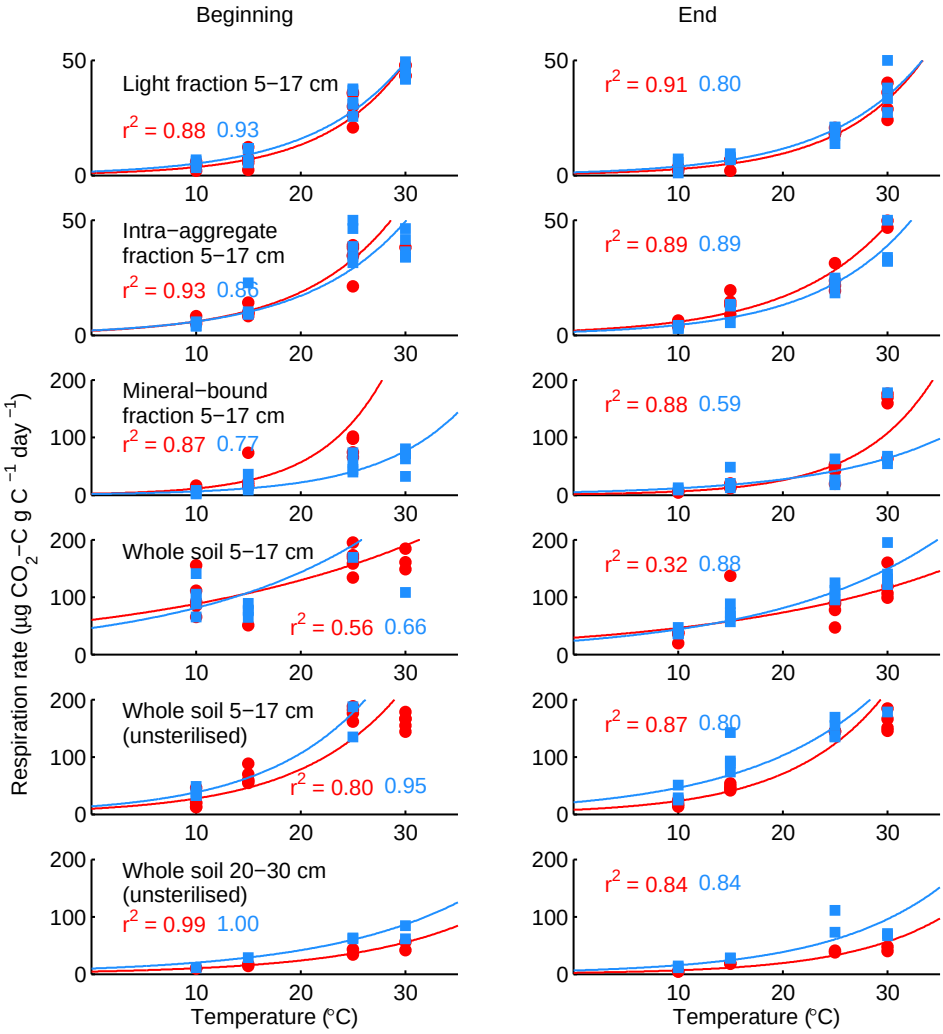

Figure 4.2: Soil respiration from three soil fractions and from whole soil at two depths during the first half and the second half of each incubation period. Note that the incubation period was shorter for the 20 - 30 cm whole soil. Lines respresent the best fit of equation 4.2 to all values at all temperatures within a single composite (40 datapoints, but n = 4). Red lines show composite A, blue lines show composite B.

4.4.2 Soil respiration from whole soils at different depths

Respiration rates per g C from 20 - 30 cm whole soils were lower than respiration rates from both 5 - 17 cm soils throughout the incubation (Fig. 4.1 Friedman test and χ^2, p <0.05). Previous research comparing respiration from the same horizons in Harwood forest similarly found that respiration from 5 - 15 cm soil was more

than twice as high as from 20 - 30 cm soil on a g-soil-C basis (Cross and Grace, 2010), although their respiration values were considerably higher than those reported here. Neither of the unsterilised whole soils (5 - 17 cm and 20 - 30 cm) showed a particular decline in respiration over time (Figs. 4.6, 4.2) although the sterilised and reioniculated whole soil from 5 - 17 cm declined over time in all but the 15 °C samples, indicating a depletion of available substrates. While the SOM substrate for sterilised and unsterilised 5 - 17 cm whole soil should have been identical, the sterilised and reinoculated whole soil contained an extra mg of labile DOC in the form of the inoculum solution. There are two possible explanations for the depletion of labile material in the sterilised soil and not the unsterilised. Either the early high respiration values represent the decomposition of labile DOM, and microbial biomass in the inoculum, and microbial necromass leftover from the sterilisation, and the later respiration values represent the true value for SOM respiration; or the decline is the result of a microbial succession during colonisation of the inoculum community, from growth-oriented r-selected communities to k-selected communities. Since the isolated fractions were also inoculated and did not show such a strong decline in respiration over time (Figs. 4.6, 4.2), it seems likely that the labile material becoming depleted in the sterilised whole soil is due to microbial necromass, since most of the microbial biomass in the fractions would have been rinsed out during fractionation. Respiration rates in some of the composite A mineral-bound fraction samples declined over time, and these samples experienced the highest proportion of total SOC consumed over the course of the incubation (see Fig. 4.7) A depletion of available substrates may explain some of the decline in respiration over time amongst the sterilised samples, but it doesn't explain the lack of decline over time in the unsterilised bulk soil.

Despite composite sampling to reduce sample variation and provide samples closer to the population mean, there were some differences in chemical characteristics between composites A and B, suggesting more humified OM was present in composite A (for example in the Alkyl-C : O-alkyl C ratio, see Fig. 3.11). Respiration

rates also showed differences between composites A and B. Composite A showed higher respiration rates in both 5 - 17 cm and 20 - 30 cm whole soils, while respiration in isolated fractions was generally higher in composite B. These differences, in the whole soils at least, are the opposite of what might be expected from the chemical characteristics of the composites.

As demonstrated in section 3.3.3, SOM at 20 - 30 cm at Harwood showed distinct chemical properties to whole soil from 5 - 17 cm SOM. In particular, the alkyl-C : O-alkyl-C ratio of 20 - 30 cm soils was around double the ratio of 5 - 17 cm soils (Fig. 3.11). Subsequent ^{14}C analysis showed that the mean residence time of 20 - 30 cm SOM was around 1000 years longer than the MRT of 5 - 17 cm soils (see Table. 5.1). The high mineral content of the 20 - 30 cm soils (Figs. 3.7 and 3.3) suggests mineral stability may be high in this horizon, while the alkyl-C : O-alkyl-C ratios suggest that this material may also be intrinsically recalcitrant, and the ^{14}C dates demonstrate that this material has been stable *in situ*.

4.4.3 Soil respiration inferred from long term accumulation of CO_2

CO_2 accumulation in the cumulative incubation showed broad agreement with the patterns in rates of respiration measured in the open incubation, although the results are not directly comparable. Respiration during the first month of the cumulative incubation was higher than recorded for the GC incubation. Respiration rates in the closed incubation were lower in isolated fractions than whole soils (2-way ANOVA, $p < 0.01$) but not significantly different between isolated fractions (2-way ANOVA, $p > 0.05$), which ranged from 32 to 100 μg CO_2-C g C^{-1} day^{-1} at 10 °C and 288 to 673 μg CO_2-C g C^{-1} day^{-1} at 30 °C. Comparing only whole soils in the cumulative incubation, respiration was slightly but not significantly lower (2-way ANOVA, $p = 0.06$) for the 20 - 30 cm whole soils than the 5 -17 cm whole soil.

4.5 Temperature sensitivity of soil respiration

Comparing the temperature sensitivity of respiration between isolated 5 - 17 cm fractions both from the GC incubation, using both exponential and Arrhenius models, and from the cumulative incubation using the Q_{10} equation directly, Q_{10} is highest in the light fraction, lower in the intra-aggregate fraction and lowest in the mineral-bound fraction (Table 4.1). These differences are significant in the cumulative incubation (1-way ANOVA, $p < 0.05$) and not significant for either model in the GC incubation. Higher temperature sensitivity in the light fraction than the intra-aggregate fraction appears to go against the hypothesis, based on Q theory, that more labile material should have lower temperature sensitivity. However, considering that the highest rates of respiration were found in the mineral-bound fraction (Fig. 4.1), a lower temperature sensitivity in this fraction is consistent with Q theory.

Only very slight differences are discernible between Q_{10} values for respiration from the other fractions and whole soils. Respiration from whole soil at 20 - 30 cm seems to have a slightly higher Q_{10} than respiration from whole soil at 5 - 17 cm, while respiration from the intra-aggregate fraction at 5- 17 cm seems to be slightly more temperature sensitive than either whole soil. In the intra-aggregate and 20 - 30 cm whole soils at least, there is a slight increase in temperature sensitivity towards the end of the incubation. Although this increase falls within the variation shown at the start of the incubation (for intra-aggregate material), the consistent trend in each of these suggests that it may be more than chance.

Sterilisation and reinoculation had a small negative effect on overall respiration rates (Fig. 4.1), but a strong negative effect on temperature sensitivity of respiration, as is apparent from comparison of the whole soils. Sterilised and reinoculated whole soil at 5 - 17 cm also showed higher variation in respiration within individual jars, which is partly reflected in the r^2 values calculated for each model fit (Table 4.1), and partly in the decline in respiration with time (Fig. 4.2),

Table 4.1: Q_{10} and E_a of respiration, calculated using an exponential model (equation 4.2) and the Arrhenius model (equation 4.3) from the GC incubation at 10, 15, 25 and 30 °C, and using the basic Q_{10} from the cumulative incubation at 10 and 30 °C. Q_{10}s given for the Arrhenius equation and E_a are for the interval 10 - 30 °C; n.d. indicates value not determined.

Fraction	Composite	Q_{10}	r^2	Q_{10}	r^2	E_a	Q_{10}
		Exponential		Arrhenius		J K^{-1} mol^{-1}	Closed inc.
Light fraction	A	3.62	(0.88)	3.62	(0.88)	9.18 x 10^4	3.18
5 - 17 cm	B	3.16	(0.86)	3.17	(0.86)	8.23 x 10^4	3.01
Intra-aggregate	A	2.95	(0.91)	2.95	(0.90)	7.73 x 10^4	2.88
5 - 17 cm	B	2.98	(0.86)	2.99	(0.87)	7.82 x 10^4	2.95
Mineral-bound	A	3.19	(0.66)	3.15	(0.67)	8.18 x 10^4	2.60
5 - 17 cm	B	2.65	(0.60)	2.67	(0.61)	7.00 x 10^4	2.54
Whole soil	A	1.59	(0.37)	1.59	(0.37)	3.30 x 10^4	1.84
5 - 17 cm	B	1.81	(0.60)	1.80	(0.59)	4.21 x 10^4	1.76
Whole soil 5 - 17 cm	A	2.96	(0.84)	2.97	(0.85)	7.78 x 10^4	n.d.
unsterilised	B	2.70	(0.83)	2.70	(0.84)	7.10 x 10^4	n.d.
Whole soil 20 - 30 cm	A	2.58	(0.85)	2.59	(0.86)	6.80x 10^4	2.62
unsterilised	B	2.43	(0.86)	2.45	(0.87)	6.39x 10^4	1.85

Considering only the sterilised and reinoculated soils, all isolated fractions showed higher Q_{10} values than whole soils, with the highest temperature sensitivity in the light fraction, in contrast to other studies showing a lower temperature sensitivity of 'labile' isolated particulate organic matter (Plante *et al.*, 2010; Leifeld and Fuhrer, 2005).

The trend in temperature sensitivity with depth is ambiguous (Table 4.1); considering only the unsterilised whole soils in the GC incubation, 20 - 30 cm whole soil seems to be slightly less temperature sensitive than 5 - 17 cm whole soil, whereas results from the cumulative incubation suggest a higher temperature sensitivity at 20 - 30 cm. Previous studies at the same site have shown an increase in Q_{10} with depth (Rey *et al.*, 2008), while other studies also report lower temperature sensitivity in mineral horizons of forest soils (Karhu *et al.*, 2010b; Gillabel *et al.*, 2010).

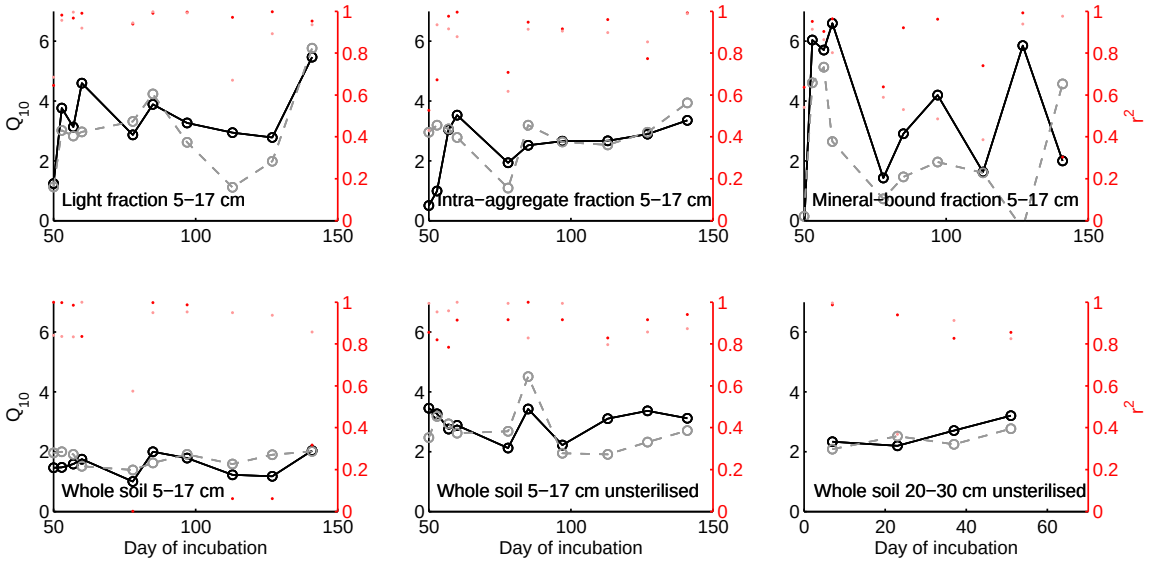

Figure 4.3: Temperature sensitivity of respiration from soil fractions and whole soil from two depths. Each black or grey point represents Q_{10} calculated from the best fit of equation 4.2 to respiration rates of four subsamples incubated at 10, 15, 25, and 30 °C. The corresponding red and pink points indicate the r^2 value showing the goodness of fit of the four points to equation 4.2. Black and red points show results from composite A subsamples, and grey and pink points show results from composite B.

4.5.1 Temperature sensitivity of depleting pools

One pitfall of the approaches described above to calculate Q_{10} is the change in substrate quality over time. In these incubations, samples with different intrinsic quality were incubated at a constant temperature over the course of the incubation; within each vessel, the most bioavailable SOM subfraction is expected to be respired first, leading to a decline in respiration rates over time (see Fig. 4.6). Since respiration are were higher at 30 °C than at 10 °C, calculating Q_{10} at one timepoint, or averaged over the same period, involves a comparison of SOM of different quality, since at any one timepoint a higher proportion of the sample at 30 ° has already been used (see Fig. 4.4). If bioavailable material is less temperature sensitive than recalcitrant material, as posited by Q theory, this would lead to an underestimation of Q_{10}.

Other researchers have avoided this problem in long-term incubations by incubating all samples at the same 'background' temperature, altering the temperature only during measurement periods, and randomising the temperature treatments during successive measurements to avoid differences in cumulative CO_2 release between treatments or effects of microbial adaptation to particular temperature regimes (Leifeld and Fuhrer, 2005). However, since microbial community adaptation to temperature regimes may be a mechanism mediating temperature effects on respiration rates, these experiments were designed with parallel temperature treatments.

An elegant solution to both problems, calculating an unbiased Q_{10} for an incubation with parallel temperature treatments, is to use the time taken to respire a set proportion of the total SOC ($Q_{10}{}^{q}$, Conant *et al.* (2008)), or to use respiration rates when a set amount of CO_2 has been released ($Q_{10const}$, Wetterstedt *et al.* (2010)), rather than the absolute rate of respiration at a fixed time. For this study, it was unfortunately not possible to use the $Q_{10}{}^{q}$ or $Q_{10const}$ as a measure of respiration, because of the long equilibration period before measurements began and the high variation in respiration rates over time. To estimate cumulative CO_2 release it was necessary to extrapolate respiration rates (linearly) from the start of the incubation to the first measurement, incorporating an unavoidable bias, underestimating cumulative respiration where the initial decline in respiration may have been highest. Using the $Q_{10}{}^{q}$ approach, comparisons were not possible between either all six treatments, or between only isolated fractions, because in all cases the samples with highest respiration had respired a higher proportion of total SOC by the first sampling point than was respired by the last sampling point in the samples with lowest respiration (Fig. 4.5). Using the $Q_{10const}$ approach, it was possible to set intermediate target values for total SOC respired, but calculation of Q_{10} required was from a single respiration rate measurement for each sample, which was problematic since respiration was very variable over time for most samples (see Fig. 4.6). A hybrid approach, calculating a $Q_{10const}$ from the time taken to respire a set amount of CO_2 at 10 and 15 °C, gave

Table 4.2: Estimated $Q_{10const}$ of respiration from the GC incubation, calculated from the estimated time taken to respire a target cumulative amount of CO_2 at 10 and 15 °C. $Q_{10const}$ were calculated using one target value for fractions and one target value for 5 - 17 cm whole soils, and so the values for fractions and whole soils are not intercomparable. There was no compatible target value for comparison of 20 - 30 cm soils with 5 - 17 cm whole soils.

		Composite A	Composite B
5 - 17 cm	Light fraction	1.8	2.1
	Intra-aggregate fraction	1.2	5.1
	Mineral-bound fraction	1.9	5.1
5 - 17 cm	Sterilised whole soil	1.5	2.4
	Unsterilised whole soils	0.7	3.1

results that showed no congruence between duplicates, and no consistent differences between fractions or depths (Table 4.2), including one sample with a negative temperature sensitivity ($Q_{10} < 1$). $Q_{10const}$ values for composite B samples were consistently higher than for composite A, which consisted of more degraded material overall (See Fig. 3.11). This could be interpreted as evidence against the hypothesis of the Q theory. However, given the inherent bias of cumulative respiration based on extrapolated early respiration rates, and the high sensitivity to measurement error due to the small subset of observations used, I consider this measure to be less useful than the fitted Q_{10} values shown in Table 4.1

Other studies have made a feature of the depletion of labile substrates over time, inferring a higher temperature sensitivity for less bioavailable SOM from Q_{10} values that increase over time as labile substrates are depleted (Hartley and Ineson, 2008; Conant *et al.*, 2008; Feng and Simpson, 2008; Karhu *et al.*, 2010a). In this experiment, Q_{10} values estimated at each timepoint (including bias due to substrate depletion) were highly variable, but did seem to increase slightly towards the end of the incubation in at least the intra-aggregate fraction (5 - 17 cm) and the 20 - 30 cm whole soil (Fig. 4.3). Since these were the two treatments that showed chemical traits suggesting intrinsic recalcitrance in Chapter 3, this tentative result suggests support for Q theory.

To test whether there was an effect of substrate depletion on the measured Q_{10}

values, I compared the proportion of SOC already respired by each sample date at 30 °C to temperature sensitivity at that timestep, calculated using only the respiration rates at 25 °C and 30 °C to minimise bias due to substrate depletion. There was no clear relationship, either from the combined measure of all time points during the GC incubation (See Fig. 4.7), or the limited information given by the cumulative incubation, where it was only possible to give a single value for each pair of samples (Fig. 4.8).

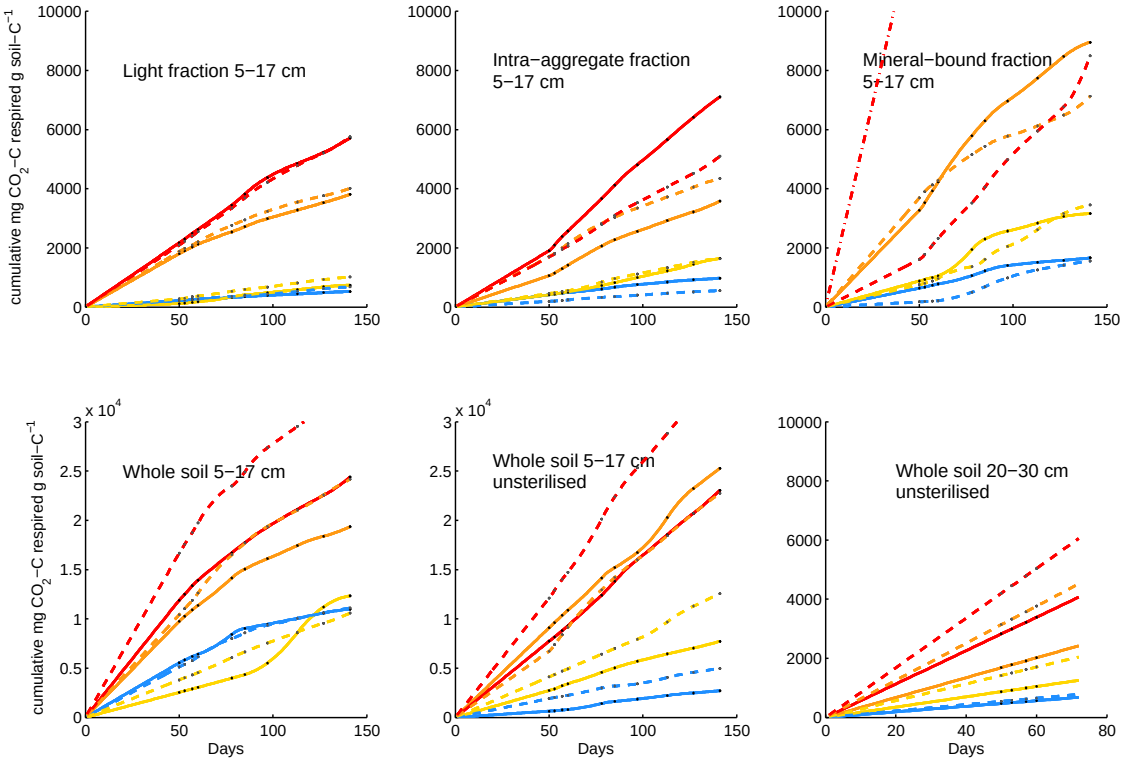

Figure 4.4: Cumulative soil respiration from three soil fractions and from whole soil at two depths over time. Respiration rates were linearly interpolated between sampling points, which are indicated in black/grey, and extrapolated before the first sampling point. Red - 30 °C, orange - 25 °C, yellow - 15 °C and blue - 10 °C. Solid lines and black points show composite A, dashed lines and grey points show composite B. Note that the incubation period was shorter for the 20 - 30 cm whole soil.

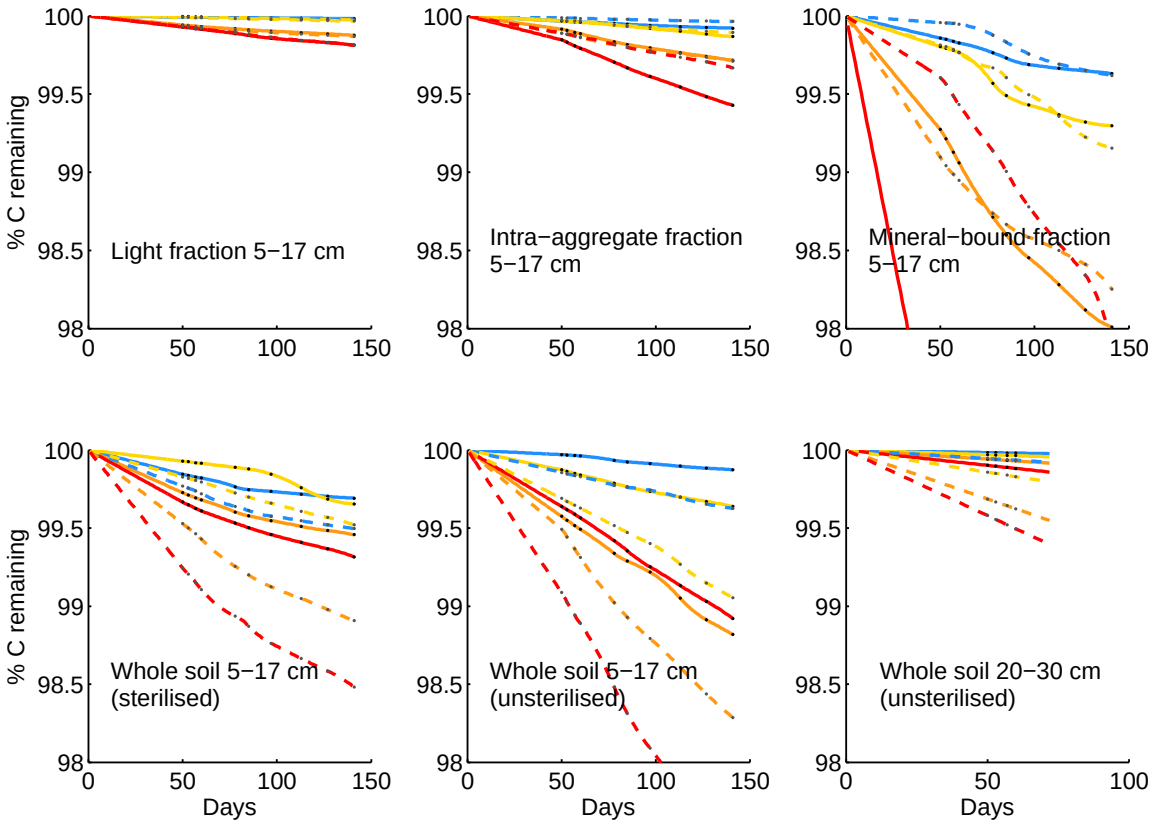

Figure 4.5: Cumulative SOC consumption from three soil fractions and from whole soil at two depths over time. Respiration rates were linearly interpolated between sampling points, which are indicated in black/grey, and extrapolated before the first sampling point. Red - 30 °C, orange - 25 °C, yellow - 15 °C and blue - 10 °C. Solid lines and black points show composite A, dashed lines and grey points show composite B. Note that the incubation period was shorter for the 20 - 30 cm whole soil.

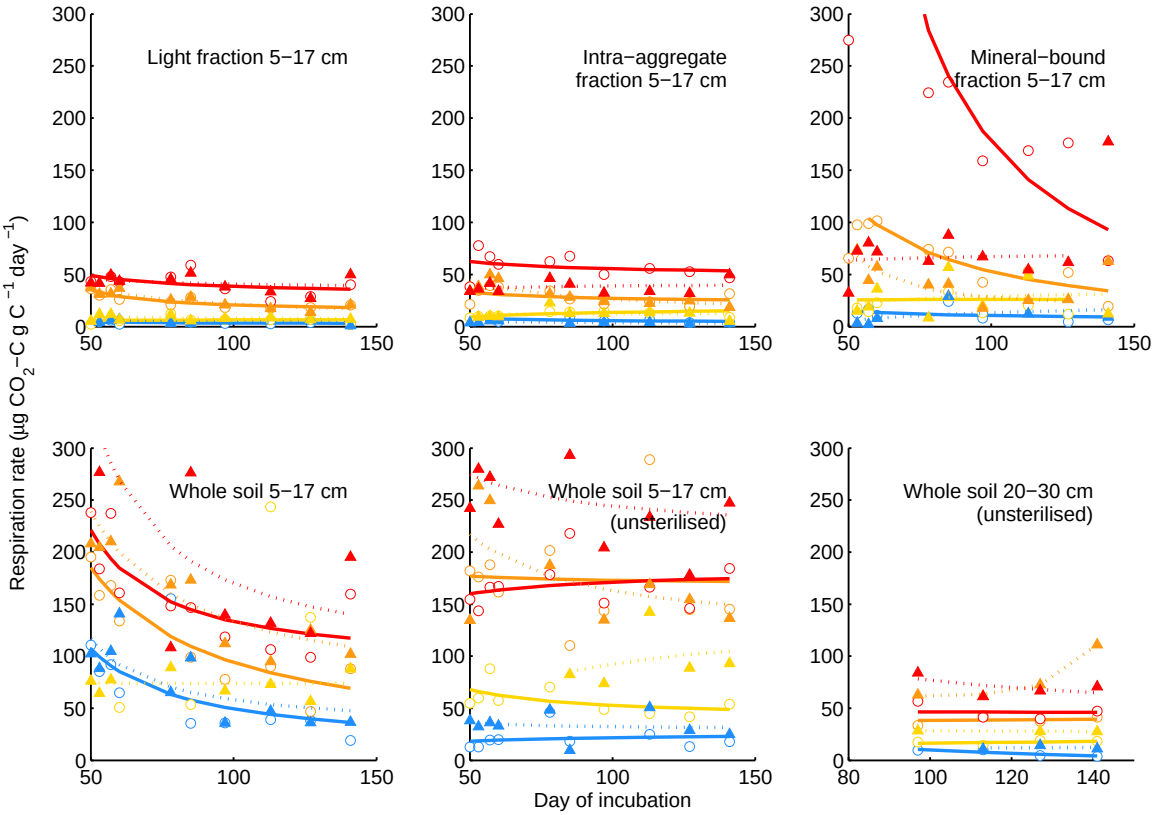

Figure 4.6: Soil respiration from three soil fractions and from whole soil at two depths over time. Each point shows the actual value recorded for a single sample. Red - 30 °C, orange - 25 °C, yellow - 15 °C and blue - 10 °C. Solid lines and circles show composite A, dashed lines and triangles show composite B. Note that the incubation period was shorter for the 20 - 30 cm whole soil.

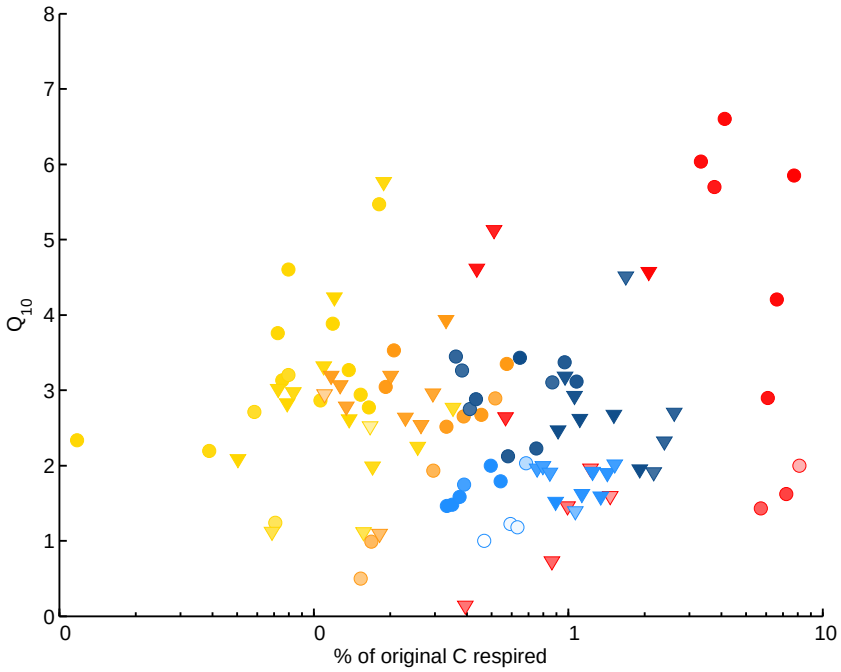

Figure 4.7: Temperature sensitivity (Q_{10}) of respiration in relation to the proportion of C respired at 30 °C during the GC incubation. Q_{10} is calculated from respiration at 25 °C and 30 °C only. Pale blue - whole soil 5 - 17 cm; dark blue - whole soil 20 - 30 cm; yellow - light fraction 5 - 17 cm ; orange - intra-aggregate 5 - 17 cm; red - mineral-bound fraction 5 - 17 cm. Circles are composite A, triangles are composite B. Each point represents one composite at a single event, incorporating two observations (25 °C and 30 °C incubations)

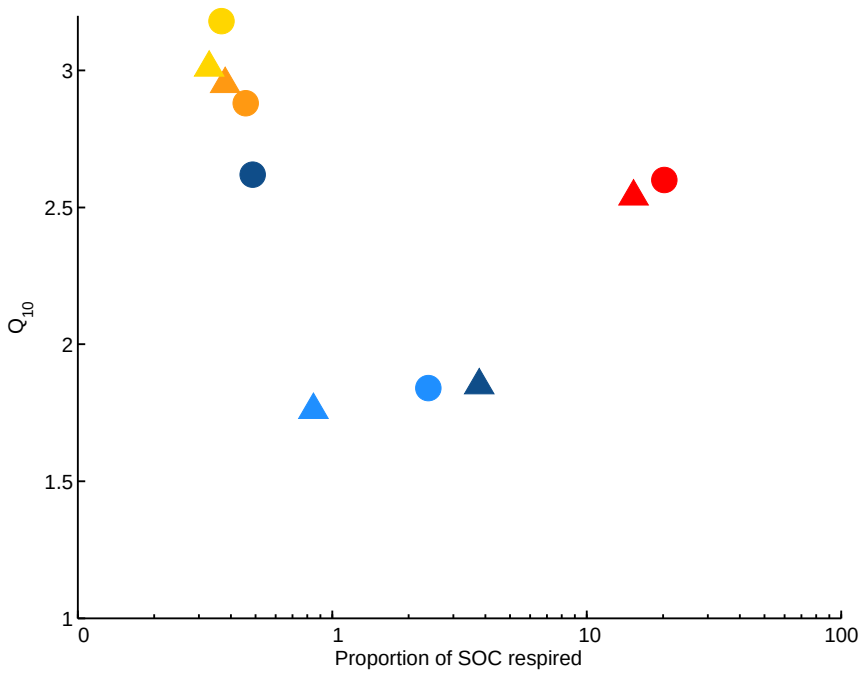

Figure 4.8: Temperature sensitivity (Q_{10}) of respiration in relation to the proportion of C respired at 30 °C during the cumulative incubation. Pale blue - whole soil 5 - 17 cm; dark blue - whole soil 20 - 30 cm; yellow - light fraction 5 - 17 cm ; orange - intra-aggregate 5 - 17 cm; red - mineral-bound fraction 5 - 17 cm. Circles are composite A, triangles are for composite B.

4.5.2 Relationship between E_a and R_{20}

A common proxy measure for comparing SOM stability in different soils is the rate of respiration at a reference temperature (Craine *et al.*, 2010; Fierer *et al.*, 2006). The respiration rate is obviously a direct measure of SOM decomposability in the circumstances given, however, it is a measure of the overall stability rather than the action of any one stabilisation mechanism. Several studies have used respiration rates or factors derived from a fitted temperature / respiration rate function (Fierer *et al.*, 2006) as surrogate measures of stability to test the predictions of the Q-theory, that chemically recalcitrant material should have a higher temperature sensitivity. Fierer *et al.* (2006) found that 45 % of the variation in temperature sensitivity could be explained

by the rate of respiration, which seems to support Q-theory. Later, an incubation of soils from across North America and a meta-analysis suggested that this could be a universal scaling relationship; (Craine *et al.*, 2010) showed that 43 % of the variation in E_a could be explained by respiration rates at 20 °C (R_{20}). Craine *et al.* (2010) anticipated the obvious criticism that an argument from comparison of respiration rates to a factor calculated from a function of the respiration rates is a circular argument- by using different subsamples of the same soils to calculate R_{20} and E_a. However, respiration rates in cores from the same original samples cannot be said to be independent from one another, and it remains to be conclusively demonstrated that this universal scaling relationship is not an artefact of the poorly fitting, simplifying model of temperature response that is still universally used (Davidson *et al.*, 2006).

I compared the respiration rates and E_a during the GC incubation to the universal scaling relationship shown by Craine *et al.* (2010); although in this comparison R_{20} and E_a were calculated from the same fitted curve, there was no correlation between R_{20} and E_a (Fig. 4.9).

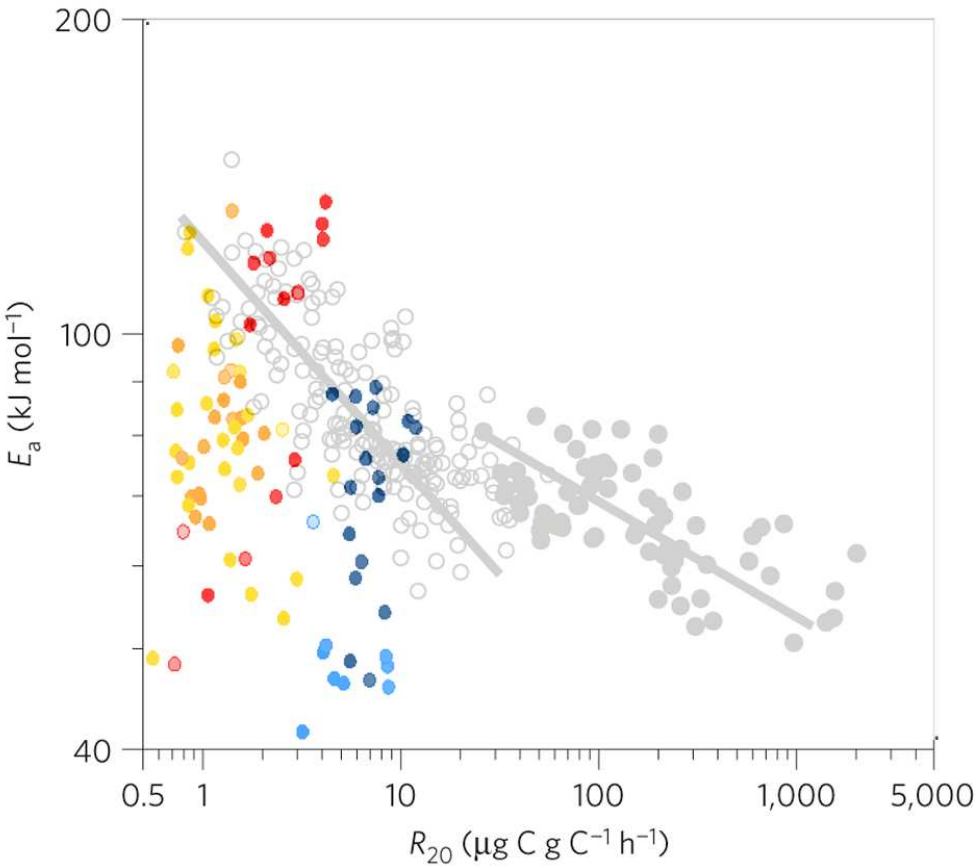

Figure 4.9: Proposed universal scaling relationship between respiration rate at a reference temperature of 20 °C (R_{20}) and E_a (a measure of temperature sensivity). Background/black and white datapoints and regression are taken from Craine *et al.* (2010). Coloured points are calculated from the results of the GC incubation, this study. Each coloured point is the product of an Arrhenius equation (equation 4.3) fitted to four incubated subsamples at 10, 15, 25 or 30 °C (one composite) on one of ten measurement dates. Each black or white point (Craine *et al.*, 2010) is the product of either: a curve fitted to respiration from five subsamples incubated at 10, 15, 20, 25 or 30 °C, on one of 15 measurement dates, or data harvested from other studies. Filled black circles show respiration of plant biomass, open black circles show respiration of SOM. From this study: pale blue - whole soil 5 - 17 cm; dark blue - whole soil 20 - 30 cm; yellow - light fraction 5 - 17 cm ; orange - intra-aggregate 5 - 17 cm; red - mineral-bound fraction 5 - 17 cm. Each coloured point is faded in proportion to the r^2 value of the fit: full colour means an r^2 of 1, no colour means an r^2 of 0.)

4.6 Conclusions

Incubation of isolated fractions showed that rates of respiration on a g soil-C^{-1} basis were equally high in the light and intra-aggregate fractions, and even higher in the mineral-bound fraction, despite the presumed stability of OM-mineral associations and the high degree of humification in the intra-aggregate fraction. Respiration rates were lower in the 20 - 30 cm soil than in 5 - 17 cm soil, indicating that 20 - 30 cm SOM is more stable, due to a combination of humification and mineral interactions. Temperature sensitivity of respiration was higher in the light fraction than in the intra-aggregate or mineral-bound fraction, and was higher in unsterilised 5 - 17 cm soil than unsterilised 20 - 30 cm soil. These results suggest that stability in the 20 - 30 cm soil is primarily due to mineral associations rather than substrate quality. Higher respiration and lower temperature sensitivity in the mineral-bound fraction, compared to the light fraction, works against the initial hypothesis that the light fraction would be the most labile and least temperature sensitive; however, interpreting the mineral-bound fraction as labile supports to the predictions of Q theory, that temperature sensitivity is higher in less bioavailable SOM.

Chapter 5

Isotopic composition of SOM respired from Harwood forest soils and density fractions

5.1 Introduction- Isotopic approaches to study SOM stability

Measurements of SOM isotopic composition ($\delta^{13}C$, ^{14}C and ^{15}N) offer many different opportunities to study SOM dynamics in situ with minimal intervention. This is as a result of many different processes causing isotope discrimination during the formation, transformation and decomposition of SOM. Initially, plant litter and root material entering the detritosphere reflects the isotopic composition of the parent plant material. The ^{14}C content of plant material reflects the ^{14}C concentration of atmospheric CO_2 at the time of CO_2 assimilation. ^{14}C currently persists in atmospheric CO_2 at a concentration of about 105.4 pMC, degrading at a rate of about 0.4 pMC y^{-1} since a high point of 185 pMC during the thermonuclear weapons testing of the 1950s and 1960s. Prior to 1955, ^{14}C accumulated in atmospheric CO_2 due to the action of cosmic rays in the upper troposphere, producing neutrons which react with

atmospheric nitrogen.

The ^{13}C isotope occurs naturally at a composition of about -8 ‰ in atmospheric CO_2, and is discriminated against by virtue of its molecular weight during photosynthesis (primarily during diffusion through the stomata and into interstitial air spaces), during synthesis of organic compounds, and during decomposition and subsequent microbial transformations. $\delta^{13}C$ signatures vary between plants with different photosynthetic pathways for CO_2 fixation; within a plant, between different compounds; and within a compound or group of compounds over time, as a result of successive microbial discrimination during decomposition. All these properties and processes causing isotopic discrimination can be useful tools for discovering the history and likely fate of organic compounds in SOM.

C isotopic fractionation occurs during synthesis of certain plant compounds, leading to distinct $\delta^{13}C$ signatures of different plant tissues. For example, lignin is typically ^{13}C depleted by 2 - 6 ‰ with respect to whole woody biomass $\delta^{13}C$ (Benner *et al.*, 1987).

The ^{13}C isotope is also subject to discrimination by physical processes in the soil which can affect measurements of the $\delta^{13}C$ of soil respiration, for example advective gas transport (leading to a ^{13}C depletion) or atmospheric incursion (leading to a ^{13}C enrichment) (Kayler *et al.*, 2010). Measurements of $\delta^{13}C$ of soil respiration are strongly dependent on precipitation, vapour pressure deficit and temperature on a diurnal scale (Bowling *et al.*, 2002). In addition, isotopic fractionation during plant CO_2 uptake is also controlled by humidity and temperature, leading to variation in $\delta^{13}C$ signatures of woody biomass and cellulose (Sidorova *et al.*, 2008). Diurnal patterns in $\delta^{13}C$ of soil respired CO_2 have been observed in an Alpine grassland, reflecting diurnal trends in photosynthesis and root exudates (Bahn *et al.*, 2009).

^{13}C fractionation during microbial respiration is responsible for a ^{13}C depletion in increasingly humified material (Ågren *et al.*, 1996). This also leads to the prediction that $\delta^{13}C$ of respired CO_2 should decline over time, as was shown by Cross

and Grace (2010) using Harwood forest soil. In the shorter term however, incubation studies often show a ^{13}C enrichment in respired CO_2 over time, attributed to the community dynamics of the establishing microbial community (Crow *et al.*, 2006). Microbial fractionation in favour of ^{13}C can also cause an accumulation of more enriched material. Etcheverria *et al.* (2009) suggest that successive ^{13}C enrichment in forest soils is partly due to the accumulation of recalcitrant products of arbuscular mycorrhizae, as Glomalin-related soil proteins are ^{13}C enriched in relation to total microbial C as well as bulk SOC. SOM $\delta^{13}C$ has also been shown to increase with depth down soil profiles (Jenkinson *et al.*, 2008). Several studies show a ^{13}C enrichment associated with mineral-bound material, increasing with density (Sollins *et al.*, 2009; Mikutta *et al.*, 2006; Quideau *et al.*, 2003), and that acid-resistant fractions are ^{13}C depleted (Quideau *et al.*, 2003; Biasi *et al.*, 2005).

In this chapter, I present data showing the ^{14}C ages and MRT of soil density fractions and whole soils from 5 - 17 cm and 20 - 30 cm, as a direct measure of the "lifetime stability" of SOM. The same fractions and whole soils were incubated at 10 or 30 °C, and the accumulated CO_2 was collected for ^{14}C dating (see section 4.3.3). Based on the chemical and physical properties of the soils and fractions, I predict that the age of fractions will follow the sequence *light «intra-aggregate <mineral-bound*, and that the 20 - 30 cm soil will be considerably older than the 5 - 17 cm soil. The Q theory of substrates with a lower intrinsic quality having a higher temperature sensitivity, if intrinsic recalcitrance is dominant over other mechanisms of stability, would suggest that there might be a general relationship between temperature and the relative age of OM respired from each fraction. This chapter also contains information on the stable isotopic ($\delta^{13}C$,$\delta^{15}N$) composition of fractions and whole soils before and after the incubation at 10 and 30 °C. The behaviour of natural abundance stable isotopes in response to temperature is more difficult to predict, however I hypothesise that material remaining after incubation of the less humified samples (light fraction, whole soil 5 - 17 cm) will be depleted in $\delta^{13}C$ after the incubation, and more

so at the higher temperature.

5.2 Approach 1: ^{14}C dating of SOM, SOM fractions and respired CO_2

The ^{14}C content of organic material is used routinely by archaeologists and palaeontologists to estimate the 'age' or time since fixation of organic carbon, for example for dating the remains of animal or plant material. ^{14}C dating of soils operates on the same principles used for archaeological ^{14}C dating, with the key difference that SOM typically consists of a heterogeneous mixture of OM from different sources, while the ^{14}C content of plant and animal remains is relatively consistent. For this reason SOM ^{14}C dating should be considered a tool for estimating mean residence times rather than assigning precise ages to materials.

5.2.1 Methods- isotopic analyses of soils and respired CO_2

Samples of all whole soils and soil fractions were combusted in an elemental analyser (Costech ECS 4010, Cernusco, Italy). The total sample carbon was converted to CO_2 by heating with CuO in a sealed quartz tube and cryogenically recovered. CO_2 from whole soils and fractions, as well as respired CO_2 collected at 10 °C and 30 °C were converted to graphite targets by Fe/Zn reduction (Slota *et al.*, 1987) at the NERC Radiocarbon Facility (Environment), East Kilbride, UK. ^{14}C analysis was performed at the Scottish Universities Environmental Research Centre (SUERC) Accelerator Mass Spectrometry (AMS) facility (East Kilbride, UK). ^{14}C results were normalised for isotopic fractionation as directed by Stuiver and Polach (1977), using $\delta^{13}C$ values measured on a dual inlet stable isotope ratio mass spectrometer (VG OPTIMA Micromass, Manchester, UK) at the NERC Radiocarbon Facility. The sample ^{14}C activity

(A_S) is then normalised (A_{NS}) to a δ^{13}C of -25 ‰ using the equation

$$A_{NS} = A_S \left(\frac{1 - 2(25 + \delta^{13}C)}{1000} \right) \tag{5.1}$$

.

For SOM originally fixed before the first major thermonuclear weapons tests (~ AD 1955), the ^{14}C content reflects its age, as ^{14}C content decreases with time due to the radioactive decay of ^{14}C; during the 1950/60s the ^{14}C content of the atmosphere almost doubled (to 190 pMC) and has subsequently declined (to current levels ~ 104 pMC). SOM with ^{14}C greater than 100 pMC unequivocally shows the presence of at least some post-1950s ^{14}C. In reality, SOM in modern samples is quite likely to be a mixture of both pre- and post-bomb, and while ^{14}C values > 104 pMC imply a substantial component of carbon fixed since the 1950/60s, it does not preclude a sizeable proportion of the carbon being fixed in pre-bomb times. Similarly, SOM with ^{14}C contents of < 100 pMC could contain some carbon fixed in the post-bomb era.

5.2.2 Technical considerations for interpreting ^{14}C age

The age of organic carbon can be estimated by comparing the ^{14}C content to the paleological record of atmospheric $^{14}CO_2$, shown in Figure 5.1. Material with ^{14}C less than 100 pMC is likely to comprise predominantly pre-bomb C sources, and is relatively straightforward to date, as atmospheric $^{14}CO_2$ increased steadily until the 20th century. Material with ^{14}C above 100 pMC contains at least some post-bomb material, but may also contain material from prior to the bomb. If it can be assumed that a sample is entirely post-bomb or entirely pre-bomb, a conventional radiocarbon age can be assigned with relatively low uncertainty; however, since most of the samples analysed for this study had ^{14}C values close to 100 pMC, and since the stand was planted 30 years ago, it is likely that all samples contain a mixture of both pre-bomb and post-bomb C, making the interpretation of dates more complicated.

5.2.3 Estimation of mean residence times from ^{14}C content

Mean residence times of isolated fractions and whole soils and from respired CO_2 were estimated from the ^{14}C activity (percent modern, pMC) of SOM, based on two commonly applied single pool models, which I will call 1) the Hsieh model and 2) the Meathrop model.

The Hsieh model was proposed by Hsieh (1993):

$$A_a = \frac{\sum_{i=b}^{p}(e^{[-(p-1)/MRT]} \times {}^{14}C_i \times e^{[-(p-i)/8268]})}{\sum_{i=b}^{p}(e^{[-(p-i)/MRT]})} \tag{5.2}$$

where A_a is the ^{14}C activity of the active pool in pMC, p is the year of soil sampling, $^{14}C_i$ is the atmospheric ^{14}C activity in the year i, b is the base year (here, set as 26000 y BP, limited by available atmospheric ^{14}C data), MRT is the mean residence time of the active pool in years, and 8268 y is the mean residence time of ^{14}C in the atmosphere. This model assumes a constant SOC input to the active pool, and a steady state system, such that inputs (of SOC) and outputs (as CO_2) are equal. In using this model to account for the ^{14}C ages of separated fractions of the same whole soil, I make two assumptions: that C enters the soil in one fraction and remains in that fraction until mineralized; and that C inputs have been constant over time during the period considered during the model run (b – present). Where there were two possible solutions for MRT (^{14}C >104 pMC), the older MRT was taken to be the most parsimonious solution as choosing the younger MRT (<11 y) reduced agreement between composites.

"The Meathrop model" is described by Harkness *et al.* (1986), and also consists of a single SOC pool with constant SOC input and equal inputs and outputs. The model is described by the equation:

$$A_t = A_{t-1} \times e^{-1/MRT} + (1 - e^{-1/MRT})A_i - A_{t-1} \times \lambda \tag{5.3}$$

where A_t is the ^{14}C activity of the pool in year t, A_{t-1} is the activity established for the year before, A_i is the input ^{14}, or the atmospheric $^{14}CO_2$ of the previous growing season (year $t-1$), and λ is the ^{14}C decay constant (1.245 $\times 10^{-4}$ year^{-1}). The Meathrop model was also initiated at t = 26000 y BP for each sample, with A_t equal to A_i for the initial year.

Both the Hsieh and Meathrop models were tested for sensitivity to date of initialisation (b in the Hsieh model, $t = 1$ in the Meathrop model) by comparing the results (R) with b = 26000 y BP (b1) and 13000 y BP (b2), and using the equation

$$S.I. = \frac{\sqrt{[(R_{b2} - R_{b1})/R_{b1}]^2}}{b2/b1} \tag{5.4}$$

Using a more recent base year leads to overestimation of MRTs in the Hsieh model, and underesimation in the Meathrop model. Both models were insensitive to base year for MRTs < 2600 y (Figure 5.2), above which the Hsieh model became more sensitive. For MRTs in the range found in this study (all < 2600) the Hsieh model is less affected by the arbitrarily set base year, so I chose to use these values in the analysis. However, using 26000 y BP as the base year for both models gives very similar results (Figure 5.2, orange line), with < 0.6 % difference between the models in the range of MRTs found here.

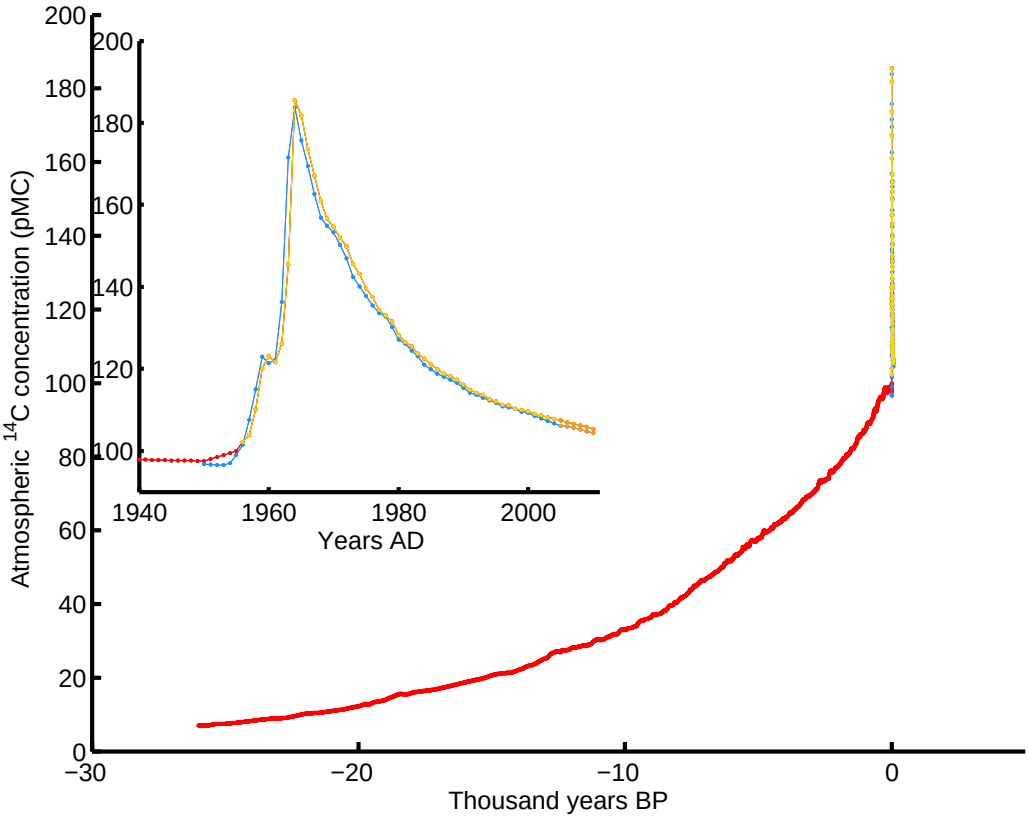

Figure 5.1: Atmospheric ^{14}C concentrations of the last 26 kyr BP, as used in MRT calculations. Red datapoints are from Reimer *et al.* (2004), blue datapoints are from Hua and Barbetti (2004), yellow datapoints are from Levin and Kromer (2004), and orange datapoints (since 2004) are extrapolated assuming a decay of 0.4 pMC year $^{-1}$.

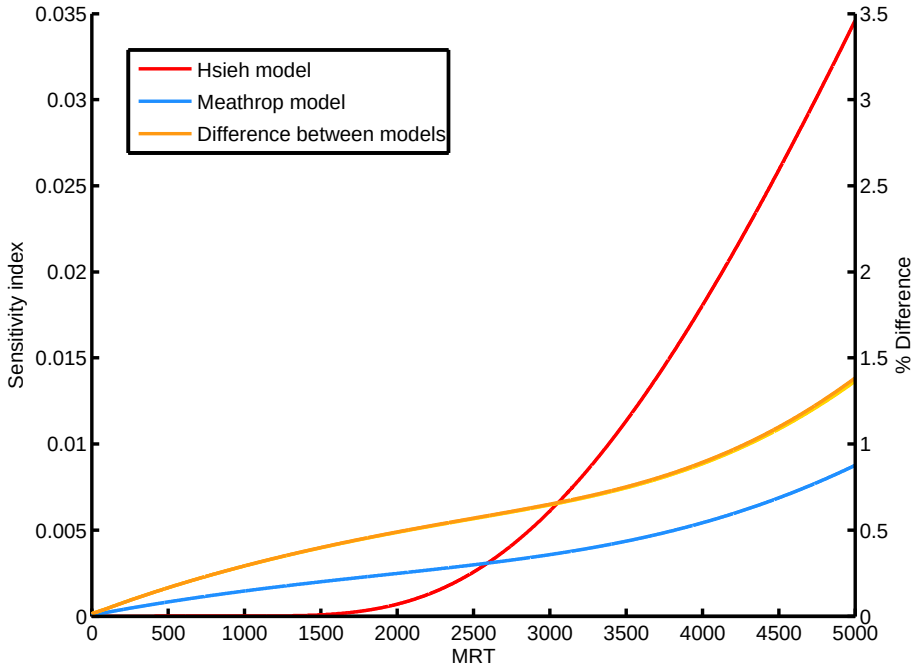

Figure 5.2: Sensitivity to base year of two models used to estimate MRT from ^{14}C dates, calculated by comparing model runs starting at 13 000 BP and 26 000 BP, using the equation 5.4. A sensitivity index of 1 would indicate that doubling the length of the run would double or halve the result. The orange line indicates the % difference between results of the two models

5.2.4 Results: ^{14}C age of SOM and respired CO_2

Solids

^{14}C dating of soils and fractions showed that all samples were relatively old in comparison to similar forest soils (Karhu *et al.*, 2010a). However, there were still significant differences in the ages of fractions and whole soils, which largely confirm the hypotheses that the stability of fractions will be in the order *light* < *intra-aggregate* < *mineral-bound*, and that whole soil SOM is considerably older at depth.

Whole soil ^{14}C contents at 5 - 17 cm were 97.8 (A) and 102.7 pMC (B), giving MRTs of 181 and 305 years, respectively (Table 5.2).

The A composite whole soil (97.8 pMC) is likely to comprise predominantly 'pre-bomb' carbon, while the B composite (102.7 pMC) whole soil also contains some 'post-bomb' carbon, however it is unlikely to be predominantly 'post-bomb' since the value is under 104 pMC. These two samples may still be quite similar in age, with slightly more younger SOC in the B composite.

Whole soil SOC at 20 - 30 cm was less ^{14}C enriched, at 76.24 (A) and 80.94 pMC (B) (MRT 1381 and 1072 y), resulting in a difference in mean residence times of around 1000 years between the 5 - 17 cm and 20 - 30 cm horizons.

Within the 5 - 17 cm samples, the light fraction was in both cases more ^{14}C enriched (younger) than the whole soil (99.52 (A) and 104.54 pMC (B), compared to 97.76 (A) and 102.71 pMC (B)) while the intra-aggregate and mineral-bound fractions were both less enriched, and hence older, than whole soil (92.57 - 94.56 pMC, compared to 97.76 (A) and 102.71 pMC (B)). The intra-aggregate and mineral-bound fractions were both significantly older than both the light fractions and the bulk material (2-way ANOVA, $p < 0.05$), but not significantly different in age themselves.

The difference in age between the two composites held for all fractions and whole soils at different depths: despite the composite sampling, composite B samples were all younger than their composite A counterparts.

Table 5.1: C, ^{13}C and ^{14}C contents and mean residence times of SOM density fractions and whole soils. Errors for C, N and C:N are 1 standard deviation of three replicates from the same subsample. All other errors presented refer to analytical confidence, and represent 1 standard deviation. CRA refers to Conventional Radiocarbon Age, in years before 1950 (y BP). A CRA values of 'mod' are given where the ^{14}C content is > 100 % modern. pMC stands for % modern carbon. Mean residence times (MRT) were calculated from the model described in equation 5.2, (Hsieh, 1993). Pub code refers to the unique publication code assigned to each sample by the NERC RCF

		C %	±	$\delta^{13}C$ (‰) ± 0.1	^{14}C (pMC)	±	CRA	±	MRT Hsieh	MRT Meathrop	Pub code
5 - 17 cm											
Whole soil	A	22.1	(6.2)	-28.6	97.76	(0.45)	182	(37)	305	302	SUERC-22680
	B	35.6	(2.3)	-28.0	102.71	(0.47)	mod		181	179	SUERC-22681
Light fraction	A	30.6	(2.0)	-28.1	99.52	(0.43)	39	(35)	255	252	SUERC-23858
	B	30.6	(1.1)	-27.8	104.54	(0.48)	mod		147	146	SUERC-23861
Intra-aggregate	A	24.9	(1.4)	-28.1	92.57	(0.43)	620	(37)	487	481	SUERC-23859
	B	30.7	(0.5)	-28.1	94.56	(0.44)	450	(37)	411	407	SUERC-23864
Mineral-bound	A	4.5	(0.7)	-28.0	92.82	(0.43)	599	(37)	477	472	SUERC-23860
	B	4.1	(0.6)	-27.6	92.69	(0.41)	609	(35)	483	477	SUERC-23865
20 - 30 cm											
Whole soil	A	28.8	(0.9)	-28.7	76.24	(0.35)	2179	(37)	1381	1361	SUERC-22679
	B	10.0	(0.4)	-28.7	80.94	(0.35)	1699	(35)	1072	1057	SUERC-28457

Respired CO_2

The ^{14}C contents of respired CO_2 (Fig. 5.3, Table 5.2) taken as a whole indicate that material respired at both 10 °C and 30 °C was more ^{14}C enriched (i.e. younger) than the incubated ('parent') soil material as a whole. This trend was consistent for the light, intra-aggregate and 5 - 17 cm whole soils, with high variation in the mineral-bound fraction and 20 - 30 cm soils. ^{14}C contents for CO_2 respired from mineral-bound fractions incubated at 10 °C were unavailable due to air contamination in one incubation jar, and insufficient CO_2 accumulation in the other.

The fact that respired CO_2 was consistently younger than parent SOM, in keeping with results from similar studies (Karhu *et al.*, 2010a), reflects the heterogeneous composition of separated fractions, whereby the younger material within a fraction is more readily respired than the older more stable subfraction. One mineral-bound fraction sample respired material much older than the incubated material, and one

light fraction sample respired material with the same MRT as incubated material. The smallest difference between ^{14}C of incubated material and $^{14}CO_2$ respired at each temperature occurred in the light fraction, confirming that this fraction is the least heterogeneous with respect to stability, reflecting a low stable SOM content.

There was no consistent relationship between temperature and the age of material respired, with composites A and B showing opposite effects in almost every pair (Fig. 5.3, Table 5.2). One exception to this was the light fraction material, where material respired at 30 °C was in both cases younger than material respired at 10 °C, demonstrated by ^{14}C contents closer to contemporary atmospheric ^{14}C. Previous studies have reported that older material is preferentially respired at higher temperatures (Bol *et al.*, 2003; Karhu *et al.*, 2010b).

Table 5.2: Elemental and isotopic composition of whole soils, SOM fractions, and respired CO_2. Errors for C, N and C:N are 1 standard deviation of three replicates from the same subsample. All other errors presented refer to analytical confidence, and represent 1 standard deviation. CRA refers to Conventional Radiocarbon Age, in years before 1950 (y BP). A CRA values of 'mod' are given where the ^{14}C content is > 100 % modern. pMC stands for % modern carbon. Mean residence times (MRT) were calculated from the model described in equation 5.2, (Hsieh, 1993). Pub code refers to the unique publication code assigned to each sample by the NERC RCF.

		SOM				Respired CO_2 (10 °C)				Respired CO_2 (30 °C)			
		^{14}C (pMC) ±	CRA (y) ±	MRT (y) Hsieh	MRT (y) Meathrop	Pub code	^{14}C (pMC) ±	CRA (y) ±	MRT (y) Hsieh	MRT (y) Meathrop	Pub code	^{14}C (pMC) ±	CRA (y) ±	MRT (y) Hsieh	MRT (y) Meathrop	Pub code
5 - 17 cm																
Whole soil	A	97.76 (0.45)	182 (37)	305	302	SUERC-22680	99.58 (0.46)	33 (37)	253	251	SUERC-27734	103.02 (0.48)	mod	174	173	SUERC-27735
	B	102.71 (0.47)	mod	181	179	SUERC-22681	109.11 (0.51)	mod	87	87	SUERC-28866	106.89 (0.50)	mod	111	111	SUERC-27728
Light fraction	A	99.52 (0.43)	39 (35)	255	252	SUERC-23858	99.53 (0.46)	38 (37)	255	252	SUERC-28855	101.82 (0.47)	mod	199	197	SUERC-27727
	B	104.54 (0.48)	mod	147	146	SUERC-23861	105.50 (0.49)	mod	132	132	SUERC-28859	107.07 (0.50)	mod	110	110	SUERC-27726
Intra-aggregate	A	92.57 (0.43)	620 (37)	487	481	SUERC-23859	97.38 (0.42)	213 (35)	316	313	SUERC-28856	96.86 (0.45)	257 (37)	333	329	SUERC-27731
	B	94.56 (0.44)	450 (37)	411	407	SUERC-23864	97.16 (0.45)	232 (37)	323	320	SUERC-28860	98.02 (0.45)	161 (37)	297	294	SUERC-27729
Mineral-bound	A	92.82 (0.43)	599 (37)	477	472	SUERC-23860	n.d.	n.d.	n.d.	n.d.		101.30 (0.47)	mod	211	209	SUERC-28861
	B	92.69 (0.41)	609 (35)	483	477	SUERC-23865	n.d.	n.d.	n.d.	n.d.		79.69 (0.42)	1824 (42)	1150	1134	SUERC28862
20 - 30 cm																
Whole soil	A	76.24 (0.35)	2179 (37)	1381	1361	SUERC-22679	71.80 (0.43)	2662 (49)	1717	1692	SUERC-28857	80.49 (0.43)	1744 (43)	1100	1085	SUERC-27730
	B	80.94 (0.35)	1699 (35)	1072	1057	SUERC-28457	93.56 (0.44)	535 (38)	449	443	SUERC-28858	84.14 (0.42)	1388 (40)	887	875	SUERC-28865

Since there was a general trend for material respired at either temperature to be younger than the incubated source material, due to the preferential respiration of a labile subfraction of each sample, it can be expected that the difference in age between respired and incubated material would be greater at earlier stages in the incubation, and decline as a larger proportion of the intial SOC is consumed and the labile substrate is depleted. During these incubations, samples were collected in batches after a threshold concentration of headspace CO_2 had been exceeded; since each sample had a different C content, there was high variation in the proportion of total sample C respired by the time the sample was taken for ^{14}C analysis. To test whether the proportion of total SOC used had an effect on the relative ^{14}C content of the respired CO_2, I estimated the proportion of total SOC used from the accumulated headspace CO_2 before sampling, and compared it to the difference between incubated and respired ^{14}C content (Fig. 5.4). Excluding the one outlying mineral-bound fraction at 30 °C which produced respired CO_2 that was considerably older than the incubated material, there would be a marginally significant weak negative correlation (r^2 = -0.48, p = 0.048) between the log of the proportion of total SOC respired and the age difference between incubated and respired material. That is to say, samples where a larger proportion of the total SOC was used would have a larger respiratory bias towards younger material. However, since only two datapoints are available for this fraction, it would be inappropriate to exclude only one; excluding both mineral-bound fraction samples, the weak negative correlation is not significant (r^2 = -0.33, p = 0.2).

While there is no significant negative correlation, the data do not show the expected positive correlation, whereby younger material would be respired first, and older material left for later. Alongside results showing similar respiration rates for isolated fractions that are 500 years apart in age (Chapter 4, Figure 4.1), this suggests that the stabilisation mechanisms responsible for the long MRT of these fractions and soils in the field may no be longer operating, under incubation conditions.

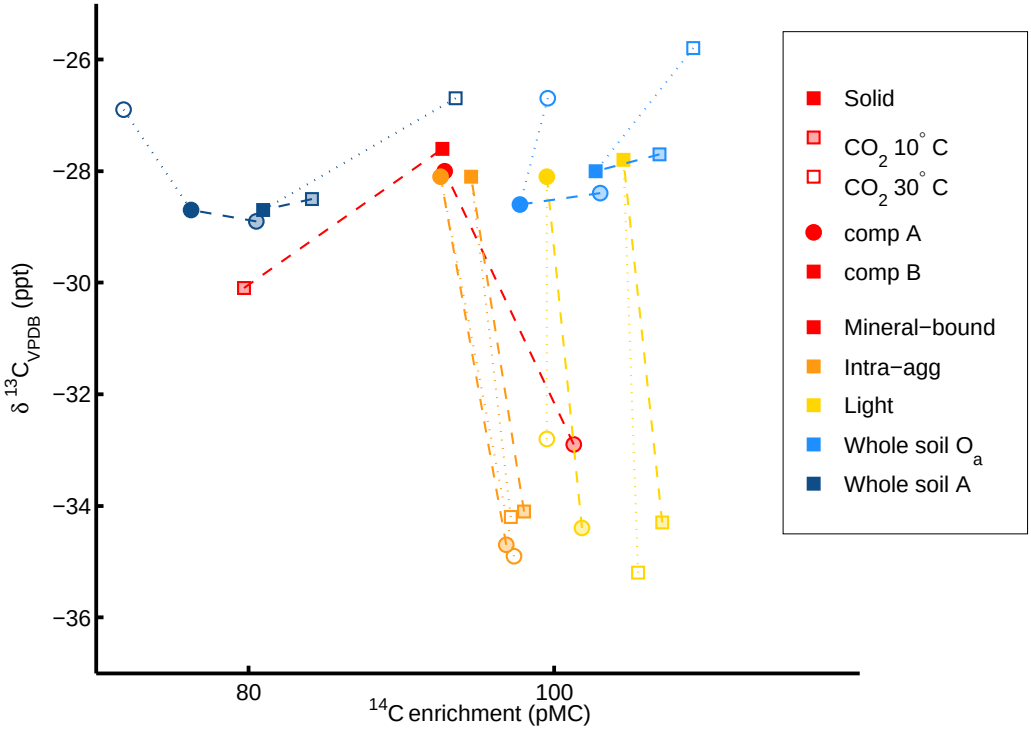

Figure 5.3: Carbon isotopic composition ($\delta^{13}C$ and ^{14}C) of initial SOM and CO_2 respired at 10 and 30 °C during the cumulative incubation. Solid points show the $\delta^{13}C$ and ^{14}C enrichment of SOM, and open points show enrichment of respired CO_2, and dashed lines connect respired CO_2 measurements to their source SOM sample.

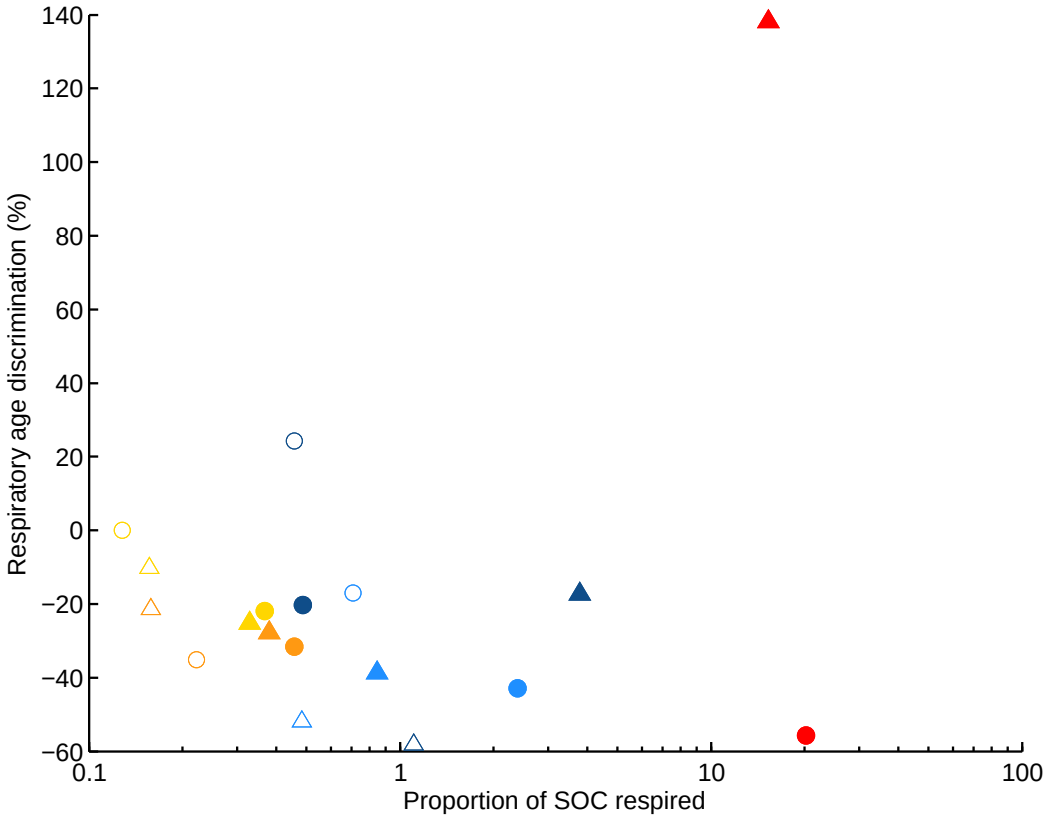

Figure 5.4: Respiratory age discrimination as a function of proportion of SOC respired. 'Respiratory age discrimination' calculated as percentage difference in MRT (Hsieh, 1993) between respired CO_2 and SOM; values above 0 indicate respired CO_2 was older than source SOM. Red –mineral bound fraction; orange –intra-aggregate fraction; yellow –light fraction; pale blue –5 - 17 cm whole soil; dark blue –20 - 30 cm whole soil. Filled markers indicate respiration at 30 °C, unfilled markers indicate respiration at 10 °C. Circles show composite A, triangles show composite B.

5.3 Approach 2: Using natural abundance $\delta^{13}C$ signatures to study SOM dynamics

Natural ^{13}C discrimination offers several different opportunities to study SOM dynamics with minimal disruption. During the cumulative incubation described in section 4.3.3, information was also gathered about the ^{13}C signature of material respired. All samples processed for ^{14}C dating (SOM fractions, whole soils and respired CO_2

from fractions and whole soils at 10 and 30 °C) were analysed for $\delta^{13}C$ in the process of ^{14}C dating, to correct for biological isotopic discrimination. In addition, at the end of each incubation the remaining material was retained for $\delta^{13}C$ and $\delta^{15}N$ analysis. In this section I present these data and discuss the implications for SOM cycling.

5.3.1 Results: Stable isotopic composition of SOM and respired CO_2

Initial solids

Isolated fractions from the 5 - 17 cm whole soil were found to be slightly enriched in ^{13}C in relation to the whole soils (Table 5.3), with the mineral-bound fraction the most enriched in both cases. DOC extracted for inoculation was ^{13}C more enriched than isolated fractions (-26.5 ‰). DOC has been shown to be ^{13}C enriched due to lower hydrophobic lignin components (Golchin *et al.*, 1994). Other studies have found that light and occluded fractions are ^{13}C-depleted in respect to whole soil (Dorodnikov *et al.*, 2011), while mineral bound material is often enriched (Crow *et al.*, 2006; Dorodnikov *et al.*, 2011; Sollins *et al.*, 2009; Mikutta *et al.*, 2006).

Whole soils at 20 - 30 cm were depleted in ^{13}C in relation to 5 - 17 cm whole soils, in contrast to the usual trends of increasing ^{13}C enrichment with depth (Amundson *et al.*, 1998; Jenkinson *et al.*, 2008). Considering that the C:N ratio in these soils also increased with depth instead of decreasing (see Fig 3.3), I suggest that this is the result of a high lignin content in the 20 - 30 cm soil (Benner *et al.*, 1987; Golchin *et al.*, 1994).

Respired CO_2

Material respired from all isolated fractions was ^{13}C-depleted by an average of 5.5 ‰ with respect to incubated material (Table 5.2, Fig. 5.3), while no such depletion was visible in any whole soil incubations. This was not explained by the addition of inoculum material, which was more ^{13}C enriched than all fractions and whole

soils. One possible cause of this isotopic fractionation is the microbial community shift associated with initial incubation conditions. Laboratory incubations of SOM (Crow *et al.*, 2006; Andrews *et al.*, 2000) and leaf residues (Schweizer *et al.*, 1999) have shown respired CO_2 with strong ^{13}C depletion in the first few days of an incubation, returning to a slightly enriched value over time. Iodine is known to contribute to changes in microbial community structure (Cotton, 1930; Amachi *et al.*, 2003). Qualitative SEM-EDX analysis (see Appendix A) revealed low levels of residual I (but no residual Na) preferentially bound to OM in the rinsed fractions, which may have contributed to the isotopic fractionation. Note that by convention ^{14}C contents were normalised to a $\delta^{13}C$ of -25 ‰, and were therefore insensitive to these fractionation effects.

There was a clear trend in the whole soil incubations for a greater ^{13}C enrichment of CO_2 respired at lower temperatures. A similar trend was also reported on whole soils from the same site by Cross and Grace (2010). Respired CO_2 from the incubation of all isolated fractions at both temperatures was depleted in ^{13}C with respect to the parent fraction or whole soil (Fig. 5.3).

Isotopic composition of remaining solids

Given the different stable isotopic composition in SOM components with different properties, in particular the ^{13}C depletion of lignin (Benner *et al.*, 1987) and observed progressive ^{13}C depletion during humification (Ågren *et al.*, 1996), it would be reasonable to expect ^{13}C discrimination to occur during respiration, and for there to be an effect of temperature on the ^{13}C discrimination experienced. However, several studies have failed to demonstrate a unifying stable isotopic fractionation effect during heterotrophic respiration, largely because of the variation in $\delta^{13}C$ of SOM and the cancelling out of any identifiable fractionation effects- such as the enrichment of mineral-bound material (Sollins *et al.*, 2009; Mikutta *et al.*, 2006; Quideau *et al.*, 2003), depletion of humified material (Ågren *et al.*, 1996) the depletion acid-insoluble

Table 5.3: $\delta^{13}C$ of density fractions and whole soils and respired CO_2 at 10 and 30 °C from the same samples

		$\delta^{13}C$ (‰, ± 0.1)		
		SOM	10 °C	30 °C
5 - 17 cm				
Whole soil	A	-28.6	-26.7	-28.4
	B	-28.0	-25.8	-27.7
Light fraction	A	-28.1	-32.8	-34.4
	B	-27.8	-35.2	-34.3
Intra-aggregate	A	-28.1	-34.9	-34.7
	B	-28.1	-34.2	-34.1
Mineral-bound	A	-28.0	-31.2	-32.9
	B	-27.6	n.d.	-30.1
20 - 30 cm				
Whole soil	A	-28.7	-26.9	-28.9
	B	-28.7	-26.7	-28.5

recalcitrant material (Biasi *et al.*, 2005; Quideau *et al.*, 2003). Despite separating a well-humified fraction and a mineral-bound fraction, I did not find differences in $\delta^{13}C$ between fractions. Therefore it should not be surprising that I also found no overall effect of respiration or incubation temperature on the $\delta^{13}C$ of soils remaining after incubation.

Conen *et al.* (2008) proposed that $\delta^{15}N$ and C:N can be used as a proxy for the degradedness of SOM, as C:N decreases and $\delta^{15}N$ increases with progressive microbial transformations. Under this model, the remaining $\delta^{15}N$ of material left after incubation should be higher than the starting $\delta^{15}N$, the C:N should be lower, and smaller differences in $\delta^{15}N$ and C:N indicate more stable initial material. Since some inorganic N was added prior to the incubation, $\delta^{15}N$ and C : N of initial substrates and remaining substrates are not comparable. This may explain the absence of a decline in the C : N ratio in the incubated material. However, the $\delta^{15}N$ and C : N

of the temperature treatments can still be interpreted: neither showed an effect of temperature.

The ^{13}C depletion observed in respired CO_2 from isolated fractions (Fig. 5.3) is not immediately mirrored by a strong enrichment $\delta^{13}C$ of remaining fractions (Fig. 5.5). However, approximation of the remaining $\delta^{13}C$ that should result from the maximum proportion of carbon lost (10 %), with the average depletion experienced by the isolated fractions (~ -5.5 ‰) and the average $\delta^{13}C$ of the initial fractions (~ -28 ‰) shows that the maximum enrichment expected of the remaining fractions is 0.37 ‰, which is within the range demonstrated (Fig. 5.5). The $\delta^{13}C$ of respired CO_2 is likely to have a lower sample error than the $\delta^{13}C$ of remaining solids, since the CO_2-C is homogenised by diffusion and the whole population was collected for analysis, whereas the solids were homogenised by grinding and a subsample was analysed.

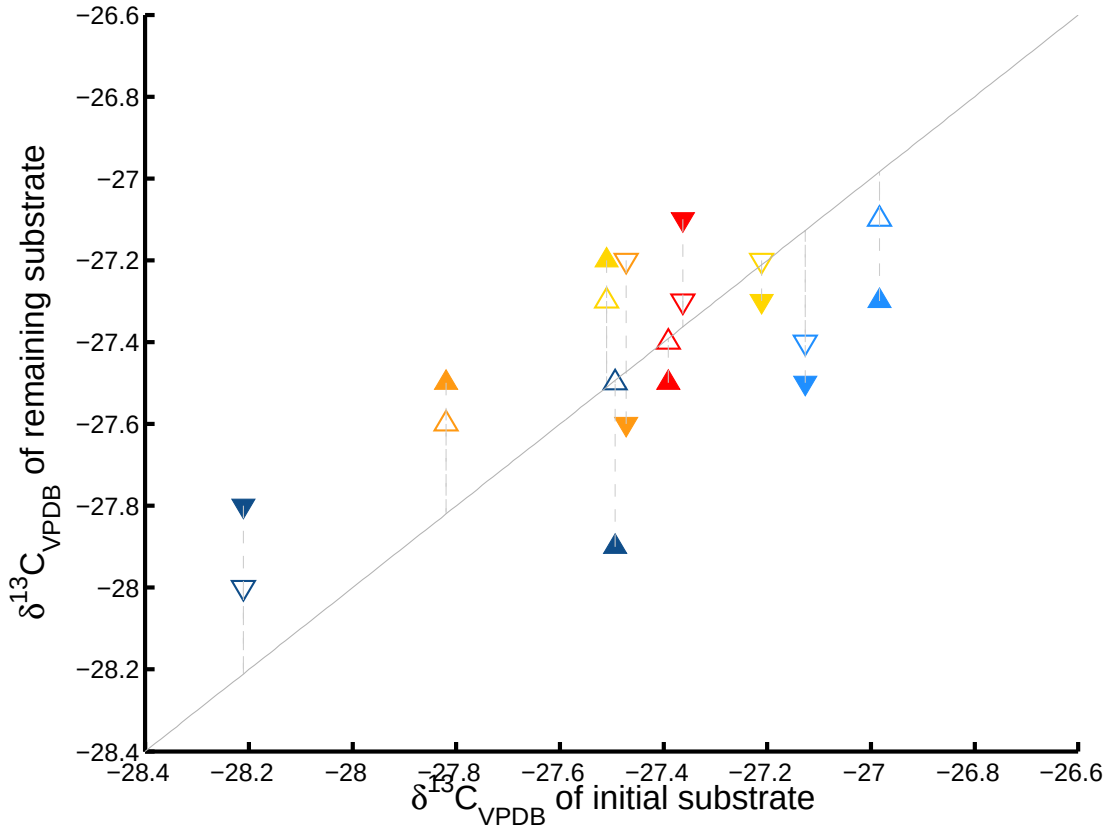

Figure 5.5: $\delta^{13}C$ of remaining SOM after incubation at 10 or 30 °C versus initial $\delta^{13}C$. Red –mineral bound fraction; orange –intra-aggregate fraction; yellow –light fraction; pale blue –5 - 17 cm whole soil; dark blue –20 - 30 cm whole soil. Open triangles–10 °C, closed triangles–30 °C. Grey line–1:1.

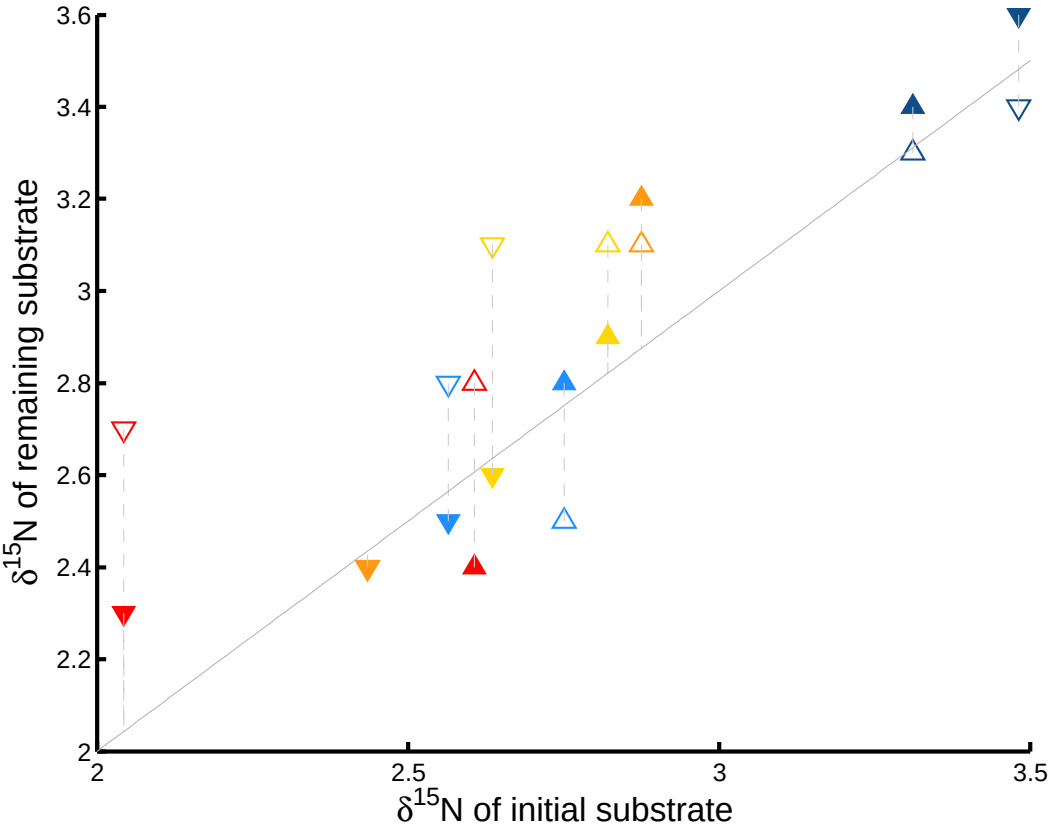

Figure 5.6: $\delta^{15}N$ of remaining SOM after incubation at 10 or 30 °C versus initial $\delta^{15}N$. Red –mineral bound fraction; orange –intra-aggregate fraction; yellow –light fraction; pale blue –5 - 17 cm whole soil; dark blue –20 - 30 cm whole soil. Open triangles–10 °C, closed triangles–30 °C. Grey line–1:1.

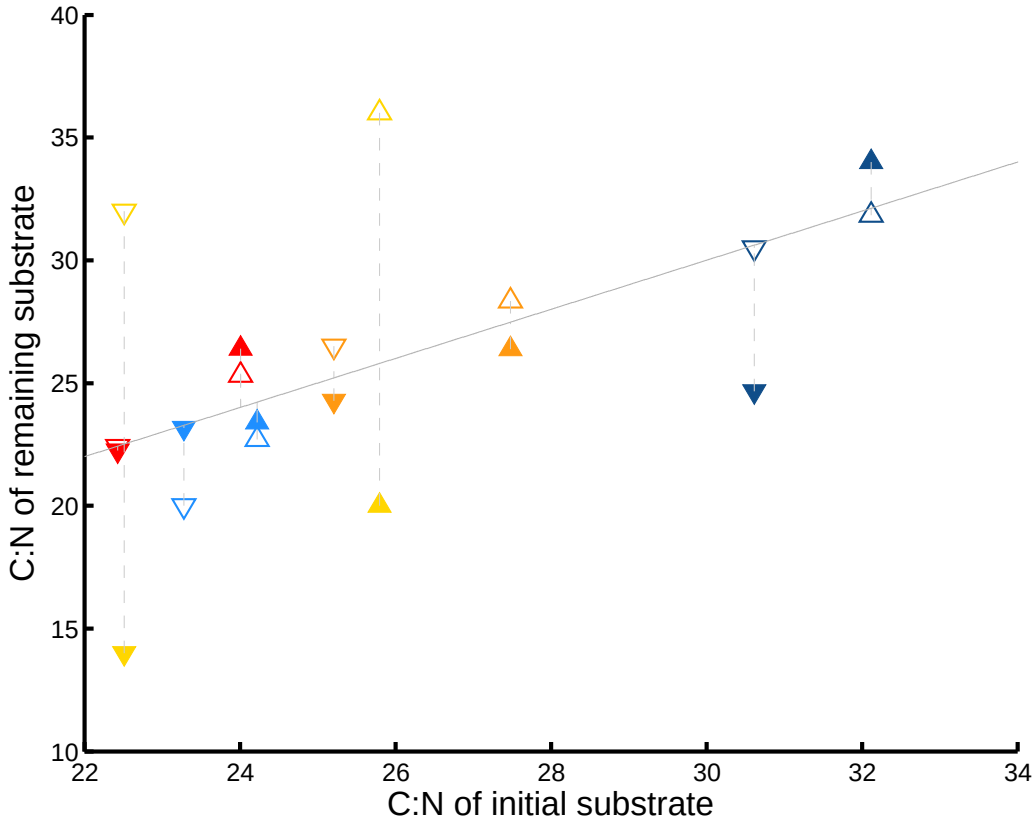

Figure 5.7: C : N ratio of remaining SOM after incubation at 10 or 30 °C versus intial C : N ratio. Red –mineral bound fraction; orange –intra-aggregate fraction; yellow –light fraction; pale blue –5 - 17 cm whole soil; dark blue –20 - 30 cm whole soil. Open triangles–10 °C, closed triangles–30 °C. Grey line–1:1.

5.4 Conclusions

In this experiment, I used the isotopic composition of respired material for insight into the temperature sensitivity of respiration. No effect of temperature was found on the ^{14}C or $\delta^{13}C$ of respired CO_2, nor on the $\delta^{15}N$, $\delta^{13}C$ or C:N ratio of remaining solids. ^{14}C dating of whole soils and fractions confirmed that SOM at 20 - 30 cm and in the mineral-bound and intra-aggregate fraction of the 5 - 17 cm soil are considerably older and more stable, at least *in situ*, than whole soil or light material. However, these age differences were not reflected by differences in the sensitivity

of respiration to temperature. Most fractions and whole soils at both 10 and 30 °C released CO_2 with a ^{14}C content indicating a younger-than-average source of respiration, but there no was effect of temperature. A positive relationship between the ^{14}C discrimination of respiration and proportion of SOM respired would indicate that progressively older SOM was respired over the course of the incubation; results here showed no such clear relationship. This may suggest that the most labile subfraction of each fraction incubated here has not yet been depleted, meaning that these incubation results don't reflect the respiration of truly 'stable' material.

There was no firm evidence of the expected positive correlation between the ^{14}C discrimination of respiration and the proportion of SOC consumed during the incubation, indicating that decomposition did not observably progress from younger to older material over the course of the incubation. This supports findings in chapter 4 that indicate the stabilisation mechanisms primarily responsible for the age of fractions were not operating at full capacity during the incubation.

Chapter 6

Priming effects of labile substrate additions in Harwood forest soil horizons

As discussed in Chapter 1, predictions of soil C storage and loss are hampered by a lack of understanding of the stability of different forms of SOM. The effective stability of SOM is manifested in the rate at which it can be mineralised by decomposers. Stability therefore depends not only on the intrinsic quality of the SOM, but also on the microbial community, which in turn is also dependent on other aspects of the soil environment such as temperature, water content and pH. What we consider to be a 'stable' pool of SOM can rapidly become labile given the right decomposer community, and labile material is effectively stable in the absence of decomposers. Since SOM in the soil matrix is a heterogeneous mixture of SOM pools, and since both the amount of microbial biomass and to an extent the microbial community, is dependent on substrate, it follows that decomposition of a given pool of SOM should be affected by the presence of adjacent substrates.

Lateral effects on respiration rate from one pool to another are often termed 'priming effects'. Numerous studies report a priming effect (PE) on soil respiration after the experimental addition of labile or nutrient-rich substrates to soil. Both positive (Ohm *et al.*, 2007) and negative priming (Guenet *et al.*, 2010) have been reported (see Table 6.1), and both are generally attributed to shifts in microbial community structure caused by the addition of the new substrate.

In laboratory studies, a range of different organic compounds have been added to soil to investigate priming effects, including sources of labile and more complex sugars, amino acids and other organic acids. Several studies have used natural abundance or radio-isotope labelling to successfully partition soil respiration after primer addition into primer-derived CO_2 and SOM-derived CO_2, distinguishing priming effects from an increase in total respiration (see Table 6.1). Labile sugars and amino acids may be 'added' to soil during rhizodeposition, microbial cell death, and may come into contact with SOM due to physical disturbance and bioturbation of soils. In practice, priming of respiration from one SOM pool to another is likely to be the result of several element interactions, as limiting nutrients may be supplied as well as limiting energy in the form of labile C; several studies have shown that mixed additions (C + N, fructose + alanine) result in higher priming effects than single additions (Hopkins *et al.*, 2008; Hamer and Marschner, 2005). In nutrient limited, C-rich soils, labile C additions alone may have no effect on SOM mineralisation, while N or other nutrient additions will (see e.g. Rinnan *et al.*, 2007). There is a wide literature on the effects of nutrient and litter additions to SOM mineralisation. As nutrient dynamics are not a major focus of the thesist, this Chapter will focus mainly on C priming effects from labile C additions.

Proposed mechanisms for positive priming effects of stable SOC due to labile OC additions include: co-metabolism of recalcitrant materials due to complementary substrate stoichiometry; incidental decomposition due to increased production of extracellular enzymes to break down the labile material, which may also be partially

effective at breaking down SOM (Fontaine *et al.*, 2004b), or due to increased overall microbial population (including some generalists).

Proposed mechanisms for negative priming effects of stable OM due to labile OM additions include preferential use of labile substrates by generalist microbes, competition (eg for water, oxygen) between labile substrate specialists and generalists/SOM specialists.

We can expect priming to be very dependent on the amount of both SOM-C and primer-C present, as well as the nutrient status of each. Blagodatskaya and Kuzyakov (2008) report a meta-analysis of priming studies, showing that priming tends to be positive and increases with labile additions up to 50% of the microbial biomass C, above which priming decreases rapidly and sometimes becomes negative.

A variety of approaches are used to distinguish between primer and primed C in respired CO_2 after primer addition, mostly using a C isotope label in order to partition respiration into at least two 'sources'. In addition, most studies invoking priming effects to explain substrate interactions make a distinction between 'apparent' priming effects (APE) and 'real' priming effects (RPE). When a labelled primer is added, an early burst of un-labelled respiration is often observed, due to the respiration of unlabelled microbial biomass-C as the primer C is consumed; since this does not reflect the incorporation of unlabelled SOM but is isotopically similar to SOM respiration, it is termed 'apparent priming'. Therefore, it is important to account for microbial biomass turnover in interpretations of priming effects.

This Chapter presents data from three successive experiments investigating the priming effects of C_4-derived sucrose additions on soil respiration from two horizons of (C_3-derived) Harwood forest soil, with or without added nutrients and soil disturbance. Where similar isotope labelling studies partiton respiration over time periods of several hours to several days, I measured respired $\delta^{13}C$ continuously at a rate of 60 Hz using TDL spectroscopy, allowing for a high temporal resolution view of substrate use during the respiratory burst following sugar addition. I compare

sucrose additions with added nutrient solution to sucrose additions without added nutrients, and two methods of applying the sucrose / nutrient mixture: with or without the physical disturbance of mixing. I am testing the hypothesis that labile sugar additions induce a higher respiration of native SOM. I predict that the more recalcitrant SOM found in 20 - 30 cm soil will show a more positive priming effect than the already labile material in the 5 - 17 cm soil, and that the addition of nutrient solution will result in a smaller priming effect.

Table 6.1: Labile substrate addition studies in the literature

Study	Soil type	Primer	Label	Application rate $\mu g\ C\ mg^{-1}$ SOC	Priming effect %	Pattern
Blagodatskaya *et al.* (2011)	loamy Gleyic Cambisol	Glucose	^{14}C glucose, ^{13}C C_3/C_4 label of 'older' SOM	100, 1000	short term- 110, 125; long term- 25, 41	PE not linear with primer conc
Blagodatskaya *et al.* (2007)	loamy Luvic Chernozem	Glucose, KNO_3 (factorial)	^{14}C	48.7, 4870		PE positive with low glucose, negative with high glucose. Lower and more negative PEs with N added.
Hamer and Marschner (2005)	Dystric Cambisol, Haplic Podzol	Fructose, alanine, catechol, oxalic acid	^{14}C	13.3, 2.2	+596 (fru + ala), -23 - 129 (fru, ala, cat, oxa)	Repeated additions led to increased mineralisation
Ohm *et al.* (2007)	Haplic Podzol size fractions	Fructose, alanine	^{14}C	3.3, 13.3	0 - +340	PE highest in clay, lowest in sand
Cheng (2009)	Mollisol	Rhizodeposits	C_3/C_4	na	0 - +380	PE diminishes over time since planting
Fangueiro *et al.* (2007)	Dystric/Eutric Cambisol	Dairy slurry size fractions	C_3/C_4	333	200 - 800	Size of PE negatively related to slurry particle size, duration of PE positively related
Fontaine *et al.* (2004b), Fontaine *et al.* (2004a)	Ultisol	Cellulose, + cellulase	^{13}C	47.1	+55	Cellulase responsible for 14 % of total PE.
Guenet *et al.* (2010)	Luvic Cambisol, 80 year fallow	Cellulose	^{13}C	100	-70	More negative priming with inoculation of FOM-specific decomposers
Hamer and Marschner (2002)	Sand mixed with peat or lignin	Glucose, fuctose, alanine, glycine, oxalic acid, acetic acid and catechol	^{14}C	13.3, 2.7	-13 (oxa + lig) to +157 (oxa + peat)	PE mostly positive, negative PE where catechol and oxalic acid were added to lignin. Alanine gave high PE in lignin, oxalic acid gave high PE in peat.
Kuzyakov and Bol (2006)	Eutric Cambisol, Dystric Gleysol	Slurry followed by sucrose	$C_3, v\ C_4$	30	na	Negative PE on SOM-C, and positive PE on slurry-C, in both soils.
Rinnan *et al.* (2007)	Arctic highly organic, moist soil	Litter (*Betula pubescens* ssp. *tortuosa*)rhizodeposits (*Carex capillaris*)	none	90 g m^{-2}	none	Bacterial growth rate and soil respiration increased in response to multiple nutrient additions, not single nutrient additions. No evidence of C limitation.
Salomé *et al.* (2010)	Eutric Cambisol / Luvisol, 5-10 cm, 80-100 cm	Fructose	^{13}C	13.3	na	Fructose additions resulted in higher soil respiration in topsoils, but not in subsoils. However, CO_2 was not partitioned to show fructose-derived and SOM-derived fractions.
Bell *et al.* (2003)	Calcidic Halpoxeroll	Wheat straw (*Triticum aestivum*)	^{14}C	0.25 $\mu g\ C\ g\ soil^{-1}$	consistently positive	PE strongly and positively correlated with fungi:bacteria ratio of all treatments.
Hamer *et al.* (2004)	Black C mixed with sand	Glucose	^{14}C	20	36 - 189	Strong correlation between glucose mineralisation and BC mineralisation, suggesting co-metabolism is responsible for PE.

6.1 Methods

Soil samples were taken from the site at Harwood Forest, as described in Chapter 2. Three soil pits were dug to 30 cm, and samples were taken from 5 - 17 cm and 20 - 30 cm in each pit. Samples were transported in a coolbox and stored in a fridge at 4°C. Once back in the laboratory, the three samples from each horizon were seived to 2 mm at field moisture to remove large roots and combined to form a single composite sample from each horizon, as described in Robertson *et al.* (1999, p.7). Soil subsamples and cane sugar samples (Sainsbury's FairTrade light brown soft sugar) were analysed for OM content, C, H and N content, water holding capacity, $\delta^{13}C$ and $\delta^{15}N$ (see Chapter 3). The priming experiment was repeated three times over the course of two years using soils collected at various dates not more than four months before the start of each incubation. Soil samples used in incubations 1 and 2 were collected in June 2009 and the incubations performed during July and August 2009. Soil samples used in incubation 3 were collected in August 2010 and the incubations performed in September 2010.

Soil samples adjusted to 65% WHC were packed into 1.8 L Kilner jars, adapted to fit TDL inlet and outlet tubes through the lid of the jar. All jars were incubated at 30 °C for at least five days until CO_2 efflux appeared to stabilise. Sugar and nutrients were added at rates described in table 6.2. During the first incubation sugar was added on a g soil $^{-1}$ basis; for the second and third incubations sugar was added on a g soil-C $^{-1}$ basis. Values used in the first experiment for sugar additions to mineral soil (in mg sugar g soil $^{-1}$) are equivalent to values used in subsequent incubations (in mg sugar g soil-C $^{-1}$), whereas additions to the 5 - 17 cm soil during incubation 1 are not strictly comparable with the other additions due to the different soil C contents of the two horizons. During incubation 2 a control jar with ashed, carbonate-free white quartz sand, soil inoculum solution (prepared as described in Chapter 4), nutrient solution and sugar was incubated alongside the soil samples.

In all three incubations, four jars from each horizon were incubated, two with sugar added and two controls. One of the primed 5 - 17 cm samples in the first incubation was abandoned due to leaks or blockages in the manifold sampling tubes.

Priming solution was prepared by added by dissolving pure cane sugar in distilled water, either on its own or containing an OM-free nutrient solution at 5 ml l^{-1} (Formulex, Growth Technology, Taunton, UK; see Appendix B). The incubation jars were reweighed on the day of sugar additions, and each jar was re-wetted to 65% WHC by adding the required dose of priming/nutrient solution topped up with distilled water. Control (unprimed) soil samples were re-wetted using distilled water including the same dosage of nutrient solution at the same time. Liquids were added with or without mixing, in the first incubation instance by pouring the liquid slowly into the soil and stirring with a large spoon to allow even contact between SOM and primer, and in the second and third incubations by spraying evenly over the top surface of the soil using a pipette.

Tunable Diode Laser determination of CO_2 and isotopic composition of CO_2

The tunable diode laser (TDL) is a high precision infrared spectrometer with a supercooled crystal source and a 1.5 m laser path. The TDL was configured for automated switching between 8 sample lines, with a sample period of 30 minutes (and a return time of 4 hours) for each line. During the 30 minute sample period, measurements alternate between input and output lines every 30 seconds, with two calibration gases (nominal values of 330 and 600 ppm CO_2) sampled for 30 seconds every 5 minutes. Within each 30 second period the sample gas, flowing at 200 ml min^{-1}, is continuously analysed for $^{12}C^{16}O_2$ and $^{13}C^{16}O_2$ every second. Air samples were drawn through a 50 L buffer volume before entering the sample headspace, to reduce variation due to atmospheric pressure fluctuations. The mass flow, pressure and sample temperature are simultaneously measured to allow accurate and high resolution determination of total CO_2 and $\delta^{13}CO_2$. Measurements of each isotope from the two

calibration gases sampled every 5 minutes were linearly interpolated to give a value for each 30 second period, and gain (G) and offset (O) factors were calculated for each isotope from the following equations:

$$G = \frac{X_C - X_B}{X_{Cm} - X_{Bm}} \tag{6.1}$$

$$O = X_C - GX_{Cm} \tag{6.2}$$

where X_C and X_B were the true mole fractions ($^{12}CO_2$ or $^{13}CO_2$) in tanks B and C, and X_{Cm} and X_{Bm} were the measured mole fractions of each tank. The sample mole fractions (X_i) were then calculated from the measured mole fractions using:

$$X_i = X_m G + O \tag{6.3}$$

Total air sample CO_2 concentrations were calculated from the following formula:

$$CO_2 = \frac{^{12}CO_2 + ^{13}CO_2}{1 - f_{other}} \tag{6.4}$$

where f_{other} is the fraction of all CO_2 isotopomers that are not $^{12}C^{16}O_2$ or $^{13}C^{16}O_2$ (0.00474). $\delta^{13}C$ was determined in ‰, relative to the international carbon isotopic standard, VPDB (0.0112372), using

$$\delta^{13}C = \left(\frac{^{13}C/^{12}C}{R_{VPDB}} - 1 \right) \times 1000 \tag{6.5}$$

The proportions of respired CO_2 derived from soil and from added sugar were calculated from the using the following equation, for each 30 second interval:

$$F_a = (\Delta_m - \Delta_s)/(\Delta_a - \Delta_s) \tag{6.6}$$

where F_a is the fraction of respired CO_2derived from the added sugar, Δ_m is the

measured $\delta^{13}C$ of respired CO_2, Δ_s is the measured $\delta^{13}C$ of solid SOM and Δ_a is the measured $\delta^{13}C$ of respired CO_2 from the soil-free sugar control used in incubation 2.

Soil microbial biomass C was measured for subsamples of the original composite samples, and for subsamples of the incubated soil from incubations 1 and 2, by the chloroform fumigation extraction method. Samples were analysed at the Scottish Agricultural College, Edinburgh campus. Total $KMnO_4$-extractable C was measured with a TOC analyser for soil samples that had been fumigated with chloroform for 24 hours, and control samples that had not. The difference in extractable C between the fumigated and control soils is attributed to dead biomass killed by fumigation. Total microbial biomass C is estimated assuming that the biomass killed during fumigation represents 45% of the total microbial biomass (Jenkinson *et al.*, 2004), although this proportion (0.45, K_{EC}) is known vary between soils, and reported values range from 0.10 to 0.73 (Martens, 1995). Unpaired Student's t-tests were used to compare microbial biomass C of treated soils in the two horizons.

$$\text{Total microbial biomass C} = (\text{Extractable C of fumigated soil} - \text{Extractable C of control soil}) / K_{EC} \quad (6.7)$$

Table 6.2: Rates and effects of sugar addition

	Depth	Sample	Sugar µg sugar-C mg soil-C^{-1}	Addition basis	Addition method	Nutrient solution	Priming
First incubation	5 - 17 cm	1	1.63	g $soil^{-1}$	Stirred	N	-
(July 2009)	20 - 30 cm	1	4.39	g $soil^{-1}$	Stirred	N	/
	20 - 30 cm	2	4.39	g $soil^{-1}$	Stirred	N	+
Second incubation	5 - 17 cm	1	4.39	g soil-C^{-1}	Stirred	Y	–
(August 2009)	5 - 17 cm	2	4.39	g soil-C^{-1}	Stirred	Y	-
	20 - 30 cm	1	4.39	g soil-C^{-1}	Stirred	Y	-
Third incubation	5 - 17 cm	1	4.39	g soil-C^{-1}	Poured	Y	++
(September 2010)	5 - 17 cm	2	4.39	g soil-C^{-1}	Poured	Y	++
	20 - 30 cm	1	4.39	g soil-C^{-1}	Poured	Y	++
	20 - 30 cm	2	4.39	g soil-C^{-1}	Poured	Y	++

6.2 Results

6.2.1 Respiration rates

All three incubations showed 20 - 30 cm soil and 5 - 17 cm soil respiring similar amounts of CO_2 per g soil-C (Figs 6.1,6.2,6.3), despite having very different soil C concentrations and microbial biomass (Table 6.3). The three incubations showed respiration rates within similar ranges, although there were differences between incubations, which can be explained by differences in the incubation conditions.

During the first incubation, respiration rates ranged from 100 to 600 μg CO_2-C g soil-C^{-1} day^{-1} for primed and unprimed soil, 5 - 17 cm and 20 - 30 cm soil alike, with no apparent patterns with depth (Fig. 6.1). Peaks from the addition of sugar were clearly visible in the $\delta^{13}CO_2$ values (Fig. 6.1), but the effect on total respiration was small, and within the range of unprimed respiration, with the exception of one jar of 5 - 17 cm soil. The small priming effect in the first incubation 5 - 17 cm jar can be attributed to the lower rate of priming per g soil-C experienced by this jar than the other incubations (see Fig. 6.1 and Table 6.2). Partitioning respiration using equation 6.6 shows that during the respiration peak after sugar addition, respiration deriving from SOM decreased slightly in the 5 - 17 cm sample and in the 20 - 30 cm sample with lower respiration, and increased slightly in the 20 - 30 cm sample with a higher respiration. Small amounts of 'sugar' respiration visible before sugar addition in the first and second incubations (Figs. 6.1 and 6.2) are due to variation in the $\delta^{13}C$ of respiration, and an average value of sugar $\delta^{13}C$ used in the partitioning equation (equation 6.6).

While there was a wide range of respiration rates in the first incubation, the second incubation showed closely matched respiration rates within treatments and a higher basal respiration rate in the 5 - 17 cm soil (300 μg CO_2-C g soil-C^{-1} day^{-1}) than in the 20 - 30 cm soil (200 - 250 μg CO_2-C g soil-C^{-1} day^{-1}) (Fig 6.2). This is attributable to the addition of nutrient solution in this incubation. Sugar additions

raised the total respiration well above the basal respiration, in contrast to the first incubation. The peaks in total respiration due to sugar addition were very similar in magnitude in the second incubation. Partitioning of sources shows a small reduction in SOM-derived respiration in all cases, with a similar magnitude for 20 - 30 cm soil as for 5 - 17 cm.

The third incubation again showed no difference in respiration rate between the 5 - 17 cm and 20 - 30 cm soil. Total respiration rates for this incubation were lower than for the first two incubations, all sitting around 100 μg CO_2-C g soil-C^{-1} day^{-1} for unprimed respiration and rising only to 500 μg CO_2-C g soil-C^{-1} day^{-1} during the sugar peak. Partitioning showed that in this incubation, in all cases SOM-derived respiration increased slightly immediately following sugar addition.

The inclusion of a nutrient solution treatment to samples in incubations 2 and 3 caused an increase in the background soil respiration rate, and arguably a higher peak in the microbial respiration of sugar, excluding the one sample in the first incubation with a very high sugar peak. Both positive and negative priming was observed with and without nutrient solution. In other studies, nutrient additions or nutrient status have proved to be an important control on priming effects; Fontaine *et al.* (2004a) found that positive priming effects after cellulose addition were higher in a low nutrient treatment than a high nutrient treatment. On the other hand Guenet *et al.* (2010) showed a consistent negative priming effect from cellulose in a soil with very low nutrient concentrations after laying bare for 80 years.

Comparing the second two incubations, where nutrient solution was applied with the same rates of sugar addition per g soil-C, the method of applying the sugar appears to control the direction of priming; stirring resulted in negative priming effects, while pouring resulted in positive effects. The disturbance effect of stirring the sugar solution into the soil has not affected the size of the measured priming effect, since the control soils used to calculate the partitioning of soil and sugar respiration were also stirred at the time of application. In any case, respiration in the control soils was

not noticeably affected by the disturbance (Figs 6.1 and 6.2). Since Blagodatskaya and Kuzyakov (2008) showed in a meta-analysis that priming effects were positive at low application rates and negative at higher application rates, I suggest that the effect of stirring or pouring the sugar solution onto the soil was a difference in local concentration. In the stirred soils, sugar was more evenly mixed through the soil. In the poured soils, sugar solution was allowed to infiltrate the soil; the distribution of sugar was more patchy, and may have been more concentrated near the surface and in macropores, but less concentrated throughout the rest of the soil. It is possible that the local sugar concentrations experienced by the majority of primable SOM in the poured treatments were considerably lower than those of the stirred treatments, with small amount of SOM experiencing very high sugar concentrations. A lower median local sugar concentration in the poured treatments would explain the positive priming in these soils and negative priming in the stirred soils.

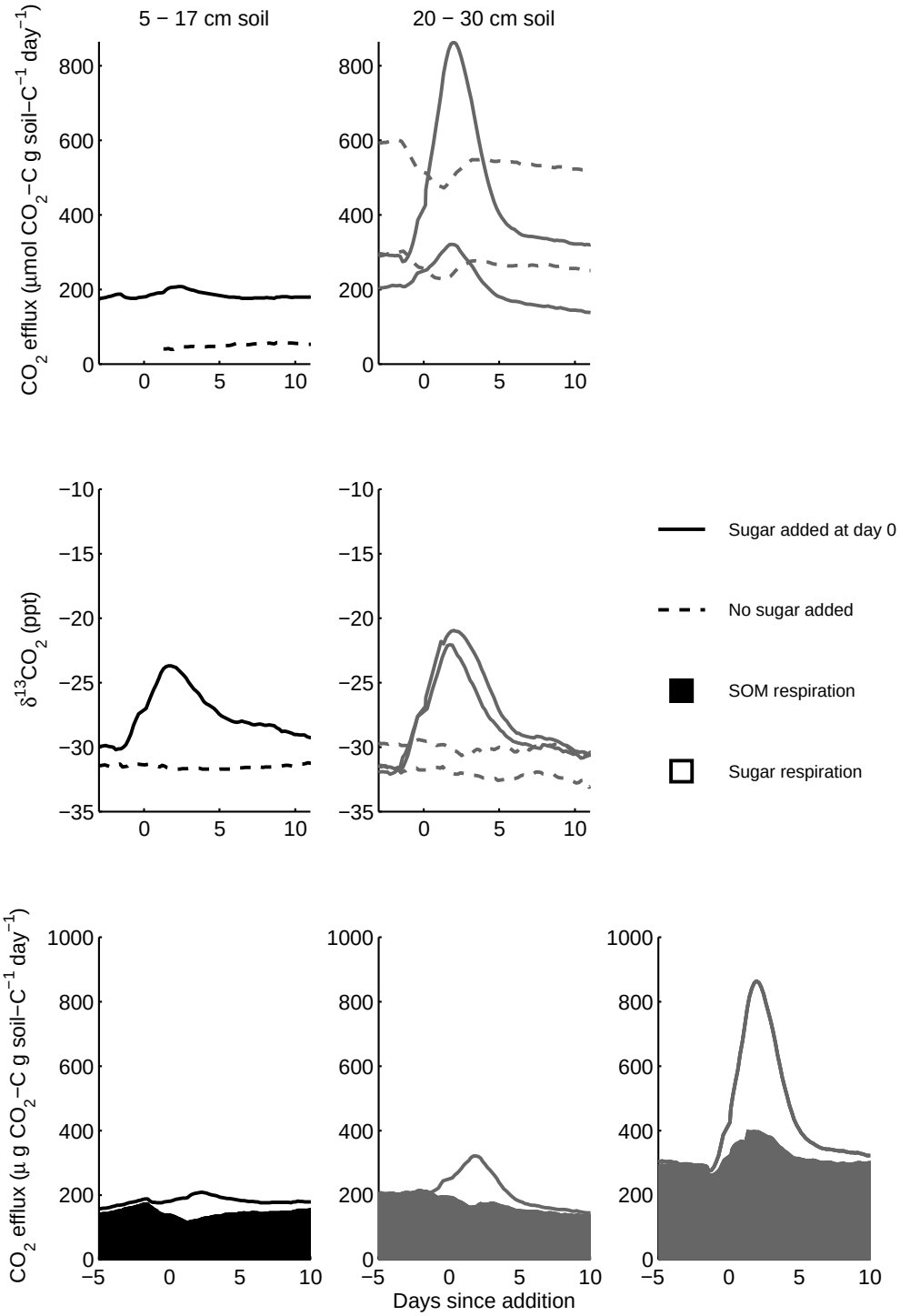
5 − 17 cm soil
20 − 30 cm soil
CO2 efflux (µmol CO2−C g soil−C−1 day−1)
δ13CO2 (ppt)
CO2 efflux (µ g CO2−C g soil−C−1 day−1)
Days since addition
Sugar added at day 0
No sugar added
SOM respiration
Sugar respiration

Figure 6.1: Priming effects during incubation 1. Upper panels show respiration rates after sugar addition, middle panels show $\delta^{13}CO_2$ of respiration, and the bottom panels show partitioning of respiration in the treated samples, where the upper lines represent total respiration and the filled area represents respiration originating from SOM. Black indicates soil respiration from 5 - 17 cm soil, grey indicates 20 - 30 cm soil. Dashed lines represent respiration from control samples, to which no sugar primer was added.

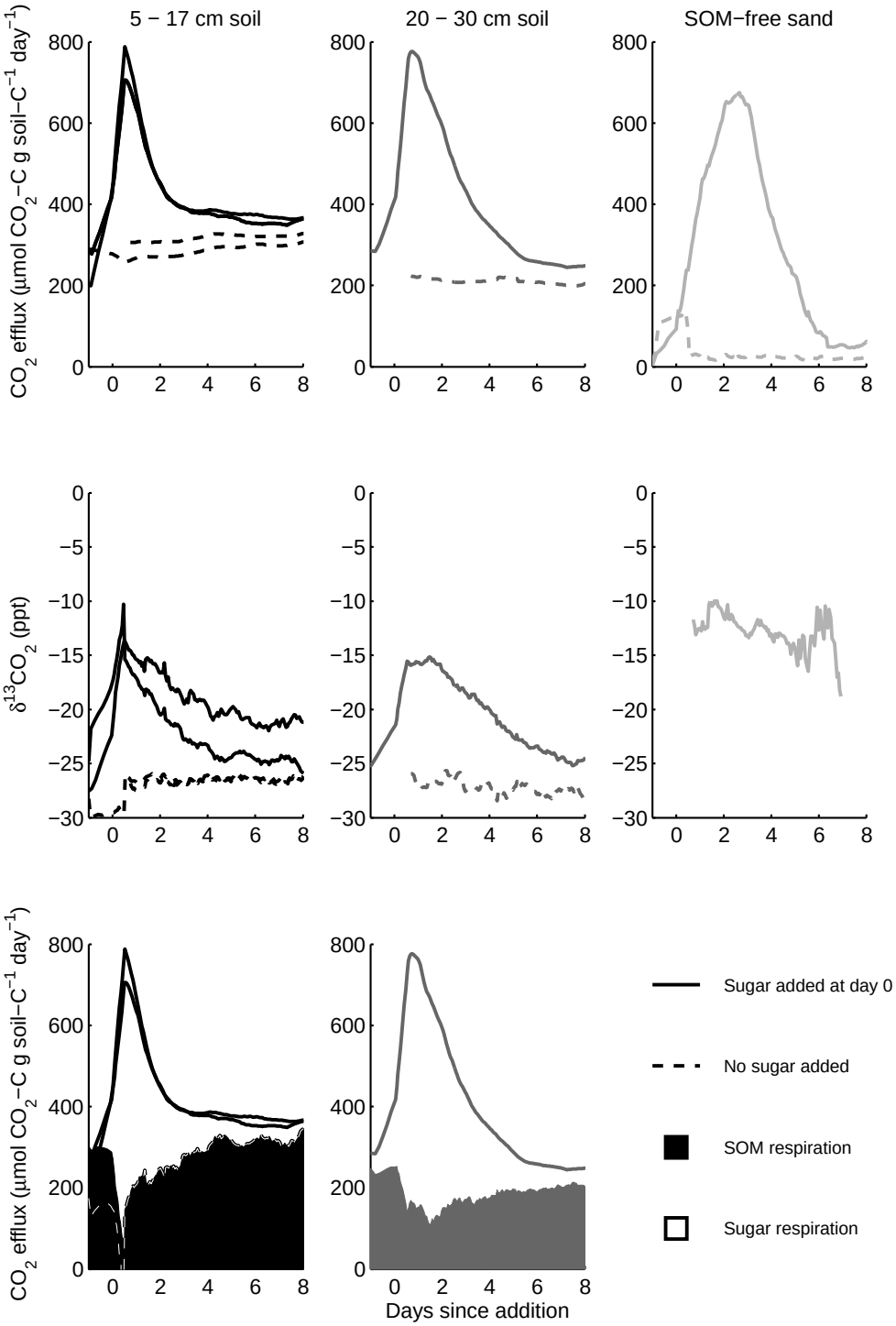
5 − 17 cm soil
20 − 30 cm soil
SOM−free sand
CO2 efflux (µmol CO2−C g soil−C−1 day−1)
δ13CO2 (ppt)
Days since addition
Sugar added at day 0
No sugar added
SOM respiration
Sugar respiration

Figure 6.2: Priming effects during incubation 2. Upper panels show respiration rates after sugar addition, middle panels show $\delta^{13}CO_2$ of respiration, and the bottom panels show partitioning of respiration in the treated samples, where the upper lines represent total respiration and the filled area represents respiration originating from SOM. Black indicates soil respiration from 5 - 17 cm soil, dark grey indicates 20 - 30 cm soil, and pale grey indicates a SOM-free quartz sand control. Respiration rates for the SOM-free control are calculated on a per g sugar-C basis, including the sand sample to which sugar was not added, to allow comparison. Dashed lines represent respiration from control samples, to which no sugar primer was added. The white dashed line in the lower panel indicates the upper bound of the hidden filled area representing the second primed 5 - 17 cm soil sample.

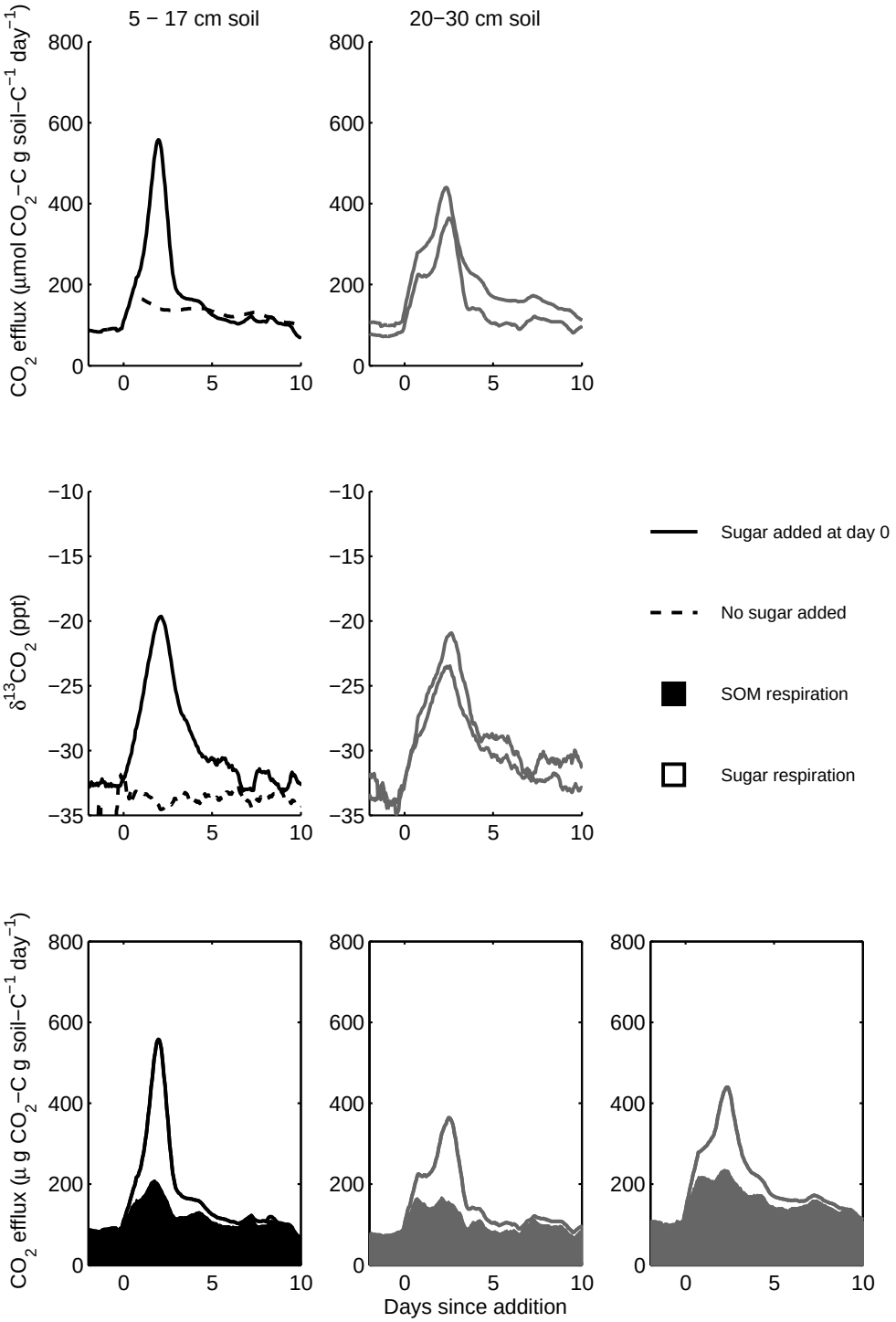
5 − 17 cm soil
20−30 cm soil
CO2 efflux (µmol CO2−C g soil−C−1 day−1)
δ13CO2 (ppt)
CO2 efflux (µ g CO2−C g soil−C−1 day−1)
Days since addition
Sugar added at day 0
No sugar added
SOM respiration
Sugar respiration

Figure 6.3: Priming effects during incubation 3. Upper panels show respiration rates after sugar addition, middle panels show $\delta^{13}CO_2$ of respiration, and the bottom panels show partitioning of respiration in the treated samples, where the upper lines represent total respiration and the filled area represents respiration originating from SOM. Black indicates soil respiration from 5 - 17 cm soil, grey indicates 20 - 30 cm soil. Dashed lines represent respiration from control samples, to which no sugar primer was added.

6.2.2 Soil microbial biomass

In several cases, the fumigated extractable C was lower than the extractable C of the control samples, leading to an apparently negative soil microbial biomass content. These negative values were found only in the 20 - 30 cm soil, which had a much lower total C content. A paired t-test showed that this difference was significant (p=0.043, n=12) and not only due to sample variation. The explanation for a loss of extractable C during choroform fumigation is not obvious, but it is possible that microbial biomass not killed by fumigation (1 - K_{EC}, assumed 55% total microbial biomass) were able to mineralise more C than was contained in the killed biomass during the 24 h fumigation period. This explanation is feasible only if K_{EC} was overestimated at 0.45, and if the actual microbial biomass C is low compared to the total extractable C.

Unpaired t-tests showed that the values given for microbial biomass C were significantly higher in 5 - 17 cm soil than 20 - 30 cm soil, including all primed, unprimed, fresh and preincubated soils ($p < 0.001$); within each horizon, mean values for microbial biomass C were higher in primed soils than in unprimed, and higher in fresh soils than in preincubated soils, but none of these comparisons were significant (all $p > 0.05$).

Table 6.3: Microbial biomass C and moisture contents of soil from organic and mineral horizons, after incubation with and without sugar additions (primed v unprimed), and for unprimed soils after fridge storage at 4 °C or preincubated at 30 °C for 1 week (fresh v incubated). n $\geq$ 3 in all cases.

	Moisture (%)	± 1 σ	Microbial biomass C (μg C g soil^{-1})	± 1 σ	Total fumigated C (μg C g soil^{-1})	± 1 σ
5 – 17 cm						
primed	67.8	2.3	582.5	292.5	2293.0	296.1
unprimed	67.0	1.7	379.3	42.1	1962.5	101.5
fresh	61.2	1.1	522.5	159.6	1507.6	44.1
incubated	68.1	0.8	208.1	83.7	2196.8	48.2
20 – 30 cm						
primed	23.8	3.3	-21.3	11.0	338.7	31.9
unprimed	27.2	1.4	-4.7	23.7	335.6	27.8
fresh	20.3	0.3	14.2	27.4	279.9	20.8
incubated	27.6	0.0	-34.4	19.1	320.8	17.1

6.3 Conclusion

Addition of labile substrates to soil did induce priming effects in the respiration of native SOM, but the priming effects measured were both negative and positive. There was no difference in priming effect between horizons. The addition of nutrient solution did not have a discernible effect on the magnitude or direction of the priming effect, although this was difficult to test due to the small sample size. Sugar additions had an insignificant positive effect on the microbial biomass C, in both horizons, and preincubating soils at 30 °C had an insignificant negative effect. The main finding of this Chapter was that the method of applying the labile substrate controlled whether the priming effect observed was positive or negative. Mixing sugar evenly into the soil resulted in negative priming of native SOM, while pouring sugar solution onto the surface and allowing it to infiltrate caused positive priming. I suggest that this difference is due to the patchy distribution of added sugar in the poured additions resulting in higher local concentrations of labile C.

Chapter 7

Soil porespace and water characteristics

7.1 Introduction

Physical location of SOM within the porespace architecture is a major control on SOM decomposition, and SOM quality is expected to vary with physical location, both with respect to position in stable aggregates, and with pore connectivity. Material protected in the inner layers of a macroaggregate by the physical occlusion of decomposers can equally be said to be protected by its lack of (or limited) connection to porespace networks. Larger pores support rapid flow of water and solutes, transporting microbial cells, and readily drain and saturate under normal field conditions. Smaller pores are less often drained, and water movement is slower. In addition to the physical inaccessibility of SOM in smaller pore spaces, soil pore water in smaller pore spaces may have limited dissolved oxygen, further repressing decomposition of SOM in the pore walls.

Because aggregate protection is an important control on SOM decomposition that is strongly affected by management practice, many studies have looked at the decomposition, quality and temperature sensitivity of SOM within aggregates, including

incubation studies of separated aggregate fractions and characterisation of aggregate fractions. (Adu and Oades, 1978; Leifeld and Fuhrer, 2005; Sey *et al.*, 2008)

SOM aggregate structure and SOM pore structure are reciprocal factors. SOM may be physically protected by aggregates, but microbes navigate the soil architecture in pore-water. Attempts to study decomposition of SOM with an aggregate approach should be balanced by *in situ* pore-oriented approaches. As results from the separation, ^{14}C dating and incubation of intra-aggregate and free light material in Chapters 3 – 5 confirm, incubation of isolated aggregate fractions results in respiration rates which reflect the intrinsic chemical properties of fractions in which in situ physical location is likely to be the main factor determining decomposition rates. To investigate the effect of physical location on respiration rates, it is necessary to keep the soil architecture intact.

The experiments described in this Chapter were aimed at comparing the respiration and temperature sensitivity of respiration between meso- and micro- pores *in situ*. The water-filled porespace of intact soil cores was altered by applying hydraulic tension to the water column in saturated cores, with the largest pores draining under the lowest tension and the smallest pores requiring a high tension or pressure to drain. The principles of this approach work under the simplifying assumptions that all macropores are connected to the bottom edge of the core; for this reason I used short (50 mm height) cores. The minimum diameter of pores drained at a certain matric potential is approximated by the formula $ø \approx 0.3/h$, where h is the matric head (Ψ_m) in cm.

Filling porespace with water in order to isolate pore classes relies on the assumption that no aerobic respiration occurs within water-filled pores, which is a blunt simplification. In addition, the treatment effect in this study can be viewed as both a difference in aerobic pore space and a difference in volumetric water content, which is itself an important control on decomposition. While total waterlogging results in anaerobic conditions where aerobic respiration is completely suppressed, in reality

the pore surfaces of matrically altered soil cores will be experiencing a broad range of water conditions.

General relationships between soil moisture and soil respiration rates are not straightforward (Adachi *et al.*, 2006; Cleveland *et al.*, 2007; Rey *et al.*, 2005; Waldrop and Firestone, 2004; Xiao *et al.*, 2007), however it is expected that soil respiration should be highest at intermediate moisture contents and temperatures (Wickland and Neff, 2008). Whether soil moisture itself significantly influences the temperature sensitivity of soil respiration or not is unclear (Niu *et al.*, 2008; Rey *et al.*, 2005), but it has been suggested that drier soil leads to more temperature sensitive decomposition as moisture attenuates changes in temperature (Niu *et al.*, 2008).

7.2 Methods, Results and Discussion

7.2.1 Sample collection

Intact 50 mm x 30 mm ø soil cores were used to investigate soil pore space. Cores were collected on the 31st July 2009 from Harwood forest. Three parallel 25 m transects (A, B and C) were drawn 10 m apart, and each was sampled every 5 m. At each point a small pit was dug to excavate an intact flat surface at the top of the O_i horizon, and 25 individual PVC corers were pressed gently into the surface at least 10 mm apart until the soil core slightly protruded (~3 mm) from the top of the ring. The cores were carefully removed from underneath, with ~10 mm intact soil protruding from the undersurface, and transported back to the laboratory in a coolbox.

7.2.2 Manipulation of soil pore space

Each core was prepared by slicing off the protruding ends with a razorblade, leaving an intact flat surface for good contact with the tension table surface. The intact cores, still surrounded by plastic tubing, were capped at both ends with a patch of nylon secured with a rubber band. The 25 cores from each pit were divided into six sets

Table 7.1: Diameter of pores drained by matric tension treatments

Matric head	Tension	Pores drained	Equilibration time	Method
-20 cm	-2 kPa	> 150 nm	24 hrs	Tension plate (Fig 7.3)
-1 m	-10 kPa	> 30 nm	96 hrs	Tension table
-5 m	-50 kPa	> 6 nm	96 hrs	Pressure table

of four and one remainder, and each set of four was combined with the five sets from each transect, resulting in six composite sets of 20 cores from each transect. The sets were assigned to six treatments: saturation in either deionised or deoxygenated water, and drained to a matric head of -20 cm, -1 m, or -5 m. The cores were saturated by placing in a shallow tray and filling the tray to half the depth of the cores (25 mm depth), leaving to equilibrate for 24 hours, filling to just below the top of the cores and equilibrating for a further 24 hours until the top surface appeared wettened, following the recommendation of Carter and Gregorich (2007).

The pressure table and the tension table apparatus were used in the soil science laboratory of the Scottish Agricultural College, Edinburgh campus. For the pressure table and tension table, silica flour and water were mixed to make a cement which acted as the contact medium. The cement was poured onto the plate surface and the cores were positioned while the cement was still wet. The tension plate was borrowed from the SIMBIOS center at the University of Abertay. The contact medium in the tension plate was a dry ceramic surface. The surface was covered with a cellulose filter paper (45 μm grade) and wettened with deionised water before contact was made.

7.3 Incubation

After adjusting the matric potential, 20 cores from each treatment from each transect were placed inside a 2 L Kilner jar fitted with gas ports in the lid, and incubated in a ramping temperature program, starting with four days at 10 °C and increasing 5 °C

per day from 10 °C to 30 °C and down again. CO_2 fluxes and $\delta^{13}C$ of respired CO_2 were measured during the incubation of transect C cores using the tunable diode laser described in section 6.1. CO_2 fluxes only were measured during the incubation of transect A cores, using the GC (section 4.3.2). Transect B cores were prepared for incubation, but measurements were abandoned due to TDL malfunction.

Both transect A and transect C incubations showed predictable increases in respiration with increasing temperature, however there was no discernible effect of either matric potential or water type on the rate or temperature response of respiration. The transect A incubation showed hysteresis in the temperature response- respiration rates were lower during the ramp up than on the ramp down; however, the transect B incubation showed the reverse. Cores with intermediate water content (drained to -1 kPa) might have been expected to show the highest overall respiration rates: this was not the case, and in fact the order of treatments with respect to respiration rate was different in each water type and from each transect.

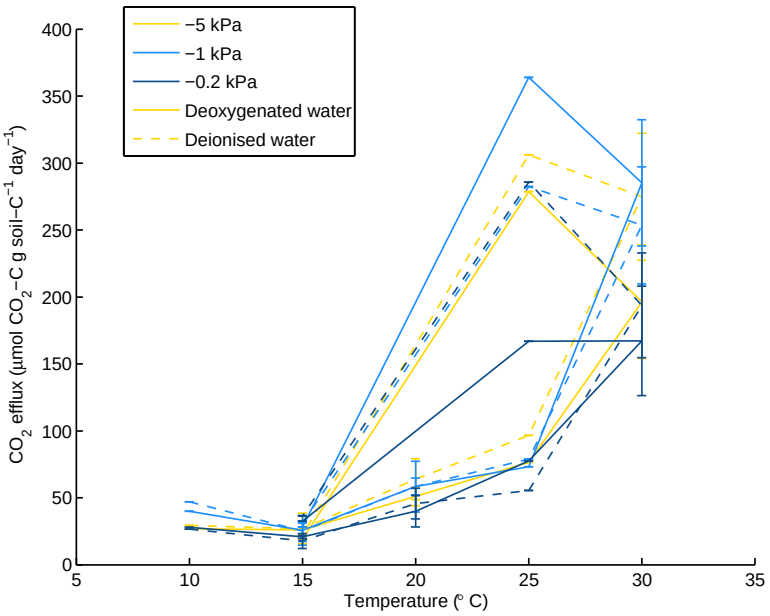

Figure 7.1: Soil respiration from intact cores at adjusted matric tension of -5, -1 and -0.2 kPa. Transect A, measured using gas chromatography. Error bars represent 1 standard deviation of three analytical replicates at each timepoint.

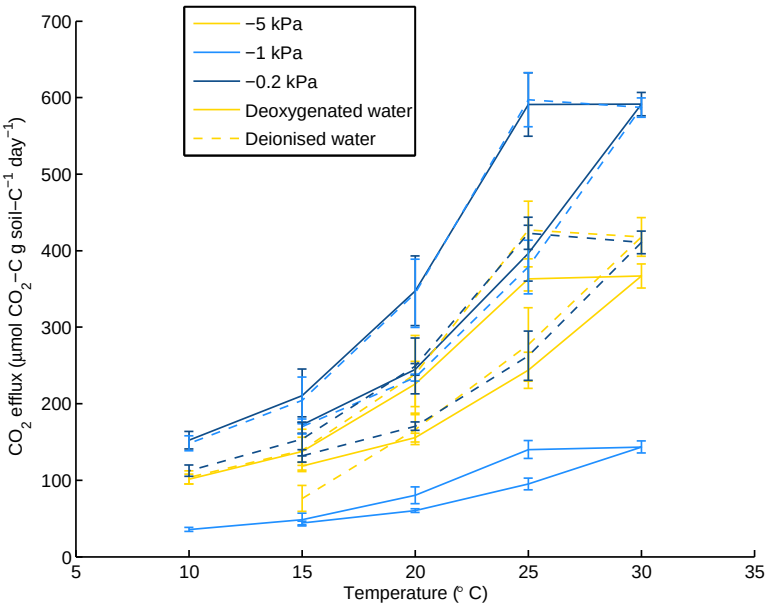

Figure 7.2: Soil respiration from intact cores at adjusted matric tension of -5, -1 and -0.2 kPa. Transect C, measured using tunable diode laser spectroscopy. Error bars represent 1 standard deviation of respiration rates within a 4-hour window.

δ^{13}C of respiration was also measured during the TDL incubation of adjusted C transect cores but are not presented here. The values remained relativey constant throughout the incubation, and did not vary with temperature, matric tension treatment or water type (multi-way ANOVA, all p >0.1). The mean δ^{13}Cof respired $CO_2$from all flasks for the whole duration was -32.1 ‰ ($\pm$ 0.1, 1 s.d.).

Figure 7.3: Tension plate apparatus

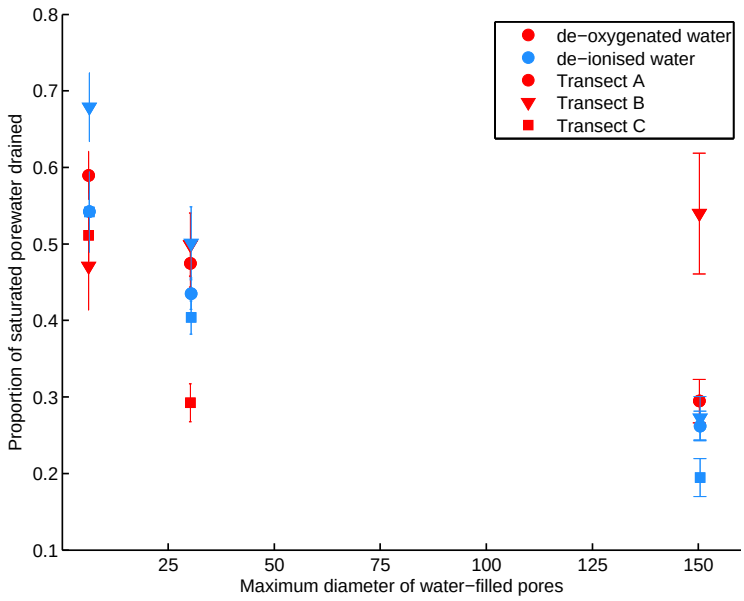

Figure 7.4: Pore size distribution determined by remaining water filled porespace at three matric tensions (-2 kPa, -10 kPa and -50 kPa)

7.4 Dry bulk density

The bulk density of cores collected in five pits along three transects indicate the scale of spatial variability of soil properties in Harwood forest. Variation within each pit (1 m^2) was very low, while variation within transects (25 m) was high, and variation between transects (30 m) was similarly high. A slight trend in bulk density was noticeable both along each transect, and also between transects (A-C).

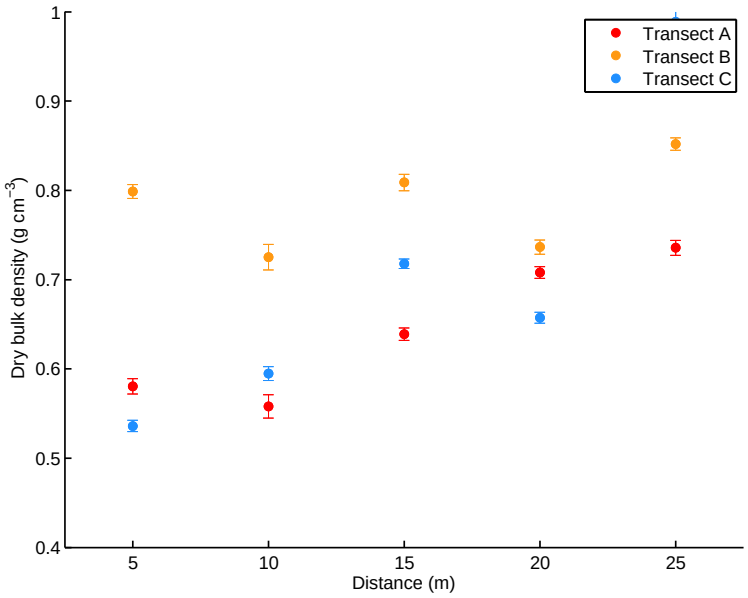

Figure 7.5: Dry bulk density of cores at 10 –15 cm depth along three 25 m transects in Harwood forest. Bars indicate standard error (n=25)

7.5 Estimation of carbon stocks using core bulk density

Dry bulk density values determined in conjunction with soil carbon concentrations in different horizons are an essential tool for measuring soil carbon stocks and monitoring small changes in soil carbon storage over time. Because carbon content and bulk

density are strongly negatively correlated, ad hoc comparisons of soil carbon storage based on carbon contents alone overestimate high values and underestimate low ones (Davidson and Ackerman, 1993). For the same reason, for accurate measurement of carbon stocks within a site, even where bulk density is not very variable, it is important to use values of bulk density, moisture content and carbon content for the same subsamples. As Conen *et al.* (2005) demonstrate, estimating area-weighted carbon stocks using mean values of carbon concentration, soil mass and bulk density result in an overestimation of carbon stocks (in their case by 13%) when compared to direct measurement of stocks on each subsample using the same data. Over the course of this PhD, carbon contents were measured without measuring the bulk density of the samples, bulk density was measured without measuring the carbon content of the samples, and bulk density was only measured at one depth. However, these values can still usefully be combined to generate a ball-park estimate of the soil carbon stocks in the top 15 cm of Harwood forest soil. Using the mean dry bulk density of all the cores in this Chapter and the mean carbon concentrations of 5 - 17 cm whole soil described in Chapter 3, and the formula

$$\text{Soil C stock (kg m}^{-2}) = \frac{\text{C content}(\%)}{100} \times \text{dry bulk density (kg m}^{-3}) \times \text{sampling depth (m)}, \tag{7.1}$$

I determined that the Harwood soil carbon stocks to 15 cm are in the order of 30.7 kg m^{-2}, $\pm$ 10.2 (1 s.d.). The error term was propogated using the formula

$$\left(\frac{\sigma_f}{f}^2\right) = \left(\frac{\sigma_A}{A}^2\right) + \left(\frac{\sigma_B}{B}^2\right) \tag{7.2}$$

.

7.6 Conclusion

Matric alteration of intact soil cores did not succeed in separating a distinct respiration response from different pore size classes. The magnitude of respiration rates in different matric potential treatments were highly variable and inconsistent, despite large differences in the water content of each treatment. Bulk density of intact cores showed a high variability in 5 m intervals, and low variability within 1 m^2 pits.

Chapter 8

Discussion

This thesis set out to investigate relationships between the stability of different forms of SOM and the temperature response of decomposition. Decomposition of SOM can be limited by a large number of different factors, including but not limited to temperature, nutrient availability, intrinsic chemical properties of SOM, physical access to SOM by decomposers, OM-mineral associations, soil pH, waterlogging, energy availability, and microbial community dynamics.

Understanding the temperature sensitivity of stable SOM is an important research goal, because of the risk of large stores of stable C in soils around the world being released to CO_2, DOC or labile SOC pools due to warming. However, long term stability of SOC can be caused by a large number of interacting factors, making it difficult to predict overall responses to temperature. Each of the limits to decomposition listed above besides temperature is likely to have an independent relationship with temperature, or with the wider effects of global climate change (von Lützow and Kögel-Knabner, 2009). The overall temperature sensitivity of respiration from stabilised SOM is a function of the underlying enzyme kinetics of the reaction, and the temperature sensitivity of each of the stabilisation mechanisms acting on that SOM. The relative importance of different stabilisation mechanisms varies enormously between biomes, between soil types, between land management types, with depth and

within soils. As a result, the temperature sensitivity of stabilised SOM as a whole is complex, and there is no consensus on the relationship between SOC age and temperature sensitivity (Kirschbaum, 2006). Two opposing approaches to characterising this complexity emerge- separating stabilisation mechanisms and characterising the individual temperature responses, or ignoring the variation in stabilisation mechanisms and aiming for a simplified relationship that can inform carbon cycle models on a global scale without the need for in depth knowledge of soil chemical and physical properties on a local scale. Both approaches are required for understanding the mechanisms of temperature response and predicting the effect of climate change on global soil carbon cycling. This thesis adopted the former approach.

8.1 Summary of results

Chapter 3

Chemical characterisation of Harwood forest soil horizons, particle size fractions and density fractions demonstrated that a range of stabilisation mechanisms may be operating in these soils. Fe concentrations were strongly correlated with C content, indicating that Fe oxides may provide some SOM stability in all fractions and depths without explaining differences between fractions. Degree of humification as measured by the Alkyl-C : O-alkyl-C ratio increased in the order *light* < *mineral-bound* < *intra-aggregate* amongst the fractions, and was considerably higher at depth in the whole soils. C:N ratios increased with depth, counter to expectations. Polysaccharides were high in the mineral-bound fraction, and were associated with the coarse sand and silt fractions. Based on these results I suggest that 20 - 30 cm soil and intra-aggregate material are likely to be intrinsically recalcitrant, while OM-mineral associations are likely to be high in the mineral bound fraction and the 20 - 30 cm soil, although Fe oxide stabilisation is likely to occur throughout the fractions and horizons.

Chapter 4

Incubation of isolated fractions showed that rates of respiration on a g soil-C^{-1} basis were equally high in the light and intra-aggregate fractions, and even higher in the mineral-bound fraction, despite the presumed stability of OM-mineral associations and the high degree of humification in the intra-aggregate fraction. Whole soil respiration rates were lower at 20 - 30 cm than at 5 - 17 cm, indicating that 20 - 30 cm SOM is more stable, due to a combination of humification and mineral interactions. Temperature sensitivity of respiration was higher in the light fraction than in the intra-aggregate or mineral-bound fraction, and was higher in unsterilised 5 - 17 cm soil than unsterilised 20 - 30 cm soil, counter to the predictions of the Q theory that more humified material should be more temperature sensitive. On the other hand, higher respiration rates and lower temperature sensitivity in the chemically labile mineral-bound fraction than the light fraction suggest some support for Q theory. These results suggest that stability at 20 - 30 cm is primarily due to mineral associations and physical protection rather than substrate quality, and that the stability of the chemically labile mineral-bound fraction owes more to the formation of microaggregates to OM-mineral bonds themselves. Respiration was suppressed in all fractions due to NaI toxicity.

Chapter 5

In Chapter 5, I used the isotopic composition of respired material for insight into the temperature sensitivity of respiration. No effect of temperature was found on the ^{14}C or $\delta^{13}C$ of respired CO_2, nor on the $\delta^{15}N$, $\delta^{13}C$ or C:N ratio of remaining solids. ^{14}C dating of whole soils and fractions confirmed that SOM in the 20 - 30 cm soil and in the mineral-bound and intra-aggregate fraction of the 5 - 17 cm soil are considerably older and more stable, at least *in situ*, than 5 - 17 cm soil whole soil or light material. However, these age differences were not reflected by differences in the

sensitivity of respiration to temperature. Most fractions and whole soils at both 10 and 30 °C released CO_2 with a ^{14}C content indicating a younger-than-average source of respiration, but there no was effect of temperature. A weak negative correlation between the ^{14}C discrimination of respiration and the proportion of SOC consumed during the incubation indicates that the expected progression from younger to older material over the course of the incubation did not occur, supporting findings in Chapter 4 that indicate the stabilisation mechanisms primarily responsible for the age of fractions were not operating during the incubation.

Chapter 6

During Chapter 6 I investigated the priming of recalcitrant SOM by labile substrate additions, to test the hypothesis that 20 - 30 cm SOM would be more susceptible to priming than 5 - 17 cm soil SOM. Naturally labelled sucrose additions provoked both positive and negative priming in the respiration of native SOM, irrespective of whether nutrient solution was added alongside. There was no difference in priming effect, background soil respiration or sugar respiration between soil depths, despite considerably lower microbial biomass C and SOC contents in the 20 - 30 cm soil. When nutrient solution was added, the difference between a positive or a negative priming effect was caused by sugar application mode. Mixing in the sugar solution caused a negative priming effect, while pouring the sugar solution on top caused a positive priming effect. Local concentrations of sugar on a small scale may have a strong effect on priming effects, and such minor differences in experimental techniques may be partly responsible for contrasting conclusions in the priming literature.

Chapter 7

I used matric tension to alter the water-filled porespace of intact Harwood forest soil cores, in an attempt to separate the temperature response of soil respiration in

micropores and macropores. There was no consistent effect of matric alteration on soil respiration or temperature response of soil respiration, despite big differences in the water-filled porespace in each treatment. Sampling a large number of intact soil cores for this experiment also provided information about the scales of spatial variation in bulk density in Harwood forest.

8.2 Dominant mechanisms of stability in Harwood Forest soil

^{14}C dating of density fractions and whole soils demonstrated that Harwood forest soil is composed of distinct SOC pools with very different turnover rates, and MRTs ranging from centuries to millenia (Chapter 5). The ^{14}C age of fractions provided information about the lifetime stability of SOM. Chemical characterisation of these fractions and whole soils in Chapter 3 provided some possible explanations for the causes of stability in the older SOM pools, from which the theoretical stability of SOM can be predicted. In Chapter 4, the isolated fractions and horizons with demonstrably different lifetime and theoretical stability were incubated, providing information about the current stability. In addition, Chapters 6 and 7 were designed to investigate further aspects of the theoretical stability of Harwood SOM; in Chapter 6, the susceptibility of SOM to priming by labile substrate co-metabolism, and in Chapter 7, physical protection of SOM within micropores. Neither Chapter 6 nor Chapter 7 conclusively demonstrated action of the mechanism of stability investigated.

8.2.1 Depth

Based on the radiocarbon ages, the strongest SOM stabilisation in Harwood occurred was related to depth. Mean residence times of 20 - 30 cm SOM were almost a millenium longer than in the horizon above (Chapter 5, table 5.2), indicating that SOM in this horizon was formed in the ericaceous moorland and survived afforestation. Decomposition of SOM at 20 - 30 cm can be expected to be hindered by seasonal

waterlogging, as drainage is an important control on CO_2 emissions at this site (Mojeremane *et al.*, 2012); it will also be limited in situ by the much lower microbial biomass (see Chapter 6, table 6.3), which is in itself a reflection of physico-chemical limits to decomposition (water, O_2 diffusion) as well as the size and quality of the available SOM pool. The 20 - 30 cm whole soil showed signs of humification (eg. high alkyl-C : O-alkyl-C ratio, Chapter 3, Fig. 3.11) and an accumulation of aromatic compounds (increasing ketone moiety with depth, Chapter 3, Fig. 3.4), indicating that intrinsic recalcitrance may play a role in SOM stabilisation. Swain *et al.* (2010) also showed increasing lignin oxidation with depth in Harwood forest, and an accumulation of phenols in the 20 - 30 cm layer attributed to profile inversion and burial of the upper organic layer during afforestation. Burial during afforestation is likely to have contributed to the stabilisation of Harwood SOM; however, the age of 20 - 30 cm material established here suggests that most of the SOM now in the 20 - 30 cm layer was already stabilised well before afforestation. Although waterlogging could be expected to be the primary source of near-permanent SOM stability in Harwood 20 - 30 cm soil, when samples were incubated under fully aerobic conditions, respiration rates were still significantly lower on a per g soil-C basis than from the 5 - 17 cm soil. This indicates that waterlogging is at least not the only control on respiration at 20 - 30 cm; I conclude that the near-permanent stabilisation of SOM in the 20 - 30 cm layer in Harwood forest is largely due to mineral-OM interactions, with some contribution from intrinsic recalcitrance. Higher Q_{10} values for respiration in the deeper soil (Table 4.1), supported by Rey *et al.* (2005) and Cross and Grace (2010), support the theory that mineral associations reduce the temperature sensitivity of soil respiration.

8.2.2 Micro-aggregates and mineral associations

The high Alkyl C : O-alkyl-C ratios of the intra-aggregate fraction indicate that humification may be responsible for the long MRT of these samples. However, when incubated, intra-aggregate and light fraction material showed similar respiration rates, indicating that the relatively long MRT of the intra-aggregate fraction is not the result of intrinic chemical properties. Furthermore, temperature sensitivity of respiration was higher in the light fraction than the intra-aggregate fraction, counter to the prediction that more humified material is more temperature sensitive. I conclude that the long MRT of intra-aggregate material is due to the physical protection of SOM within aggregates.

The very strong correlation between Fe concentration and C content suggests that OM stabilised by Fe oxides and in Fe-humus complexes are high in all fractions, which should be an important source of SOM stability in this soil type (Sollins *et al.*, 2009). However, the fact that this relationship holds even for the samples with a relatively young ^{14}C age indicates that Fe stabilisation is not responsible for the stability of the older SOM fractions.

The long MRT of the mineral-bound fraction suggests that this material is resistant to decomposition in situ. Relatively high levels of polysaccharides, low Alkyl-C : O-alkyl C ratio and high thermal lability of this fraction indicate that this fraction is stabilised by mineral associations and physical stabilisation rather than chemical properties. However, when incubated this fraction showed a higher rate of respiration per g soil-C than the light or intra-aggregate fractions, indicating that physical stability of aggregates, rather than mineral associations, is responsible for the long MRT of the mineral-bound fraction. Mineral associations are supposed to provide SOM stability on a near-permanent basis (Marschner *et al.*, 2008; Kögel-Knabner *et al.*, 2008); other studies of the age of density fractions have shown that mineral-bound material is considerably older than intra-aggregate material (Dorodnikov *et al.*, 2011).

In this study intra-aggregate SOM was just as old as mineral-bound SOM, which supports the idea that physical protection is the primary cause of stability in both, rather than recalcitrance and mineral interactions respectively.

8.2.3 Differences between composited duplicates

Despite compositing samples to reduce sample variation, consistent differences appeared between composite A and composite B. Composite A samples were consistently older than composite B within each category (Table 5.2); Alkyl-C : O-alkyl-C ratios, indicating humification, were higher in composite A than composite B (Fig 3.11). Fe : C ratios were also consistently higher in composite A than composite B (Fig 3.13). Despite these differences, respiration rates were not detectably higher in composite B samples within each category. This suggests that although Fe oxide stabilisation and the intrinsic recalcitrance of humified material contributed to the lifetime stability of SOM, the current stability during incubations was determined by another factor. This supports the idea that both Fe oxide interactions and humification provide stability via physical protection in microaggregates, and not directly.

8.3 Temperature sensitivity of soil respiration

The Q_{10}s of respiration from isolated fractions and whole soils as determined in Chapter 4 showed that the light fraction was more sensitive to temperature than the intra-aggregate and mineral-bound fractions, despite the fact that intra-aggregate and mineral-bound material was more humified, and previous studies have shown more humified material to be more temperature sensitive (Leifeld and Fuhrer, 2005; Plante *et al.*, 2010). Karhu *et al.* (2010a) used the ^{14}C ages of physical fractions to partition respiration from forest soils into 'younger' and 'older' sources, and found that respiration from older SOC (based on a heavy fraction) was more temperature-sensitive than young (light) in the 5 - 17 cm soil, but in the upper mineral horizon

light fraction material was more temperature sensitive. It is tempting to conclude from my results comparing the three isolated fractions that 'younger', light material is more sensitive to temperature; however, the youngest fraction that I identified had a MRT of 146 years, qualifying for the stable pool in most soil carbon models. The highest modelled temperature sensitivities found by Karhu *et al.* (2010a) were in pools with MRTs of 7 - 16 years, and showed Q_{10} around six while all other pools showed a $Q_{10} \sim 3$. It is highly probable that the light fractions I isolated contain a subfraction of younger SOM that in the decadal turnover pool, which might drive the temperature sensitivity of the whole fraction. However, the ^{14}C of respired CO_2 from the light fraction showed that the MRT of respired material was >110, suggesting that the decadal pool does not dominate respiration in this soil.

The temperature sensitivity of mineral-bound fractions in this study are to be interpreted with caution, since there was high variation in respiration over time and between composites. Mineral-bound fraction respiration was particularly variable because of the very low total respiration rates. Mineral-bound OM can be expected to have a lower temperature sensitivity, since mineral-OM bonds are known to be thermally stable and formation of mineral-OM associations is itself temperature sensitive (Thornley and Cannell, 2001). In addition, the mineral-bound material in this study was high in labile SOC components, high in polysaccharides and with a high C : N ratio, which would be consistent with a low temperature sensitivity according to Q-theory, despite contrasting results from similar studies (Leifeld and Fuhrer, 2005). The low temperature sensitivity, high relative respiration rate and long MRT are consistent with this fraction as an entrapped labile pool under physical protection from microaggregates.

The net temperature sensitivity of soil respiration is not only affected by the kinetics of an individual reaction: temperature-dependent processes affecting the supply and transport of substrates, oxygen, water and decomposers also affect the measured result. Davidson *et al.* (2006) suggest that Q_{10} values above 2.5 are an indication of

interacting substrate supply issues. Here, only the sterilised 5 - 17 cm whole soils showed Q_{10} values under 2.5. This might suggest that high Q_{10} values amongst the fractions are partly down to the separation of co-limiting substrates; however this argument is weakened by the fact that all but one of the unsterilised whole soils also had Q_{10} values over 2.5.

8.4 Limitations

8.4.1 Sampling strategy and experimental design of incubations

The incubation experiments described in this thesis were hampered by an initial sampling strategy with inadequate replication. Composite sampling is a useful shortcut for incorporating a representation of population variation into a small number of samples to reduce analysis costs and processing time; Robertson *et al.* (1999) recommend that composited soil samples should at least be duplicated. However, most useful statistical tests require a minimum of n = 3. Incubation experiments in particular require replication to represent not only the soil population variation, but the variation in incubation conditions and microbial community dynamics. The decision to use only two composite replicates for this study was made on the basis of the time-consuming density fractionation procedure; an improved design taking the same amount of processing time would have been to use smaller subsamples, three temperature treatments, and three composited replicates for the GC incubation. In addition, replicated CO_2 measurements of each sample at each sampling event would have reduced the variation in respiration rates between sampling events, allowing improved estimates of temperature sensitivity. The GC incubations were performed in small vials to allow rapid buildup of measurable CO_2 concentrations, and CO_2 was sampled only once, at the end of the sealed period, the length of which was determined by estimating the time taken to build up a similar headspace CO_2 concentration in

each vial. If the experiment were to be repeated, an improved method of determining CO_2 concentrations taking into account the non-linear buildup of headspace CO_2 due to diffusion and CO_2 saturation would be to use larger headspace vessels and longer sealed periods, measuring headspace CO_2 from each vessel repeatedly and calculating the rate of CO_2 production from the CO_2 accumulation curve.

Techniques have been developed for measuring CO_2 evolution from soils on a very small scale, in modified 96-well MicroResp™ plates. While short-term, a microresp incubation could have provided a low-cost, well-replicated supplement to the long-term incubation experiments described, using only small amounts of soil.

Radiocarbon dating of Harwood forest density fractions validated our approach to separating SOM pools, confirming that density separation isolated two fractions that were stable in terms of lifetime stability. However, the remaining light fraction also showed relatively long mean residence times (147 and 255 y), was not demonstrably labile with respect to measured respiration rates (current stability) and held 82 % of the total 5 - 17 cm SOC. Crow *et al.* (2007) demonstrated that during density fractionation with SPT a significant SOM fraction is solubilized into the separation medium, and that this fraction is both functionally separate from the light and heavy fractions and highly soil-specific, although widely discarded in density fractionation experiments. Undoubtedly some fraction of SOM was also lost to the NaI solution during this experiment.

Further separation of the light fraction, perhaps using a lower-density medium, or including isolation of acid-resistant fractions and retention of the DOM lost during fractionation, might have allowed separation of a younger and more truly labile fraction for comparison. Other studies have already demonstrated the importance of lignin chemistry for the Harwood SOC stocks (Swain *et al.*, 2010); further investigation of the chemistry of the light fraction could have allowed a fuller understanding of the importance of intrinsic chemical recalcitrance for Harwood SOM stabilisation.

By far the most stable OM analysed by radiocarbon dating was the 20 - 30 cm

whole soil (1381 and 1072 y), which was not fractionated, as it was only included in the experimental plan at the last minute. Given that this horizon is within the rooting zone, it is very likely that this horizon contains young SOM as well as highly stabilised SOM. A fuller investigation of the relative importance of different stabilisation mechanisms in Harwood would have included characterisation and incubation of density fractions from 20 - 30 cm soil also.

8.4.2 Microbial heterotrophic respiration in isolation from plant inputs

Soil incubation studies are an important tool for understanding SOM processes in depth; the ability to manipulate soils and exclude external variables allows a detailed analysis of individual processes that is near impossible in field studies. However, the extent to which incubation of soils in laboratory conditions give a realistic picture of *in situ* soil C cycling is highly questionable. Taken out of the field, soils are cut off from litter and rhizodeposit inputs, mycelial transport networks are cut, macrobiota are excluded and groundwater flow is removed. Each of these features of soil contribute considerably to soil carbon cycling and are also temperature sensitive (Briones *et al.*, 2008; Hawkes *et al.*, 2008). Removal of roots results in the loss of a large proportion of the soil microbial biomass (De Neergaard and Magid, 2001), as well as labile carbon inputs that can have a strong influence on the decomposition of bulk SOM (Bais *et al.*, 2006; Blagodatskaya and Kuzyakov, 2008). Harwood forest has an abundant ectomycorrhizal community, with close to 100 % of root tips colonised (Palfner *et al.*, 2005), which will act as a C and N distribution network. Since this thesis concerned stabilisation factors affecting the SOM decomposition in bulk soil, it was reasonable to exclude rhizosphere and mycorrhizal processes, but the lack of labile substrate additions should be taken into consideration. Similarly, incubating isolated fractions involves separating substrate pools that are likely to interact in field conditions, either through co-metabolism or microbial community shifts.

8.4.3 NaI toxicity

In addition to standard sample preparation, the isolated density fractions incubated in Chapter 4 were also exposed to a strong NaI solution during fractionation. Iodine is well known to have a toxic effect (Cotton, 1930) so efforts were taken to thoroughly rinse the samples with water, and fractions were sterilised and then reinoculated before incubation. However, some I residues remained, and seemed to be selectively sorbed to OM (see Appendix A). These I residues seem likely to be the reason why respiration rates were strongly suppressed in all isolated fractions, compared to the whole soil (Fig. 4.1). NaI was chosen in preference to the alternative widely used density agent, SPT, which is known to be toxic to soil microorganisms and to affect clay mineral structure (Magid *et al.*, 1996; Swanston *et al.*, 2002; von Lützow *et al.*, 2007). Crow *et al.* (2007) found a suppression of respiration in forest soil fractions separated with NaI, but conclude that the toxicity was not high enough to account for the suppression. Sollins *et al.* (1984) explicitly tested the effect of residual NaI on anaerobic microbial N mineralisation, and found no effect.

8.4.4 Substrate quality changes over time

Soils or soil fractions isolated from carbon inputs progressively change in composition over time, as the stock of undecomposed material declines and humified microbial products accumulate. As a result, incubation experiments frequently show that initially high incubation responses tail off rapidly (Townsend *et al.*, 1997). This pattern was explained by some as the acclimation of the microbial community to a new temperature regime (Luo *et al.*, 2001; Giardina and Ryan, 2000), used to argue that observed increases in soil respiration are artefacts of temperature manipulation experiments. Subsequently several modelling studies showed that the temporal response is explained just as well by the depletion of labile substrates (Kirschbaum, 2004; Knorr *et al.*, 2005) and later experiments confirm a lack of microbial acclimation

to temperature changes (Vicca *et al.*, 2009).

This progression offers opportunities to compare the decomposition of humified and fresh SOM (Hartley and Ineson, 2008), but it also presents a problem for the determination of temperature responses from soil incubations. Identical soil samples incubating for the same length of time at different temperatures will degrade to a different degree over the course of the incubation depending on the decomposition rate, leading to a comparison of respiration rates from unequal SOM sources (Conant *et al.*, 2008). Conant *et al.* (2011) warn that this discrepancy leads to a consistent bias towards results that indicate a higher temperature sensitivity of older material. Although attempts were made to estimate the temperature sensitivity corrected for substrate depletion during these incubations (section 4.5.1), experimental design precluded useful interpretation of these results. Incubation studies comparing samples with different expected respiration rates should not be preceded by an unmeasured equilibration period. Allowing respiration rates to equilibrate before measurements begin is only appropriate where the samples can be expected to have similar respiration rate, and the temperature of equilibration is constant for all samples.

8.5 Further work

Results from Chapters 3 and 4 suggested that the spatial location of SOM in the soil matrix is important for the stabilisation of SOM. Physical occlusion of SOM is sensitive to management and indirectly to global change, but is likely to be more impacted by changes to the water cycle than direct effects of temperature on decomposition. More research is needed to focus on the spatial distribution of different forms of SOM and in particular differences in microbial communities within the porespace. During Chapter 7 I attempted to address this question, but the method of manipulating pore space by matric alterations was not effective. Rather than attempting to

separate respired CO_2 from different spatial locations in the soil, or balancing manipulation of soil pore space with minimal disruption of structure, a more effective approach to this question might be to incubate intact cores at different temperatures, and characterise the remaining SOM in pore walls for evidence of decomposition and microbial transformation using structure-preserving micro-spatial approaches such as microtomography or nanoSIMS.

I did not conclusively demonstrate whether the Harwood 20 - 30 cm whole soil is predominantly mineral-stabilised or aggregate-stabilised. This is an important question with impacts for the management of UK forests. Organic-rich, acidic mineral soils are common under forests in the UK, partly due to the practice of afforesting moorlands for timber production. This mineral soil had a relatively high, and very old, OM content. If the SOM in this horizon is impermanently stabilised in intra-aggregate form, it is likely to be vulnerable to SOC losses due to physical disturbance during felling and ground preparation. If permanent mineral associations are more dominant, it may be more stable. A fuller investigation of the clay mineralogy and metal oxide status of these soils is necessary to determine their vulnerability to disturbance. Characterisation of the density fractions of 20 - 30 cm

As mentioned previously, the youngest fractions isolated in these soils had a MRT that put it in the decadally cycling SOC pool. This fraction almost certainly contains a more active subfraction, with an MRT of years less. A full picture of the carbon cycling of Harwood forest soil would need to involve separating this active subfraction from the light material. Relatively high metal concentrations in the light material suggested that a more stabilised subfraction could have been separated by fractionation at a lower density. Alternatively, isolating and characterising an acid-resistant subfraction from the light fraction would give information about the active fraction by subtraction.

8.6 Conclusions

This thesis investigated the various mechanisms of SOM stability. I separated soil fractions and soil horizons which had very different turnover rates; 20 - 30 cm whole soil was in the millenial SOC turnover pool, while mineral-bound and intra-aggregate material formed a multi-centennial turnover pool. Light material showed the shortest residence times, but was still around 100 years old. Stability implied by respiration rates during a laboratory incubation was not consistent with the turnover rates shown by ^{14}C dating. In particular, old, mineral-bound material respired more per g C than younger light material, while old and humified intra-aggregate material respired just as much. A very old 20 - 30 cm soil horizon showed some signs of stability during incubation experiments, chemical characteristics indicating humification, as well as a lower temperature sensitivity. I suggest that a combination of mineral associations and aggregate protection provides stability to the 20 - 30 cm SOM. Contrary to expectations, the 20 - 30 cm soil was no more susceptible to priming by labile substrates; slight differences in methodology controlled whether a positive or a negative priming effect was observed. The most temperature sensitive SOC pool investigated in this study was the youngest and least humified, in contrast to predictions based on enzyme kinetics and thermodynamics. However, this youngest pool contained OM that was around 100 years old; high temperature sensitivity of this fraction relative to fresh material would be consistent with established theory. Temperature sensitivity of respiration in the 20 - 30 cm soil and the mineral bound fraction were lower, supporting the hypothesis that the formation of mineral associations is also sensitive to temperature, attenuating the temperature sensitivity of soil respiration. Above all, there is no clear relationship between age or degradedness of SOM and the temperature sensitivity of respiration. Representation of the complexity of SOM stabilisation mechanisms in SOC models is critical for coupling climate models to the terrestrial carbon cycle, but considerably more work is necessary before a consensus is reached.

Bibliography

Adachi M, Bekku YS, Rashidah W, Okuda T, Koizumi H (2006) Differences in soil respiration between different tropical ecosystems. *Applied Soil Ecology*, **34**, 258–265.

Adu JK, Oades JM (1978) Physical factors influencing decomposition of organic materials in soil aggregates. *Soil Biology and Biochemistry*, **10**, 109–115.

Ågren GI, Bosatta E, Balesdent J (1996) Isotope discrimination during decomposition of organic matter: A theoretical analysis. *Soil Science Society of America Journal*, **60**, 1121–1126.

Ågren GI, Wetterstedt JM (2007) What determines the temperature response of soil organic matter decomposition? *Soil Biology and Biochemistry*, **39**, 1794–1798.

Amachi S, Kasahara M, Hanada S, Kamagata Y, Shinoyama H, Fujii T, Muramatsu Y (2003) Microbial participation in iodine volatilization from soils. *Environmental Science & Technology*, **37**, 3885–3890.

Amundson R, Stern L, Baisden T, Wang Y (1998) The isotopic composition of soil and soil-respired CO_2. *Geoderma*, **82**, 83–114.

Andrews JA, Matamala R, Westover KM, Schlesinger WH (2000) Temperature effects on the diversity of soil heterotrophs and the $\delta^{13}C$ of soil-respired CO_2. *Soil Biology and Biochemistry*, **32**, 699–706.

D'Angelo EM, Kovzelove CA, Karathanasis, AD (2009) Carbon Sequestration Processes in Temperate Soils With Different Chemical Properties and Management. *Soil Science*, **174**, 45–55.

Arrhenius S (1915) *Quantitative laws in biological chemistry*. G. Bell & sons, London.

Bahn M, Schmitt M, Siegwolf R, Richter A, Brüggemann N (2009) Does photosynthesis affect grassland soil-respired CO_2 and its carbon isotope composition on a diurnal timescale? *New Phytologist*, **182**, 451–460.

Bais H, Weir T, Perry L, Gilroy S, Vivanco J (2006) The role of root exudates in rhizosphere interactions with plants and other organisms. *Annual Reviews in Plant Biology*, **57**, 233–266.

Baisden WT, Amundson R, Cook AC, Brenner DL (2002) Turnover and storage of c and N in five density fractions from California annual grassland surface soils. *Global Biogeochemical Cycles*, **16**, 16 PP.

Balesdent J, Balabane M (1996) Major contribution of roots to soil carbon storage inferred from maize cultivated soils. *Soil Biology and Biochemistry*, **28**, 1261 – 1263.

Baldock J, Masiello CA, Gélinas Y, Hedges JI (2004) Cycling and composition of organic matter in terrestrial and marine ecosystems. *Marine Chemistry*, **92**, 39–64.

Ball BC, Watson CA, Baddeley JA (2007a) Soil physical fertility, soil structure and rooting conditions after ploughing organically managed grass/clover swards. *Soil Use and Management*, **23**, 20–27.

Ball T, Smith KA, Moncrieff JB (2007b) Effect of stand age on greenhouse gas fluxes from a Sitka spruce [Picea sitchensis (Bong.) Carr.] chronosequence on a peaty gley soil. *Global Change Biology*, **13**, 2128–2142.

Ball T, Smith KA, Garnett MH, Moncrieff JB, Zerva A (2011) An assessment of the effect of sitka spruce (picea sitchensis bong. carr) plantation forest cover on carbon turnover and storage in a peaty gley soil. *European Journal of Soil Science*, **62**, 560–571.

Batjes N (1996) Total carbon and nitrogen in the soils of the world. *European Journal of Soil Science*, **47**, 151–163.

Bell JM, Smith JL, Bailey VL, Bolton H (2003) Priming effect and C storage in semi-arid no-till spring crop rotations. *Biology and Fertility of Soils*, **37**, 237–244.

Bellamy PH, Loveland PJ, Bradley RI, Lark RM, Kirk GJD (2005) Carbon losses from all soils across England and Wales 1978-2003. *Nature*, **437**, 245–248.

Benner R, Fogel ML, Sprague EK, Hodson RE (1987) Depletion of ^{13}C in lignin and its implications for stable carbon isotope studies. *Nature*, **329**, 708–710.

BEST (2011) Berkeley earth surface temperature group website. http://www.berkeleyearth.org

Biasi C, Rusalimova O, Meyer H, *et al.* (2005) Temperature-dependent shift from labile to recalcitrant carbon sources of arctic heterotrophs. *Rapid Communications in Mass Spectrometry*, **19**, 1401–1408.

Blagodatskaya E, Blagodatsky S, Anderson TH, Kuzyakov Y (2007) Priming effects in chernozem induced by glriucose and n in relation to microbial growth strategies. *Applied Soil Ecology*, **37**, 95 – 105.

Blagodatskaya E, Kuzyakov Y (2008) Mechanisms of real and apparent priming effects and their dependence on soil microbial biomass and community structure: critical review. *Biology and Fertility of Soils*, **45**, 115–131.

Blagodatskaya E, Yuyukina T, Blagodatsky S, Kuzyakov Y (2011) Three-source-partitioning of microbial biomass and of co_2 efflux from soil to evaluate mechanisms of priming effects. *Soil Biology and Biochemistry*, **43**, 778 – 786.

Bol R, Bolger T, Cully R, Little D (2003) Recalcitrant soil organic materials mineralize more efficiently at higher temperatures. *Journal of Plant Nutrition and Soil Science*, **166**, 300–307.

Bond-Lamberty B, Thomson A (2010) Temperature-associated increases in the global soil respiration record. *Nature*, **464**, 579–582.

Bosatta E, Ågren GI (1999) Soil organic matter quality interpreted thermodynamically. *Soil Biology and Biochemistry*, **31**, 1889–1891.

Bowling D, McDowell N, Bond B, Law B, Ehleringer J (2002) ^{13}C content of ecosystem respiration is linked to precipitation and vapor pressure deficit. *Oecologia*, **131**, 113–124.

Briones MJI, Ostle NJ, Piearce TG (2008) Stable isotopes reveal that the calciferous gland of earthworms is a CO_2-fixing organ. *Soil Biology and Biochemistry*, **40**, 554–557.

Brown S, Lugo AE (1984) Biomass of tropical forests: a new estimate based on forest volumes. *Science*, **223**, 1290–1293.

Caesar-TonThat TC, Caesar AJ, Gaskin JF, Sainju UM, Busscher WJ (2007) Taxonomic diversity of predominant culturable bacteria associated with microaggregates from two different agroecosystems and their ability to aggregate soil in vitro. *Applied Soil Ecology*, **36**, 10–21.

Cannell MGR, Dewar RC, Pyatt DG (1993) Conifer plantations on drained peatlands in britain: a net gain or loss of carbon? *Forestry*, **66**, 353–369.

Carney KM, Hungate BA, Drake BG, Megonigal JP (2007) Altered soil microbial community at elevated CO_2 leads to loss of soil carbon. *Proceedings of the National Academy of Sciences of the United States of America*, **104**.

Carter M, Gregorich E (2007) *Soil sampling and methods of analysis*. CRC Press, New York, 2 edition.

Chefetz B, Hader Y, Chen Y (1998) Dissolved organic carbon fractions formed during composting of municipal solid waste: Properties and significance. *Acta Hydrochimica et Hydrobiologica*, **26**, 172–179.

Cheng W (2009) Rhizosphere priming effect: Its functional relationships with microbial turnover, evapotranspiration, and C-N budgets. *Soil Biology and Biochemistry*, **41**, 1795 – 1801.

Clay D, Carlson G, Schumacher T, Owens V, Mamani-Pati F (2010) Biomass estimation approach impacts on calculated soil organic carbon maintenance requirements and associated mineralization rate constants. *Journal of Environmental Quality*, **39**, 784–790.

Cleveland C, Nemergut D, Schmidt S, Townsend A (2007) Increases in soil respiration following labile carbon additions linked to rapid shifts in soil microbial community composition. *Biogeochemistry*, **82**, 229–240.

Cloy J, Wilson C, Graham M (2011) The role of Fe and Al oxides in the stabilisation of organic matter in gleyed soils under different hydrological regimes. *In Prep*

Cloy JM, Farmer JG, Graham MC, MacKenzie AB, Cook GT (2008) Historical records of atmospheric Pb deposition in four Scottish ombrotrophic peat bogs: An isotopic comparison with other records from western Europe and Greenland. *Global Biogeochemical Cycles*, **22**, 16 PP.

Conant RT, Drijber RA, Haddix ML, *et al.* (2008) Sensitivity of organic matter decomposition to warming varies with its quality. *Global Change Biology*, **14**, 868–877.

Conant RT, Ryan MG, Ågren GI, *et al.* (2011) Temperature and soil organic matter decomposition rates – synthesis of current knowledge and a way forward. *Global Change Biology*, **17**, 3392–3404.

Conen F, Leifeld J, Seth B, Alewell C (2006) Warming mineralises young and old soil carbon equally. *Biogeosciences*, **3**, 515–519.

Conen F, Zerva A, Arrouays D, Jolivet C, Jarvis PG, Grace J, Mencuccini M (2005) The carbon balance of forest soils: detectability of changes in soil carbon stocks in temperate and boreal forests. *SEB Experimental Biology Series*, pp. 235–249.

Conen F, Zimmermann M, Leifeld J, Seth B, Alewell C (2008) Relative stability of soil carbon revealed by shifts in δ^{15}N and C:N ratio. *Biogeosciences*, **5**, 123–128.

Cotton M (1930) Toxic effects of iodine and nickel on buckwheat grown in solution cultures. *Bulletin of the Torrey Botanical Club*, **57**, 127–140.

Coumou D, Rahmstorf S (2012) A decade of weather extremes. *Nature Climate Change*, **2**, 491–496.

Cox PM, Betts RA, Jones CD, Spall SA, Totterdell IJ (2000a) Acceleration of global warming due to carbon-cycle feedbacks in a coupled climate model. *Nature*, **408**, 184–187.

Cox RJ, Peterson HL, Young J, Cusik C, Espinoza EO (2000b) The forensic analysis of soil organic C by FTIR. *Forensic Science International*, **108**, 107–116.

Craine JM, Fierer N, McLauchlan KK (2010) Widespread coupling between the rate and temperature sensitivity of organic matter decay. *Nature Geosci*, **3**, 854–857.

Creamer C, Filley T, Boutton T, Oleynik S, Kantola I (2011) Controls on soil carbon accumulation during woody plant encroachment: Evidence from physical fractionation, soil respiration, and δ^{13}C of respired CO_2. *Soil Biology and Biochemistry*, **43**, 1678 – 1687.

Cross A, Grace J (2010) The effect of warming on the CO_2 emissions of fresh and old organic soil from under a Sitka spruce plantation. *Geoderma*, **157**, 126–132.

Crow S, Swanston C, Lajtha K, Brooks J, Keirstead H (2007) Density fractionation of forest soils: methodological questions and interpretation of incubation results and turnover time in an ecosystem context. *Biogeochemistry*, **85**, 69–90.

Crow SE, Sulzman EW, Rugh WD, Bowden RD, Lajtha K (2006) Isotopic analysis of respired CO_2 during decomposition of separated soil organic matter pools. *Soil Biology and Biochemistry*, **38**, 3279–3291.

Dalal RC (1998) Soil microbial biomass—what do the numbers really mean? *Aust. J. Exp. Agric.*, **38**, 649–665.

Davidson EA, Ackerman IL (1993) Changes in soil carbon inventories following cultivation of previously untilled soils. *Biogeochemistry*, **20**, 161–193.

Davidson EA, Janssens IA (2006) Temperature sensitivity of soil carbon decomposition and feedbacks to climate change. *Nature*, **440**, 165–173.

Davidson EA, Janssens IA, Luo Y (2006) On the variability of respiration in terrestrial ecosystems: moving beyond Q_{10}. *Global Change Biology*, **12**, 154–164.

Dawson TE, Mambelli S, Plamboeck AH, Templer PH, Tu KP (2002) Stable isotopes in plant ecology. *Annual Review of Ecology and Systematics*, **33**, 507–559.

De Neergaard A, Magid J (2001) Influence of the rhizosphere on microbial biomass and recently formed organic matter. *European Journal of Soil Science*, **52**, 377–384.

Dengel S, Grace J (2010) Carbon dioxide exchange and canopy conductance of two coniferous forests under various sky conditions. *Oecologia*, **164**, 797–808.

Dorodnikov M, Kuzyakov Y, Fangmeier A, Wiesenberg GL (2011) C and N in soil organic matter density fractions under elevated atmospheric CO_2: Turnover vs. stabilization. *Soil Biology and Biochemistry*, **43**, 579–589.

Ducaroir J, Lamy I (1995) Evidence of trace metal association with soil organic matter using particle size fractionation after physical dispersion treatment. *The Analyst*, **120**, 741.

Eswaran H, Vandenberg E, Reich P (1993) Organic carbon in soils of the world. *Soil science society of America Journal* **57**, 192–194

Etcheverria P, Huygens D, Godoy R, Borie F, Boeckx P (2009) Arbuscular mycorrhizal fungi contribute to ^{13}C and ^{15}N enrichment of soil organic matter in forest soils. *Soil Biology and Biochemistry*, **41**, 858–861.

Fangueiro D, Chadwick D, Dixon L, Bol R (2007) Quantification of priming and CO_2 emission sources following the application of different slurry particle size fractions to a grassland soil. *Soil Biology and Biochemistry*, **39**, 2608–2620.

Fellbaum CR, Gachomo EW, Beesetty Y, *et al.* (2012) Carbon availability triggers fungal nitrogen uptake and transport in arbuscular mycorrhizal symbiosis. *Proceedings of the National Academy of Sciences*.

Feng X, Simpson AJ, Wilson KP, Williams DD, Simpson MJ (2008) Increased cuticular carbon sequestration and lignin oxidation in response to soil warming. *Nature Geoscience*, **1**, 836–840.

Feng X, Simpson MJ (2008) Temperature responses of individual soil organic matter components. *Journal of Geophysical Research*, **113**, G03036.

Fierer N, Colman BP, Schimel JP, Jackson RB (2006) Predicting the temperature dependence of microbial respiration in soil: A continental-scale analysis. *Global Biogeochemical Cycles*, **20**, GB3026.

Filley TR, Boutton TW, Liao JD, Jastrow JD, Gamblin DE (2008) Chemical changes to nonaggregated particulate soil organic matter following grassland-to-woodland transition in a subtropical savanna. *Journal of Geophysical Research*, **113**, G03009.

Fontaine S, Bardoux G, Abbadie L, Mariotti A (2004a) Carbon input to soil may decrease soil carbon content. *Ecology Letters*, **7**, 314–320.

Fontaine S, Bardoux G, Benest D, Verdier B, Mariotti A, Abbadie L (2004b) Mechanisms of the priming effect in a savannah soil amended with cellulose. *Soil Science Society of America Journal*, **68**, 125–131.

Friedlingstein P, Cox P, Betts R, *et al.* (2006) Climate–Carbon cycle feedback analysis: Results from the C^4MIP model intercomparison. *Journal of Climate*, **19**, 3337–3353.

Gartzia-Bengoetxea N, González-Arias A, Merino A, de Arano IM (2009) Soil organic matter in soil physical fractions in adjacent semi-natural and cultivated stands in temperate Atlantic forests. *Soil Biology and Biochemistry*, **41**, 1674–1683.

Ghashghaie J, Badeck FW, Lanigan G, *et al.* (2003) Carbon isotope fractionation during dark respiration and photorespiration in C_3 plants. *Phytochemistry Reviews*, **2**, 145–161.

Giardina CP, Ryan MG (2000) Evidence that decomposition rates of organic carbon in mineral soil do not vary with temperature. *Nature*, **404**, 858–861.

Gillabel J, Cebrian-Lopez B, Six J, Merckx R (2010) Experimental evidence for the attenuating effect of SOM protection on temperature sensitivity of SOM decomposition. *Global Change Biology*, **16**, 2789–2798.

Gleixner G, Bol R, Balesdent J (1999) Molecular insight into soil carbon turnover. *Rapid Communications in Mass Spectrometry*, **13**, 1278–1283.

Gleixner G, Poirier N, Bol R, Balesdent J (2002) Molecular dynamics of organic matter in a cultivated soil. *Organic Geochemistry*, **33**, 357 – 366.

Godbold D, Hoosbeek M, Lukac M, *et al.* (2006) Mycorrhizal hyphal turnover as a dominant process for carbon input into soil organic matter. *Plant and Soil*, **281**, 15–24.

Golchin A, Oades JM, Skjemstad JO, Clarke P (1994) Soil structure and carbon cycling. *Australian Journal of Soil Research*, **32**, 1043–1068.

Grandy AS, Neff JC, Weintraub MN (2007) Carbon structure and enzyme activities in alpine and forest ecosystems. *Soil Biology and Biochemistry*, **39**, 2701–2711.

Guenet B, Leloup J, Raynaud X, Bardoux G, Abbadie L (2010) Negative priming effect on mineralization in a soil free of vegetation for 80 years. *European Journal of Soil Science*, **61**, 384–391.

Guo L, Wang M, Gifford R (2007) The change of soil carbon stocks and fine root dynamics after land use change from a native pasture to a pine plantation. *Plant and Soil*, **299**, 251–262.

Guggenberger G, Christensen BT, Zech W (1994) Land-use effects on the composition of organic matter in particle-size separates of soil: I. Lignin and carbohydrate signature. *European Journal of Soil Science*, **45**, 449–458.

Haberhauer G, Rafferty B, Strebl F, Gerzabek MH (1998) Comparison of the composition of forest soil litter derived from three different sites at various decompositional stages using FTIR spectroscopy. *Geoderma*, **83**, 331–342.

Haider K, Martin JP (1975) Decomposition of specifically carbon-14 labeled benzoic and cinnamic acid derivatives in soil. *Soil Science Society of America Journal*. **39**,657–662.

Hamer U, Marschner B (2002) Priming effects of sugars, amino acids, organic acids and catechol on the mineralization of lignin and peat. *Journal of Plant Nutrition and Soil Science*, **165**, 261–268.

Hamer U, Marschner B (2005) Priming effects in soils after combined and repeated substrate additions. *Geoderma*, **128**, 38 – 51.

Hamer U, Marschner B, Brodowski S, Amelung W (2004) Interactive priming of black carbon and glucose mineralisation. *Organic Geochemistry*, **35**, 823 – 830.

Hardie SML, Garnett MH, Fallick AE, Rowland AP, Ostle NJ (2005) Carbon dioxide capture using a zeolite molecular sieve sampling system for isotopic studies (^{13}C and ^{14}C) of respiration. *Radiocarbon*, **47**, 441–451.

Harkness DD, Harrison AF, Bacon PJ (1986) The temporal distribution of 'bomb' ^{14}C in a forest soil. *Radiocarbon*, **28**, 328–337.

Hartley IP, Ineson P (2008) Substrate quality and the temperature sensitivity of soil organic matter decomposition. *Soil Biology and Biochemistry*, **40**, 1567–1574.

Hawkes CV, Hartley IP, Ineson P, Fitter AH (2008) Soil temperature affects carbon allocation within arbuscular mycorrhizal networks and carbon transport from plant to fungus. *Global Change Biology*, **14**, 1181–1190.

Hedges JI, Cowie GL, Ertel JR, Barbour RJ, Hatcher PG (1985) Degradation of carbohydrates and lignins in buried woods. *Geochimica et Cosmochimica Acta*, **49**, 701 – 711.

Hickman L (2011) Global warming policy foundation donor funding levels revealed | environment | the guardian. http://www.guardian.co.uk/environment/2011/jan/20/global-warming-policy-foundation-donors.

Hopkins DW, Sparrow AD, Shillam LL, *et al.* (2008) Enzymatic activities and microbial communities in an Antarctic dry valley soil: Responses to C and N supplementation. *Soil Biology and Biochemistry*, **40**, 2130–2136.

Houghton JT, Filho LG, Intergovernmental Panel on Climate Change, Callander BA, Harris N, Kattenburg A, Maskell K (1996) *Climate Change 1995: the science of climate change*. Cambridge University Press, Cambridge.

Hsiang SM, Meng KC, Cane MA (2011) Civil conflicts are associated with the global climate. **476**, 438–441.

Hsieh YP (1993) Radiocarbon signatures of turnover rates in active soil organic carbon pools. *Soil Science Society of America Journal*, **57**, 1020–1022.

Hua Q, Barbetti M (2004) Review of tropospheric bomb-^{14}c data for carbon cycle modeling and calibration purposes. *Radiocarbon*, **46**, 1273–1298

Ingwersen J, Poll C, Streck T, Kandeler E (2008) Micro-scale modelling of carbon turnover driven by microbial succession at a biogeochemical interface. *Soil Biology and Biochemistry*, **40**, 864–878.

IPCC (2007) Contribution of working group I to the fourth assessment report of the intergovernmental panel on climate change. Cambridge University Press.

IPCC (2007) Working group II report "Impacts, adaptation and vulnerability".

Irvine MR, Gardiner BA, Hill MK (1997) The Evolution Of Turbulence Across A Forest Edge *Boundary-layer Meteorology*, **84**, 467.

Jeffries TW, Choi S, Kirk TK (1981) Nutritional regulation of lignin degradation by phanerochaete chrysosporium. *Appl. Environ. Microbiol.*, **42**, 290–296.

Jenkinson DS, Brookes PC, Powlson DS (2004) Measuring soil microbial biomass. *Soil Biology and Biochemistry*, **36**, 5 – 7.

Jenkinson DS, Poulton PR, Bryant C (2008) The turnover of organic carbon in subsoils. part 1. natural and bomb radiocarbon in soil profiles from the Rothamsted long-term field experiments. *European Journal of Soil Science*, **59**, 391–399.

John B, Ludwig B, Potthoff M, Flessa H (2004) Carbon and nitrogen mineralization after maize harvest between and within maize rows: a microcosm study using ^{13}C natural abundance. *Journal of Plant Nutrition and Soil Science*, **167**, 270–276.

John B, Yamashita T, Ludwig B, Flessa H (2005) Storage of organic carbon in aggregate and density fractions of silty soils under different types of land use. *Geoderma*, **128**, 63 – 79.

Jones C, McConnell C, Coleman K, Cox P, Falloon P, Jenkinson D, Powlson D (2005) Global climate change and soil carbon stocks; predictions from two contrasting models for the turnover of organic carbon in soil. *Global Change Biology*, **11**, 154–166.

Kaiser K, Guggenberger G (2000) The role of DOM sorption to mineral surfaces in the preservation of organic matter in soils. *Organic Geochemistry*, **31**, 711–725.

Kaiser K, Zech W (2000) Sorption of dissolved organic nitrogen by acid subsoil horizons and individual mineral phases. *European Journal of Soil Science*, **51**, 403–411.

Kaiser M, Ellerbrock RH, Gerke HH (2007) Long-term effects of crop rotation and fertilization on soil organic matter composition. *European Journal of Soil Science*, **58**, 1460–1470.

Kaiser M, Walter K, Ellerbrock R, Sommer M (2011) Effects of land use and mineral characteristics on the organic carbon content, and the amount and composition of na-pyrophosphate-soluble organic matter, in subsurface soils. *European Journal of Soil Science*, **62**, 226–236.

Kalbitz K, Kaiser K (2008) Contribution of dissolved organic matter to carbon storage in forest mineral soils. *Journal of Plant Nutrition and Soil Science*, **171**, 52–60.

Kalbitz K, Kaiser K, Bargholz J, Dardenne P (2006) Lignin degradation controls the production of dissolved organic matter in decomposing foliar litter. *European Journal of Soil Science*, **57**, 504–516.

Karhu K, Fritze H, Hämäläinen K, *et al.* (2010a) Temperature sensitivity of soil carbon fractions in boreal forest soil. *Ecology*, **91**, 370–376.

Karhu K, Fritze H, Tuomi M, Vanhala P, Spetz P, Kitunen V, Liski J (2010b) Temperature sensitivity of organic matter decomposition in two boreal forest soil profiles. *Soil Biology and Biochemistry*, **42**, 72–82.

Kayler ZE, Sulzman EW, Rugh WD, Mix AC, Bond BJ (2010) Characterizing the impact of diffusive and advective soil gas transport on the measurement and interpretation of the isotopic signal of soil respiration. *Soil Biology and Biochemistry*, **42**, 435 – 444.

Kirschbaum MUF (2004) Soil respiration under prolonged soil warming: are rate reductions caused by acclimation or substrate loss? *Global Change Biology*, **10**, 1870–1877.

Kirschbaum MUF (2006) The temperature dependence of organic-matter decomposition- still a topic of debate. *Soil Biology and Biochemistry*, **38**, 2510–2518.

Kleber M, Sollins P, Sutton R (2007) A conceptual model of organo-mineral interactions in soils: self-assembly of organic molecular fragments into zonal structures on mineral surfaces. *Biogeochemistry*, **85**, 9–24.

Kleber M, Nico PS, Plante A, Filley T, Kramer M, Swanston C, Sollins P (2011) Old and stable soil organic matter is not necessarily chemically recalcitrant: implications for modeling concepts and temperature sensitivity. *Global Change Biology*, **17**, 1097–1107.

Knorr W, Prentice IC, House JI, Holland EA (2005) Long-term sensitivity of soil carbon turnover to warming. *Nature*, **433**, 298–301.

Kögel-Knabner I, Guggenberger G, Kleber M, *et al.* (2008) Organo-mineral associations in temperate soils: Integrating biology, mineralogy, and organic matter chemistry. *Journal of Plant Nutrition and Soil Science*, **171**, 61–82.

Kögel-Knabner I, Hatcher PG, Tegelaar EW, de Leeuw JW (1992) Aliphatic components of forest soil organic matter as determined by solid-state ^{13}C NMR and analytical pyrolysis. *Science of The Total Environment*, **113**, 89–106.

Kramer C, Gleixner G (2008) Soil organic matter in soil depth profiles: Distinct carbon preferences of microbial groups during carbon transformation. *Soil Biology and Biochemistry*, **40**, 425–433.

Krull ES, Baldock JA, Skjemstad JO (2003) Importance of mechanisms and processes of the stabilisation of soil organic matter for modelling carbon turnover. *Functional Plant Biology*, **30**.

Kuzyakov Y, Bol R (2006) Sources and mechanisms of priming effect induced in two grassland soils amended with slurry and sugar. *Soil Biology and Biochemistry*, **38**, 747–758.

Lamparter A, Bachmann J, Goebel MO, Woche SK (2009) Carbon mineralization in soil: Impact of wetting-drying, aggregation and water repellency. *Geoderma*, **150**, 324–333.

Le Quere C, Raupach MR, Canadell JG, Marland et al G (2009) Trends in the sources and sinks of carbon dioxide. *Nature Geosci*, **2**, 831–836.

Lehmann J, Kinyangi J, Solomon D (2007) Organic matter stabilization in soil microaggregates: implications from spatial heterogeneity of organic carbon contents and carbon forms. *Biogeochemistry*, **85**, 45–57.

Leifeld J, Fuhrer J (2005) The temperature response of CO_2 production from bulk soils and soil fractions is related to soil organic matter quality. *Biogeochemistry*, **75**, 433–453.

Leifeld J, Zimmermann M, Fuhrer J (2008) Simulating decomposition of labile soil organic carbon: Effects of pH. *Soil Biology and Biochemistry*, **40**, 2948–2951.

Leifeld J, Zimmermann M, Fuhrer J, Conen F (2009) Storage and turnover of carbon in grassland soils along an elevation gradient in the Swiss Alps. *Global Change Biology*, **15**, 668–679.

Levin I, Kromer B (2004) The tropospheric $^{14}CO_2$ level in mid latitudes of the Northern Hemisphere (1959-2003). *Radiocarbon*, **46**, 1261–1272.

Lobell DB, Burke MB, Tebaldi C, Mastrandrea MD, Falcon WP, Naylor RL (2008) Prioritizing climate change adaptation needs for food security in 2030. *Science*, **319**, 607–610.

Lockwood M (2010) Solar change and climate: an update in the light of the current exceptional solar minimum. *Proceedings of the Royal Society A: Mathematical, Physical and Engineering Science*, **466**, 303 –329.

Luke CM, Cox PM (2011) Soil carbon and climate change: from the jenkinson effect to the compost-bomb instability. *European Journal of Soil Science*, **62**, 5–12.

Luo Y, Wan S, Hui D, Wallace LL (2001) Acclimatization of soil respiration to warming in a tall grass prairie. *Nature*, **413**, 622–625.

Magid J, Gorissen A, Giller KE (1996) In search of the elusive "active" fraction of soil organic matter: Three size-density fractionation methods for tracing the fate of homogeneously ^{14}c-labelled plant materials. *Soil Biology and Biochemistry*, **28**, 89–99.

Marschner B, Brodowski S, Dreves A, *et al.* (2008) How relevant is recalcitrance for the stabilization of organic matter in soils? *Journal of Plant Nutrition and Soil Science*, **171**, 91–110.

Martens R (1995) Current methods for measuring microbial biomass C in soil: Potentials and limitations. *Biology and Fertility of Soils*, **19**, 87–99.

Mikutta R, Kleber M, Torn M, Jahn R (2006) Stabilization of soil organic matter: Association with minerals or chemical recalcitrance? *Biogeochemistry*, **77**, 25–56.

Millard P, Midwood AJ, Hunt JE, Whitehead D, Boutton TW (2008) Partitioning soil surface CO_2 efflux into autotrophic and heterotrophic components, using natural gradients in soil δ^{13}C in an undisturbed savannah soil. *Soil Biology and Biochemistry*, **40**, 1575–1582.

Mitchell JT, Harrison G (2010) CO_2 payback time for a wind farm on afforested peatland in the uk. *Mires and Peat*, **4**.

Mojeremane W, Rees RM, , Mencuccini M (2012) The effects of site preparation practices on carbon dioxide, methane and nitrous oxide fluxes from a peaty gley soil. *Forestry*, **85**, 1–15.

Murage EW, Voroney PR, Kay BD, Deen B, Beyaert RP (2007) Dynamics and turnover of soil organic matter as affected by tillage. *Soil Science Society of America Journal*, **71**, 1363.

NASA (2011) NASA research finds 2010 tied for warmest year on record. http://www.nasa.gov/topics/earth/features/2010-warmest-year.html *12 Jan 2011*

NASA (2012) Satellites see unprecedented greenland ice sheet surface melt. http://www.nasa.gov/topics/earth/features/greenland-melt.html.

Niu S, Wu M, Han Y, Xia J, Li L, Wan S (2008) Water-mediated responses of ecosystem carbon fluxes to climatic change in a temperate steppe. *New Phytologist*, **177**, 209–219.

Ohm H, Hamer U, Marschner B (2007) Priming effects in soil size fractions of a podzol Bs horizon after addition of fructose and alanine. *Journal of Plant Nutrition and Soil Science*, **170**, 551–559.

Osborne CP, Beerling DJ (2006) Nature's green revolution: the remarkable evolutionary rise of C_4 plants. *Philosophical Transactions of the Royal Society B: Biological Sciences*, **361**, 173 –194.

Overpeck J, Udall B (2010) Dry times ahead. *Science*, **328**, 1642–1643.

Palfner G, Casanova-Katny M, Read D (2005) The mycorrhizal community in a forest chronosequence of Sitka spruce [*Picea sitchensis*; (bong.) carr.] in northern England. *Mycorrhiza*, **15**, 571–579.

Patz JA, Campbell-Lendrum D, Holloway T, Foley JA (2005) Impact of regional climate change on human health. *Nature*, **438**, 310–317.

Paul S, Flessa H, Veldkamp E, López-Ulloa M (2008a) Stabilization of recent soil carbon in the humid tropics following land use changes: evidence from aggregate fractionation and stable isotope analyses. *Biogeochemistry*, **87**, 247–263.

Paul S, Martinson GO, Veldkamp E, Flessa H (2008b) Sample pretreatment affects the distribution of organic carbon in aggregates of tropical grassland soils. *Soil Science Society of America Journal*, **72**, 500.

Plante AF, Conant RT, Carlson J, Greenwood R, Shulman JM, Haddix ML, Paul EA (2010) Decomposition temperature sensitivity of isolated soil organic matter fractions. *Soil Biology and Biochemistry*, **42**, 1991–1996.

Powlson DS, Whitmore AP, Goulding KWT (2011) Soil carbon sequestration to mitigate climate change: a critical re-examination to identify the true and the false. *European Journal of Soil Science*, **62**, 42–55.

Prescott C (2008) Soil science: Heat-proof carbon compound. *Nature Geoscience*, **1**, 815–816.

Quideau SA, Graham RC, Feng X, Chadwick OA (2003) Natural isotopic distribution in soil surface horizons differentiated by vegetation. *Soil Science Society of America Journal*, **67**, 1544–1550.

Rahmstorf S (2010) A new view on sea level rise. *Nature Reviews Climate Change*, **4**, 44–45.

Rasmussen C, Southard RJ, Horwarth WR (2008) Litter type and soil minerals control temperate forest soil carbon response to climate change. *Global Change Biology*, **14**, 2064–2080.

Reimer PJ, Baillie MGL, Bard E, *et al.* (2004) IntCal04 terrestrial radiocarbon age calibration, 0-26 cal kyr BP. *Radiocarbon*, **46**, 1029–1058.

Rey A, Petsikos C, Jarvis PG, Grace J (2005) Effect of temperature and moisture on rates of carbon mineralization in a Mediterranean oak forest soil under controlled and field conditions. *European Journal of Soil Science*, **56**, 589–599.

Rey A, Pegoraro E, Jarvis PG (2008) Carbon mineralization rates at different soil depths across a network of european forest sites (FORCAST). *European Journal of Soil Science*, **59**, 1049–1062.

Rillig M, Caldwell B, Wösten H, Sollins P (2007) Role of proteins in soil carbon and nitrogen storage: controls on persistence. *Biogeochemistry*, **85**, 25–44.

Rinnan R, Michelsen A, Bååth E, Jonasson S (2007) Mineralization and carbon turnover in subarctic heath soil as affected by warming and additional litter. *Soil Biology and Biochemistry*, **39**, 3014–3023.

Robertson GP, Coleman DC, Bledsoe CS, Sollins P (1999) *Standard Soil Methods for Long-term Ecological Research*. Oxford University Press, Oxford.

Rochette P, Flanagan LB, Gregorich EG (1999) Separating soil respiration into plant and soil components using analyses of the natural abundance of carbon-13. *Soil Science Society of America Journal*, **63**, 1207–1213.

Rovira P, Kurz-Besson C, Coûteaux M, Vallejo VR (2008) Changes in litter properties during decomposition: A study by differential thermogravimetry and scanning calorimetry. *Soil Biology and Biochemistry*, **40**, 172–185.

Salomé C, Nunan N, Pouteau V, Lerch TZ, Chenu C (2010) Carbon dynamics in topsoil and in subsoil may be controlled by different regulatory mechanisms. *Global Change Biology*, **16**, 416–426.

Sample I (2007) Scientists offered cash to dispute climate study | environment | the guardian. http://www.guardian.co.uk/environment/2007/feb/02/frontpagenews.climatechange.

Schmidt MW, Torn MS, Abiven S, *et al.* (2011) Persistence of soil organic matter as an ecosystem property. *Nature*, **478**, 49–56.

Schweizer M, Fear J, Cadisch G (1999) Isotopic (^{13}C) fractionation during plant residue decomposition and its implications for soil organic matter studies. *Rapid Communications in Mass Spectrometry*, **13**, 1284–1290.

Smith P, Fang C (2010) Carbon cycle: A warm response by soils. *Nature*, **464**, 499–500.

Seeber J, Scheu S, Meyer E (2006) Effects of macro-decomposers on litter decomposition and soil properties in alpine pastureland: A mesocosm experiment. *Applied Soil Ecology*, **34**, 168–175.

Sey B, Manceur A, Whalen J, Gregorich E, Rochette P (2008) Small-scale heterogeneity in carbon dioxide, nitrous oxide and methane production from aggregates of a cultivated sandy-loam soil. *Soil Biology and Biochemistry*, **40**, 2468–2473.

Sidorova OV, Siegwolf RTW, Saurer M, Naurzbaev MM, Vaganov EA (2008) Isotopic composition (δ^{13}C, δ^{18}O) in wood and cellulose of Siberian larch trees for early Medieval and recent periods. *Journal of Geophysical Research*, **113**, G02019.

Six J, Callewaert P, Lenders S, *et al.* (2002) Measuring and understanding carbon storage in afforested soils by physical fractionation. *Soil Science Society of America Journal*, **66**, 1981–1987.

Sleutel S, Leinweber P, Begum SA, Kader MA, Neve SD (2009) Shifts in soil organic matter composition following treatment with sodium hypochlorite and hydrofluoric acid. *Geoderma*, **149**, 257–266.

Slota P, Jull A, Linick T, Toolin L (1987) Preparation of small samples for ^{14}C accelerator targets by catalytic reduction of CO. *Radiocarbon*, **29**, 303–306.

Sohi SP, Mahieu N, Arah JRM, Powlson DS, Madari B, Gaunt JL (2001) A procedure for isolating soil organic matter fractions suitable for modeling. *Soil Science Society of America Journal*, **65**, 1121–1128.

Sohi SP, Yates HC, Gaunt JL (2010) Testing a practical indicator for changing soil organic matter. *Soil Use and Management*, **26**, 108–117.

Sollins P, Kramer M, Swanston C, *et al.* (2009) Sequential density fractionation across soils of contrasting mineralogy: evidence for both microbial- and mineral-controlled soil organic matter stabilization. *Biogeochemistry*, pp. 209–231.

Sollins P, Spycher G, Glassman C (1984) Net nitrogen mineralization from light- and heavy-fraction forest soil organic matter. *Soil Biology and Biochemistry*, **16**, 31 – 37.

Sollins P, Swanston C, Kleber M, *et al.* (2006) Organic C and N stabilization in a forest soil: Evidence from sequential density fractionation. *Soil Biology and Biochemistry*, **38**, 3313 – 3324.

Sollins P, Swanston C, Kramer M (2007) Stabilization and destabilization of soil organic matter– a new focus. *Biogeochemistry*, **85**, 1–7.

Solomon S, Plattner GK, Knutti R, Friedlingstein P (2009) Irreversible climate change due to carbon dioxide emissions. *Proceedings of the National Academy of Sciences*, **106**, 1704–1709.

Spaccini R, Piccolo A, Haberhauer G, Gerzabek MH (2000) Transformation of organic matter from maize residues into labile and humic fractions of three european soils as revealed by ^{13}C distribution and CPMAS-NMR spectra. *European Journal of Soil Science*, **51**, 583–594.

Spielvogel S, Prietzel J, Kögel-Knabner I (2008) Soil organic matter stabilization in acidic forest soils is preferential and soil type-specific. *European Journal of Soil Science*, **59**, 674–692.

Stemmer M, Gerzabek MH, Kandeler E (1998) Organic matter and enzyme activity in particle-size fractions of soils obtained after low-energy sonication. *Soil Biology and Biochemistry*, **30**, 9–17.

Stemmer M, Von Lützow M, Kandeler E, Pichlmayer F, Gerzabek MH (1999) The effect of maize straw placement on mineralization of C and N in soil particle size fractions. *European Journal of Soil Science*, **50**, 73–85.

Stevenson FJ (1994) *Humus chemistry: genesis, composition, reactions.* Wiley, New York.

Stuiver M, Polach HA (1977) Discussion: Reporting of ^{14}C data. *Radiocarbon*, **19**, 355–363.

Swain EY, Perks MP, Vanguelova EI, Abbott GD (2010) Carbon stocks and phenolic distributions in peaty gley soils afforested with sitka spruce (picea sitchensis). *Organic Geochemistry*, **41**, 1022—1025.

Swanston CW, Caldwell BA, Homann PS, Ganio L, Sollins P (2002) Carbon dynamics during a long-term incubation of separate and recombined density fractions from seven forest soils. *Soil Biology and Biochemistry*, **34**, 1121 – 1130.

Taylor BR, Parkinson D, Parsons WFJ (1989) Nitrogen and lignin content as predictors of litter decay rates: A microcosm test. *Ecology*, **70**, pp. 97–104.

Thornley JHM, Cannell MGR (2001) Soil carbon storage response to temperature: an hypothesis. *Annals of Botany*, **87**, 591–598.

Tonon G, Sohi S, Francioso O, *et al.* (2010) Effect of soil pH on the chemical composition of organic matter in physically separated soil fractions in two broadleaf woodland sites at Rothamsted, UK. *European Journal of Soil Science*, **61**, 970–979.

Torn MS, Trumbore SE, Chadwick OA, Vitousek PM, Hendricks DM (1997)Mineral control of soil organic carbon storage and turnover. *Nature*, **389**, 170–173.

Townsend AR, Vitousek PM, Desmarais DJ, Tharpe A (1997) Soil carbon pool structure and temperature sensitivity inferred using CO_2 and $^{13}CO_2$ incubation fluxes from five Hawaiian soils. *Biogeochemistry*, **38**, 1–17.

Trumbore S (2000) Age of soil organic matter and soil respiration: radiocarbon constraints on belowground C dynamics. *Ecological Applications*, **10**, 399–411.

Trumbore S (2009) Radiocarbon and soil carbon dynamics. *Annual Review of Earth and Planetary Sciences*, **37**, 47–66.

Turchenek L, Oades J (1979) Fractionation of organo-mineral complexes by sedimentation and density techniques. *Geoderma*, **21**, 311 – 343.

UN Department of Economic and Social Affairs (2004) World population to 2300.

Uvarov AV, Scheu S (2004) Effects of density and temperature regime on respiratory activity of the epigeic earthworm species *Lumbricus rubellus* and *Dendrobaena octaedra* (Lumbricidae). *European Journal of Soil Biology*, **40**, 163–167.

Vanhala P, Karhu K, Tuomi M, Sonninen E, Jungner H, Fritze H, Liski J (2007) Old soil carbon is more temperature sensitive than the young in an agricultural field. *Soil Biology and Biochemistry*, **39**, 2967–2970.

Vicca S, Fivez L, Kockelbergh F, *et al.* (2009) No signs of thermal acclimation of heterotrophic respiration from peat soils exposed to different water levels. *Soil Biology and Biochemistry*, **41**, 2014–2016.

von Lützow M, Kögel-Knabner I (2009) Temperature sensitivity of soil organic matter decomposition– what do we know? *Biology and Fertility of Soils*, **46**, 1–15.

von Lützow M, Kögel-Knabner I, Ekschmitt K, Flessa H, Guggenberger G, Matzner E, Marschner B (2007) SOM fractionation methods: Relevance to functional pools and to stabilization mechanisms. *Soil Biology and Biochemistry*, **39**, 2183–2207.

Wadhams P (2012) Arctic ice cover, ice thickness and tipping points. *Ambio*, **41**, 23–33.

Wagai R, Mayer LM, Kitayama K (2009) Nature of the "occluded" low-density fraction in soil organic matter studies: A critical review. *Soil Science and Plant Nutrition*, **55**, 13–25.

Waldrop MP, Firestone MK (2004) Altered utilization patterns of young and old soil C by microorganisms caused by temperature shifts and N additions. *Biogeochemistry*, **67**, 235–248.

Webster EA, Chudek JA, Hopkins DW (2000) Carbon transformations during decomposition of different components of plant leaves in soild. *Soil Biology and Biochemistry*, **32**, 301–314.

Wetterstedt JÅ, Persson T, Ågren G (2010) Temperature sensitivity and substrate quality in soil organic matter decomposition: results of an incubation study with three substrates. *Global Change Biology*, **16**, 1806.

Wickland K, Neff J (2008) Decomposition of soil organic matter from boreal black spruce forest: environmental and chemical controls. *Biogeochemistry*, **87**, 29–47.

Xiao C, Janssens IA, Liu P, Zhou Z, Sun OJ (2007) Irrigation and enhanced soil carbon input effects on below-ground carbon cycling in semiarid temperate grasslands. *New*, **174**, 835–846.

Yafa C, Farmer JG (2006) A comparative study of acid-extractable and total digestion methods for the determination of inorganic elements in peat material by inductively coupled plasma-optical emission spectrometry. *Analytica Chimica Acta*, **557**, 296 – 303.

Zerva A, Ball T, Smith KA, Mencuccini M (2005) Soil carbon dynamics in a Sitka spruce (Picea sitchensis (Bong.) carr.) chronosequence on a peaty gley. *Forest Ecology and Management*, **205**, 227–240.

Zerva A, Mencuccini M (2005) Carbon stock changes in a peaty gley soil profile after afforestation with sitka spruce (*Picea sitchensis*). *Annals of Forest Science*, **62**, 873–880.

Zerva A, Mencuccini M (2005) Short-term effects of clearfelling on soil CO_2, CH_4, and N_2O fluxes in a Sitka spruce plantation. *Soil Biology and Biochemistry*, **37**, 2025–2036.

Zhang H (1994) Organic matter incorporation affects mechanical properties of soil aggregates. *Soil and Tillage Research*, **31**, 263 – 275.

Zimmermann M, Leifeld J, Schmidt MWI, Smith P, Fuhrer J (2007) Measured soil organic matter fractions can be related to pools in the RothC model. *European Journal of Soil Science*, **58**, 658–667.

Appendix A

SEM-EDX of density fractions and whole soils

Figure A.1: Organic horizon whole soil

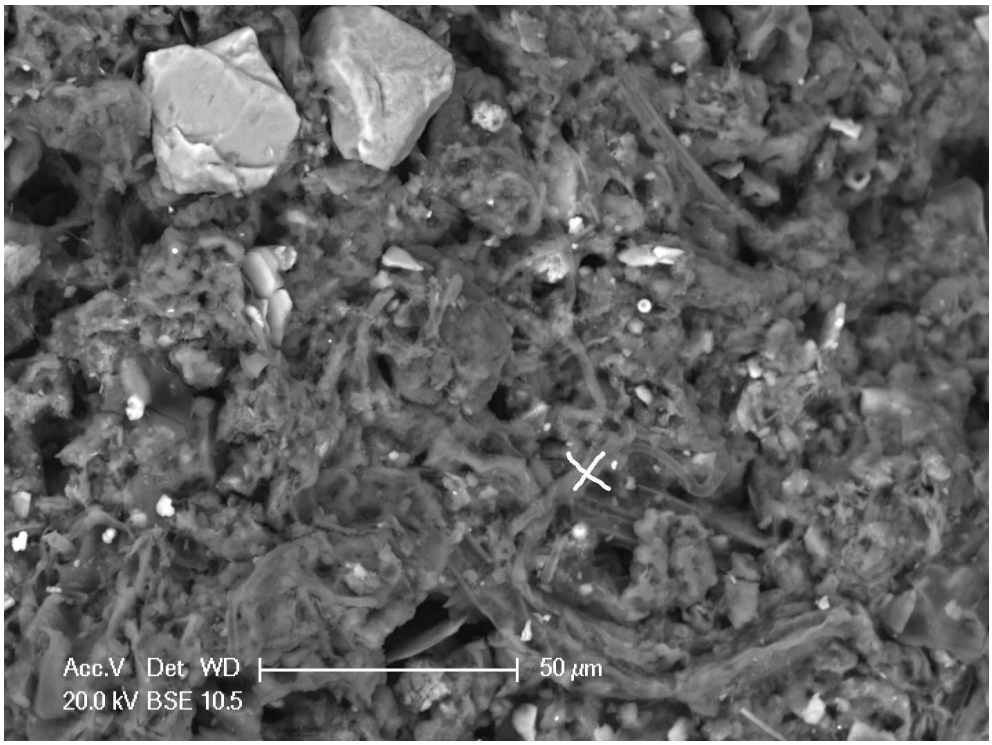

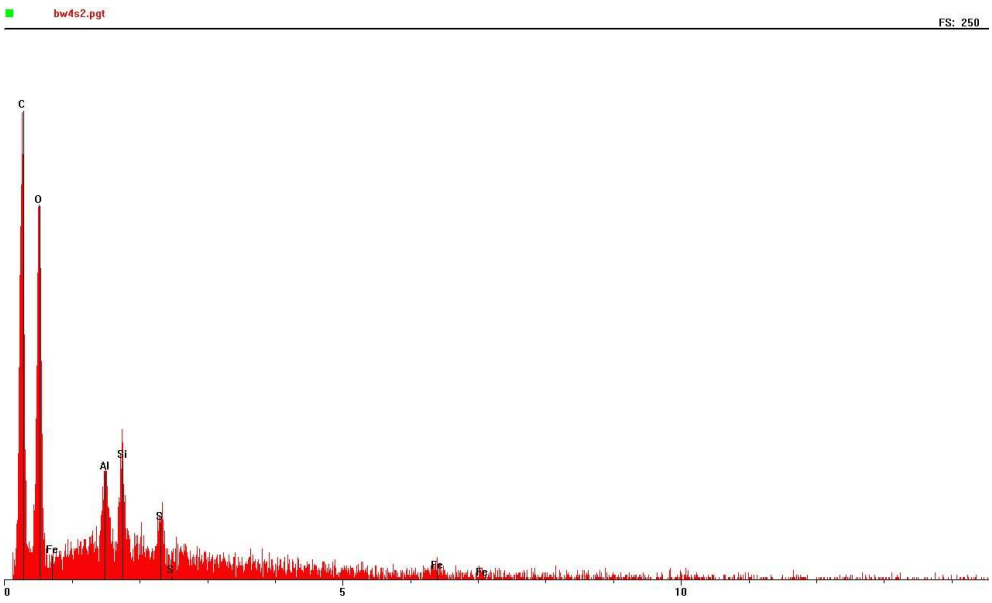

Figure A.2: Organic horizon light fraction

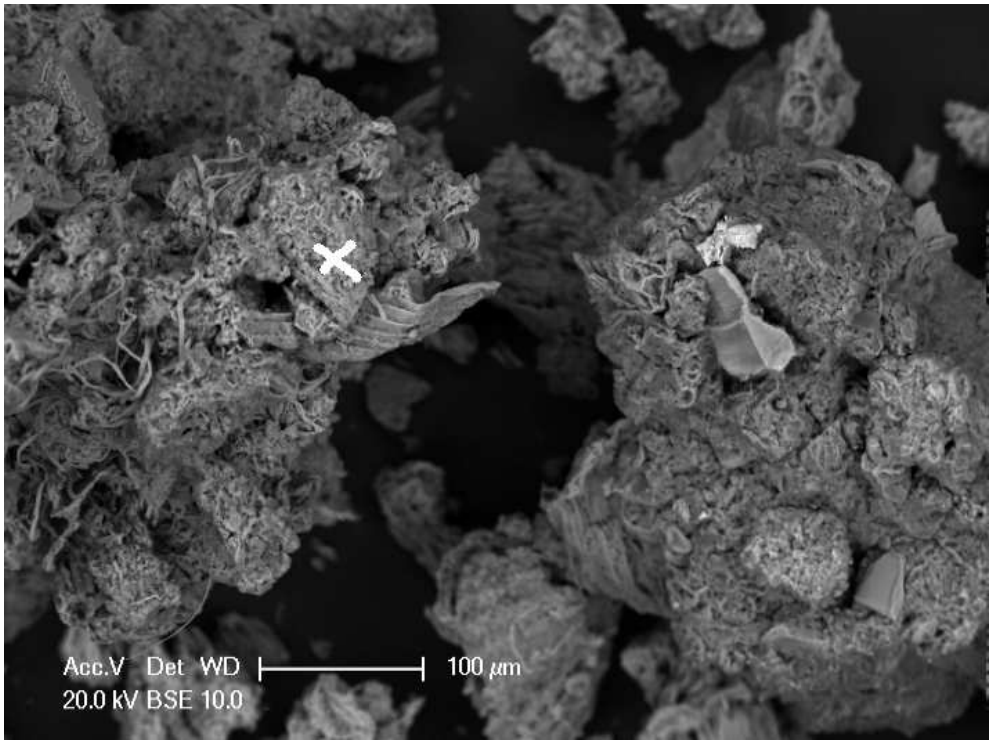

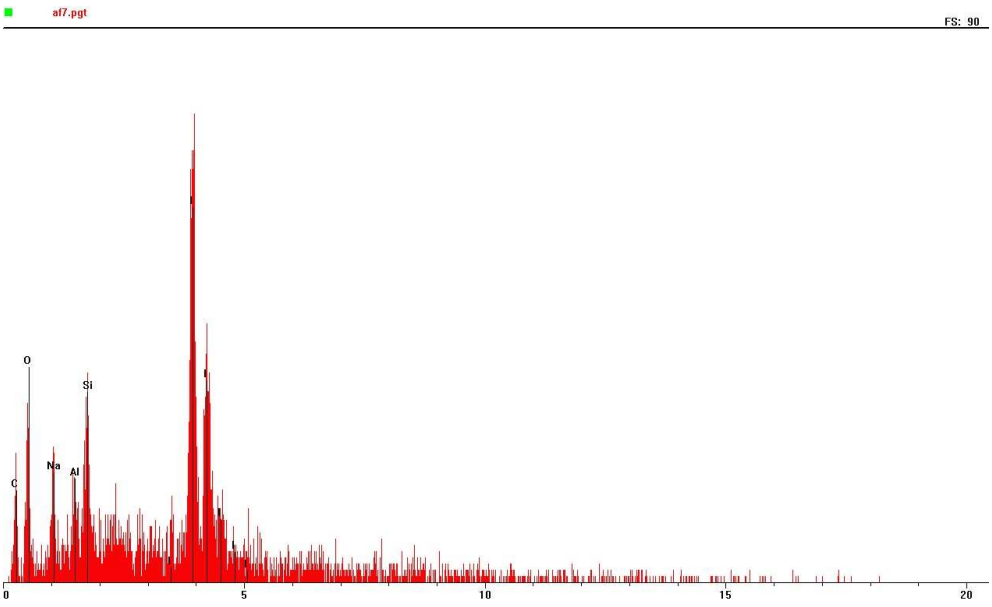

Figure A.3: Organic horizon intra-aggregate fraction

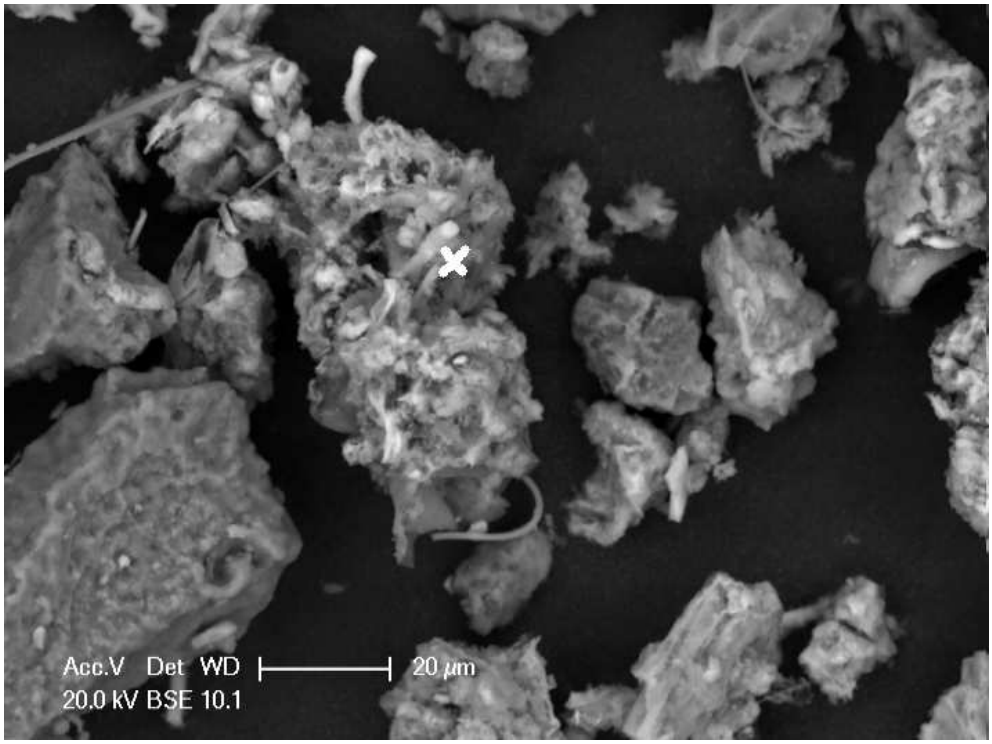

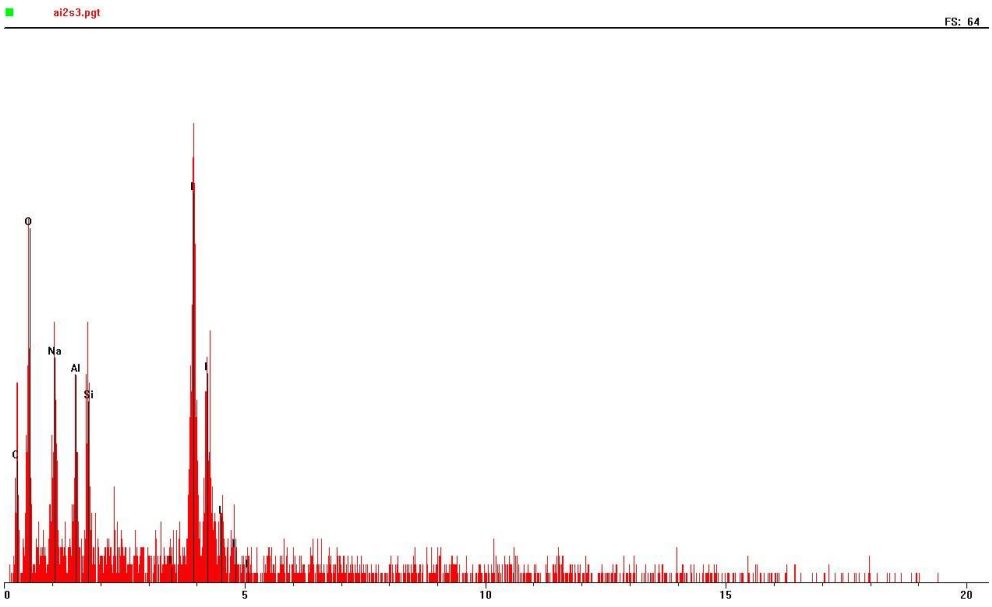

Figure A.4: Organic horizon mineral-bound fraction

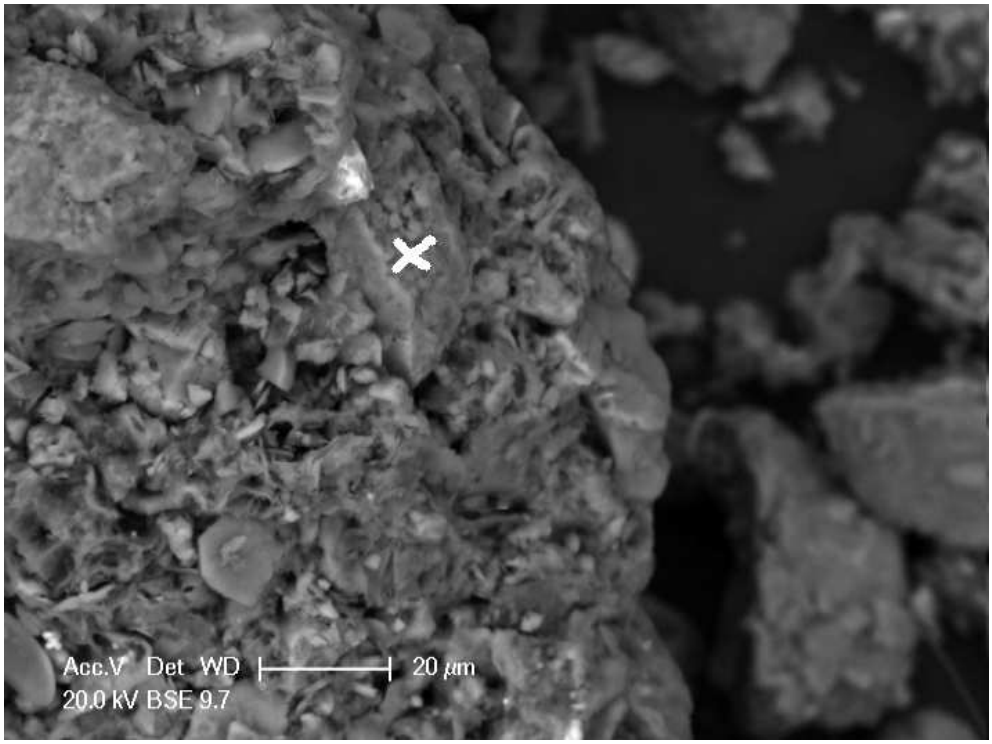

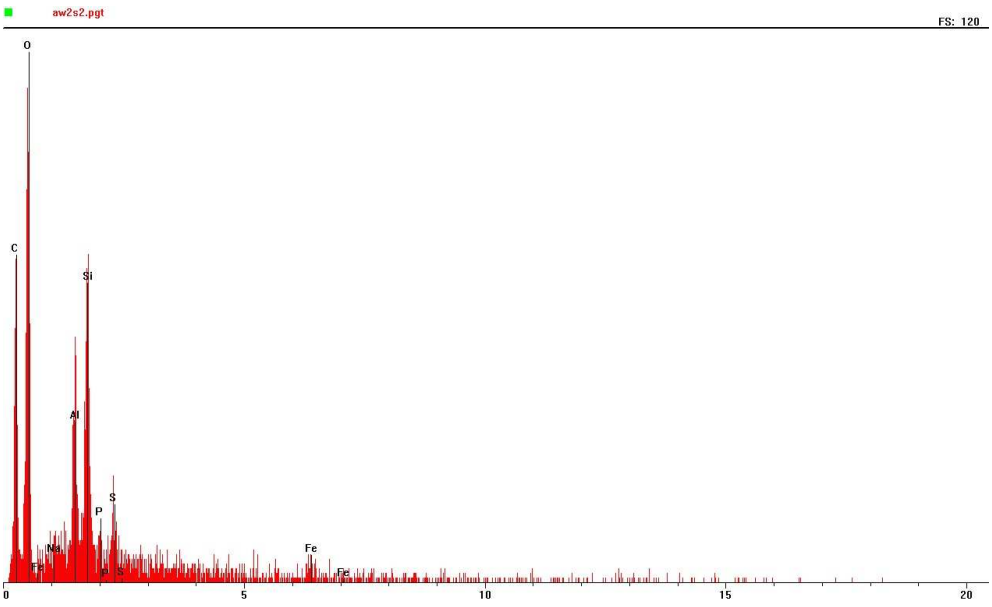

Figure A.5: Mineral horizon whole soil

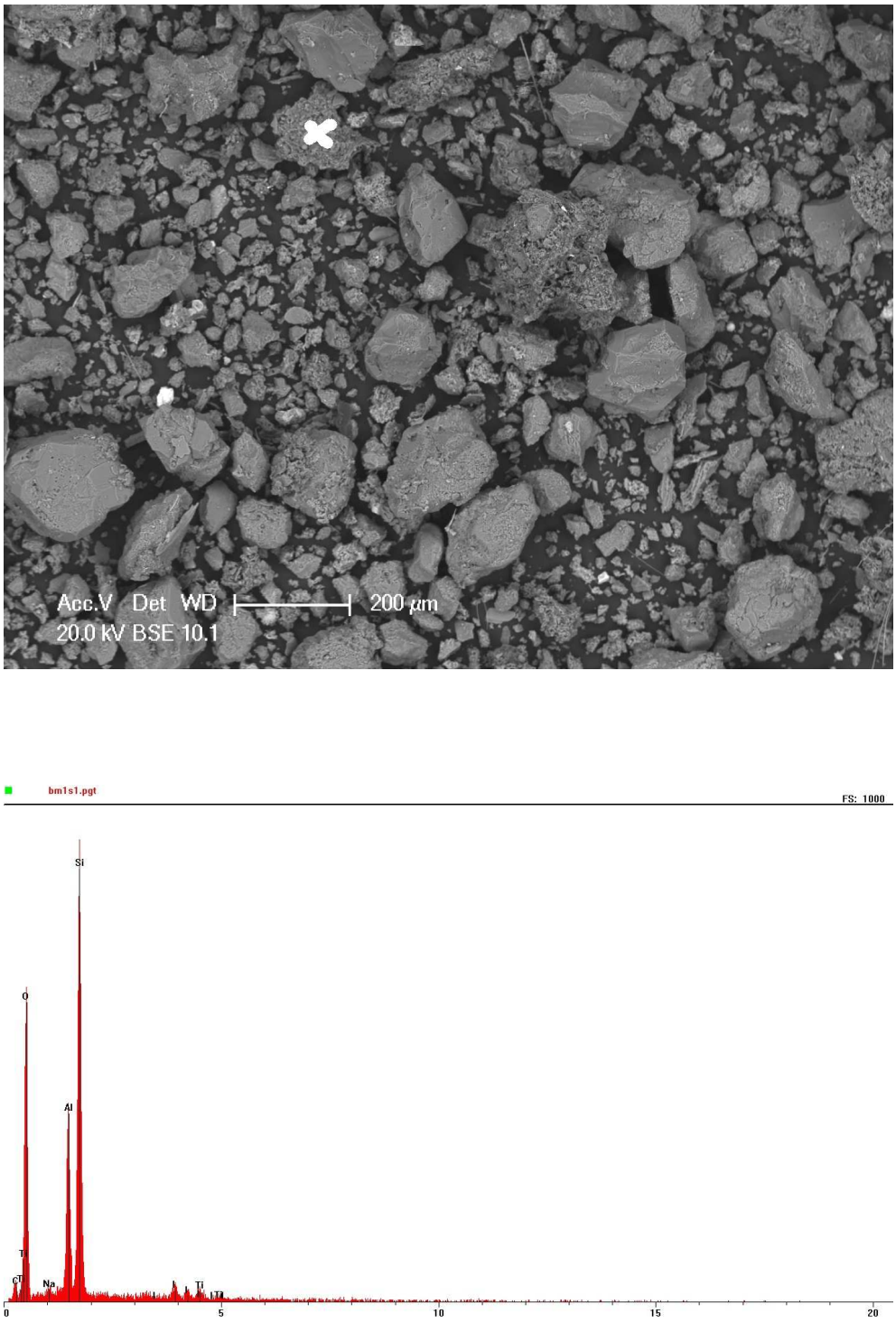

Appendix B

Formulex nutrient solution specification sheet

Formulex

Spec Sheet

Analysis of Concentrate (Elements)	% W/V	g/L	% W/W	ppm w/soln
Nitrate-Nitrogen	2.09	21.92	1.987975	219
Ammonium-Nitrogen	0.20	2.12	0.192386	21
Total Nitrogen	2.29	24.04	2.18	240
Phosphorous-P	0.35	3.72	0.336984	37
Phosphorus pentoxide – P2O5	0.81	8.52	0.772366	85
Potassium – K	2.65	27.84	2.525123	278
Potassium oxide – K2O	3.19	33.55	3.042773	335
Calcium – Ca	1.26	13.20	1.197259	132
Calcium oxide – CaO	1.76	18.47	1.675445	185
Magnesium – Mg	0.29	3.04	0.275963	30
Magnesium oxide – MgO	0.4805	5.05	0.457619	50
Sulphate – SO4	0.39	4.12	0.374091	41
Sulphur – S	0.130801	1.37	0.12	14
Iron	0.050	0.53	0.048	5.26
Manganese	0.012	0.131	0.012	1.309
Zinc	0.0034	0.036	0.0032	0.35756
Boron	0.0102	0.108	0.0098	1.075
Copper	0.0023	0.025	0.0022	0.25
Molybdenum	0.0012	0.012	0.0011	0.1237052
Cobalt	0.0006	0.006	0.0006	0.064388881
Nickel	0.0006	0.006	0.0006	0.064760709
NPK (using %W/V)	2.29	0.35	2.65	
N:P2O5:K2O (using %W/V)	2.29	0.81	3.19	
NPK (using %W/W)	2.180361	0.336984	2.525123	
N : P2O5 : K2O (using %W/W)	2.180361	0.772366	3.043	
% of N from ammonium	8.82%			
K/N ratio =	1.16			
Specific Gravity =	1.05			

Constituent Compounds	CAS #	%W/V	g/L	%W/W
Magnesium Carbonate	23389-33-5	0.52	5.50	0.498684807
Phosphoric Acid	7664-38-2	1.38	14.51	1.316462585
Potassium Sulphate	7778-80-5	0.71	7.49	0.679092971
Calcium Nitrate Prill	13477-34-4	6.77	71.13	6.452063492
Calcium Nitrate tetrahydrate				
Potassium Nitrate	7757-79-1	6.03	63.30	5.74122449
Magnesium Nitrate	13446-18-9	1.47	15.39	1.395464853
Ammonium Nitrate	6484-52-2	0.65	6.86	0.621950113
Fe 13 % EDTA	15708-41-5	0.3810	4.00	0.363
Mn-EDTA	5375-84-5	0.0890	0.94	0.085
Solubor	1303-96-4	0.0476	0.50	0.045
Zn-EDTA	4025-21-9	0.0243	0.26	0.023
Cu-EDTA	4025-15-1	0.0167	0.175	0.016
Moly	13106-76-8	0.0030	0.031	0.0028
Cobalt Nitrate	14216-74-1	0.0030	0.032	0.0029
Nickel Sulphate	10101-97-0	0.0028	0.029	0.0026
Humic Acid	NIL	NIL	NIL	NIL

Formulex

analysis for labels statutory layout

N : P2O5 : K2O	2.289	0.811	3.195
Nitrogen-N			
Nitrate-N	2.087	%W/V	
Ammoniacal-N	0.202	%W/V	
Phosphorus pentoxide (P2O5) water soluble (P)	0.811	0.354	%W/V
Potassium oxide (K2O) (K)	3.195	2.651	%W/V
Calcium oxide (CaO) (Ca)	1.759	1.257	%W/V
Magnesium oxide (MgO) (Mg)	0.480	0.290	%W/V
Sulphate (SO4) (S)	0.393	0.131	%W/V
Boron (B)	0.0102	%W/V	
Cobalt (Co)	0.0006	%W/V	
Copper (Cu)	0.0023	%W/V	
Iron (Fe)	0.0501	%W/V	
Manganese (Mn)	0.0125	%W/V	
Molybdenum (Mo)	0.0012	%W/V	
Nickel (Ni)	0.0006	%W/V	
Zinc (Zn)	0.0034	%W/V	